RIVAS

Railway Induced Vibration Abatement Solutions

Collaborative project

Description of test procedures based on laboratory tests and field tests including validation

Deliverable D1.10

Submission date: 31/12/2013

Project Coordinator:

Wolfgang Behr

International Union of Railways (UIC)

ext.behr@uic.org

Title	**Description of test procedures based on laboratory tests and field tests including validation (Deliverable D1.10)**
Domain	**WP 1.2**
Date	**31/12/2013**
Author/Authors	Rüdiger Garburg, Dorothée Stiebel (DB), Vicente Cuellar (CEDEX),
Partner	DB, CEDEX, BAM, ER,
Document Code	rivas_db_wp1_d1_10__test_procedures_V_1.0_final (07-05-14)
Version	1.0
Status	Final

Dissemination level:

Project co-funded by the European Commission within the Seventh Framework Programme		
Dissemination Level		
PU	Public	X
PP	Restricted to other programme participants (including the Commission Services)	
RE	Restricted to a group specified by the consortium (including the Commission) Services)	
CO	Confidential, only for members of the consortium (including the Commission Services)	

Document history		
Revision	Date	Description
0.02	24/10/2013	First Draft
0.04	17/12/2013	Complete revision, Chapter 6 & 7 added
1.0	31/12/2013	Final

1. EXECUTIVE SUMMARY

The aim of the RIVAS project is to reduce the environmental impact of railway induced vibration by providing a set of vibration mitigation measures. These measures may affect the rolling stock, the track or the soil below or in the immediate vicinity of the track. For an accurate assessment of different mitigation measures, standardized measurement procedures are required. The establishment of test procedures to efficiently monitor and control the performance of vibration mitigation measures under realistic conditions and their effect on residents is one of the main scopes within WP1.

Not in all cases it is possible to determine the mitigation effect, the so called insertion loss (IL), of e.g. different mitigation measures directly in tracks with running trains. Before installation in commercial tracks a long process of construction, prototype development and homologation procedures for new components or measures have to be performed. For an early evaluation of different mitigation measures, for parametric studies or for relative comparison of different solutions, also alternative procedures in laboratory or admitted for full-scale test track installations are required.

This deliverable describes the investigation within RIVAS for testing procedures with artificial vibration excitations compared to installations in a commercial track in DB's network. The test and evaluation procedures described in this report can be used for the determination of resilient elements in track-systems, either in real track or in full-scale test-installation. Furthermore the investigations are closely linked to the developed mitigation measures for ballasted tracks (RIVAS WP 3.2) and slab tracks (RIVAS WP 3.4). So the procedures with the artificial vibration excitation are focused on resilient elements in track, in particular under sleeper pads (USP) combined with different types of sleepers. The conclusions cannot be transferred to further resilient elements.

Following a short introduction, chapter 4 gives an overview on different procedures to determine the IL with artificial vibration excitations.

Chapter 5 describes the performed evaluation procedures and the results obtained:

- In a first step, a special force controlled hydraulic shaker was used. A special focus was laid on studying the influence of sprung and unsprung masses on the determination of IL. A special procedure has to be found how to bring adequate masses on the track within short track possessing time and without hindrance of the train traffic. The investigation is described in chapter 5.1.
- An analogical procedure was used for determining the dynamic characteristics of the different mitigation measures installed within the investigation in WP 3.2 and WP 3.4 on a special test field of RIVAS partner Eiffage Rail. This is described in chapter 5.2.
- As an additional investigation, some track configurations were also measured in the CEDEX laboratory with their special test-rig (chapter 5.3). In contrast to use of the stationary shaker, it is possible to simulate moving loads within the CEDEX track box. Some proposals for a better understanding of the theoretical background as well for a further development of the track box are given.

The chapters 6 and 7 describe additional questions which were not initially planned within RIVAS but raised up within the project duration. In chapter 6 two different methods of data analysis of measurement were compared. On the one hand the easier and most common way with the "fast max-hold 1/3 octave spectra" and the data analysis of the energy over the time signal over the pass by time are compared. It could be shown that for the determination of IL

the different analysis methods lead to similar results. In chapter 7 an additional procedure for the determination of subsoil correction functions with the line mobility transfer function was tested.

The report closes in chapter 8 with a summary of the main conclusions. The investigations show that a procedure to determine the dynamic characteristics in track with stationary vibration excitation including the simulation of the different masses could be found.

The determination of IL by train passages show that in the low frequency part the IL depends significantly on the different train categories. This is caused by a reduction of the parametric excitation due to the installation of USP. Therefore it is not possible to have only one definite reference IL for the comparison of train passing's and artificial excitation.

For determination of the insertion loss, the soil correction of the different sections (e.g. with transfer mobility functions) was found to be essential to obtain reliable results.

The test with artificial excitation is capable to investigate the dynamic characteristics of a track. The results for the IL by the shaker excitation showed a good agreement with the expected results compared to calculation methods based on dynamic models with mass-spring-systems or impedance models [20]. The results of IL by train passages show particularly for the lower frequency range some additional positive mitigation effects which are not possible to explain with these simple models. This phenomenon has been considered before in several other investigations as described in [21] and [22] and further publications. Compared to other resilient elements (under ballast mats, floating slab-systems), the reduction of the parametric excitation due to the USP has a more dominant effect.

This clearly shows that the USP have some additional positive side-effects on vibration mitigation which cannot be described with simple models as well as with the stationary harmonic artificial excitation. This mitigation effects based on mechanical behaviour e.g. due to embedding the ballast stones in resilient material with an increase of contact area together with an decrease of contact forces between ballast and sleeper [23], the better load-distribution in longitudinal direction as well as the general better track quality (e.g. avoiding of hanging sleepers) cannot be detected by stationary excitation. This gives also an explanation that the mitigation effect of USP is underestimated when using dynamic prediction models.

In addition to the stationary tests at the free field, laboratory tests were performed at the CEDEX track box which allows simulating the pass-by of a train considering also the real dynamic loads depending on the track configuration. As a result, a positive efficiency was found in the low frequency part which is in a very good agreement with the pass-by measurements. Because this effect could not be measured with the stationary tests mentioned above, the test at the CEDEX track box is considered to be a complementary test. For the higher frequencies, the agreement between the measurements at the CEDEX track box and the measurements by using train pass-by was not as good as expected. Therefore, a procedure was developed how the CEDEX track box can be used in future to obtain the trend of the IL's values expected in the free field at some distance of the track.

Finally, four different annexes are added to the report describing the performed measurements in detail.

2. TABLE OF CONTENTS

3. INTRODUCTION AND SCOPE

It is a prerequisite to determine the effectiveness of vibration mitigation measures as exact as possible both for the vibration prediction within the environmental impact assessment studies in the planning phase for new railway lines as well as for cost-benefit-analyses to decide between different mitigation measures proposed for a specific site.

In general, vibration mitigation can be described by the “insertion loss” (IL) which quantifies the relative mitigation effect compared to a specified reference situation (e.g. the standard ballasted track).

For the detection of the mitigation-measure efficiencies, a procedure based on vibration measurements during train passage was developed within the RIVAS project [1] and described in a basic deliverable [2] and [3]. But for some reasons, a simple to handle measurement procedure with artificial excitation has significant advantages. Thus, reduction of costs is possible when homologation of the new products is not needed before testing and the installation cost is low (installation of some meters of the new product instead of minimum 100 m as required in [2] and [3]).

Therefore, alternative measurement methods to detect mitigation-measure efficiencies by using artificial excitation at field or in laboratory were investigated within RIVAS. Even if the absolute values of the mitigation-measure efficiencies are not the same as in measurement during train passage, at least a relative comparison of different mitigation measures was expected to be possible with artificial excitation. Considering resilient elements in the track, effects due to the isolation-effect and due to the long-term reduction of track irregularities could be separated.

Subsequently this procedure was used to compare the effectiveness of mitigation measures at different track sections with configurations of heavy sleepers and under-sleeper-pads (USP) in different stiffness categories including a slab-track configuration. These tests were carried out at a full-scale test-field of the RIVAS partner “Eiffage Rail” (ER) within RIVAS in WP 3.2 and 3.4.

In contrast to use the stationary shaker, the so called CEDEX track box opens the possibility to simulate moving loads within a full-scale test in laboratory. Some investigations have been performed and considerations for a better understanding of the theoretical background as well as proposals for a further development of the track box are given.

The test and evaluation procedures described in this report are capable to determine the effect of resilient elements in track systems, either in real track or in full-scale test-installation but not necessarily to determine mitigation effects on other parts of the “vibration systems” (e.g. methods on buildings, on transmission part or for vehicles). Furthermore the investigations are focused on USP (under sleeper pads), the conclusions cannot be transferred by implication to other resilient elements.

4. DETERMINATION OF MITIGATION-MEASURE EFFICIENCIES

4.1 DEFINITION AND MEASUREMENT PROCEDURES

In general, the vibration reduction of mitigation measures is quantified by means of the "insertion loss" (IL). The insertion loss describes the relative abatement effect of a mitigation measure compared to a reference situation. Typically, the reference situation is a standard ballast track system without any mitigation measures. Quantitatively, the insertion loss shows the change of the third-octave spectrum of structure-/ground borne noise if a mitigation measure were installed, assuming all other influences remain constant (e.g. the same vehicle, velocity, rail roughness etc.):

$$D_e(f_{Tn}) = L_{v,1}(f_{Tn}) - L_{v,2}(f_{Tn}) \quad (1.)$$

with:

- $D_e(f_{Tn})$: insertion loss
- $L_{v,1}(f_{Tn})$: third-octave spectrum of ground vibration at the reference track
- $L_{v,2(}f_{Tn})$: third-octave spectrum of vibration at the track with mitigation measure

The standard procedure to determine IL is to compare the ground vibration measured during train passages at a specific site before and after the installation of a mitigation measure (the so called "left/right" method or "Procedure 1") or during the same train passages at two adjacent track sections with and without measure (the "before/after" or "Procedure 2" method) as described in the RIVAS measurement protocol [2] and outlined in Figure 4-1.

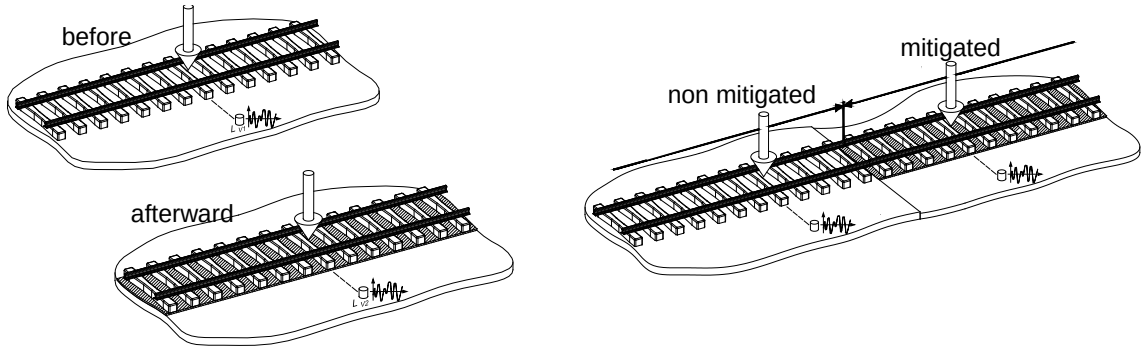

Figure 4-1: Basic principle of determining the IL with the two procedures, the "before/afterwards" method or procedure 2 on the left and the "left/right"-method or procedure 1 on the right side.

Each method has its particular advantages: While working with the left/right method the identical train is considered in both sections and therefore the influence of different trains is negligible. On the other hand, it has to be ensured that the conditions of the subsoil, the ground and within the transmission paths in general are identical at both sections. Alternatively, results have to be normalised by an appropriate correction term.

On the other hand, the before/afterwards method is not influenced by different subsoil conditions, but since it is not possible to measure the identical trains, it has to ensure that the trains and their passage speeds within the both measurement campaigns are comparable. Measuring a high number of train passages for each train category is essential to obtain statistical valid results. Furthermore, the before/afterwards method determines the mitigation effect in total which means that very often the mitigation effect is not only caused by introducing the resili-

ent element alone, but also by the better track quality in consequence of its renewal, new ballast and further influencing parameters and it is not possible to separate the effect of e.g. the elastic element.

In order to obtain the full information of reliable data, the so called “combined procedure” with the application of both methods is generally recommended in the RIVAS measurement protocol [2].

In general, the mentioned procedures are possible to be applied to train passage measurements as well as to a stationary, artificial vibration excitation e.g. by a (force-controlled) shaker or by impact loads. To ensure that the influence of excitation is eliminated in both procedures it is required to know the input forces.

The diagram in Figure 4-2 shows an overview on the particular procedures and methods for the determination of IL in a general overview. The general determination procedures and the different excitation mechanism are further discussed within the document.

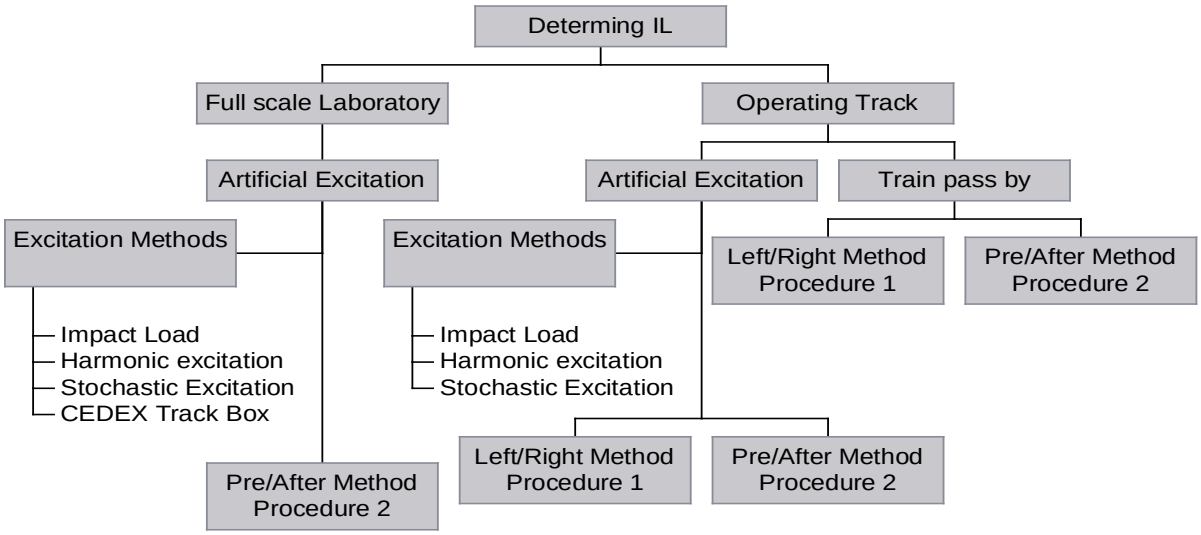

Figure 4-2: Schema of different methodologies for the determination of the Insertion loss (IL)

4.2 VIBRATION GENERATION DURING TRAIN PASSAGE

For the generation of ground borne noise and vibration, different types of excitation are responsible as shown e.g. in RIVAS Deliverable D 1.2 Annex, [3]:

- The main excitation is described as **a relative displacement** at the wheel and rail contact point. It is usually referred to as wheel and rail unevenness and can include the description of isolated defects (such as wheel flats, welded joints…) as long as no loss of contact occurs.
- The **quasi-static excitation**, related to the train load moving at a given speed, will depend on the magnitude of the speed and the magnitude and geometric distribution of the vertical loads along the train.
- The **parametric excitation** is related to the stiffness variation of the track. It generates high vibration levels at the sleeper frequency and its harmonics, but can also include lower frequency, that can be described by random variation of the ballast stiffness for instance. Unlike the unevenness, the parametric excitation depends on the train static load (the higher the load, the higher the contact force) and also depends on the track stiffness (the lower the stiffness, the lower the excitation).

These effects of vibration generation cannot be reproduced by stationary artificial vibration generations.

4.3 VIBRATION GENERATION WITH ARTIFICIAL EXCITATION

For determinations with stationary vibration generation, different methodologies and types of vibration generators are possible. Each method has their particular advantages and disadvantages.

Depending on the scope of the investigation, an adequate preload has to be considered as discussed later on within this report.

Impact load

The procedure to excite the track by impact load is in general capable for determination of the dynamic characteristics of resilient elements of rail-fastenings systems (e.g. railpads) or systems installed in the track or in special test-rig installation as long as the input energy is high enough to generate vibration signals at the measurement points which are significant above the background vibration level.

For the impact load a falling mass (Figure 4-3) as well as an impact-hammer can be used. For the determination it is essential to use a hammer with input-force measurement device. With impact-load it is possible to generate vibration impacts within a frequency range between 5 and 200 Hz.

Figure 4-3: Hydraulic driven drop weight "DYNPACT®"as an example for falling mass as used within RIVAS project WP 1 and WP 3 (picture Detusche Bahn AG R. Garburg)

Using a falling mass (hydraulic driven drop weight) enables much more input energy as by simple hammers. The repeatability of each impact is very high, so that the number of repetitions can be limited.

Harmonic excitation

For the harmonic excitation vibration, generators acting as an unbalanced mass generator as well as hydraulic or electro-dynamic shaker are used. These generators offer continuous fre-

quency sweeps or act in a mono-frequent mode varying the frequency in 1/3 octave or narrow band steps.

For investigation of the transfer-mobility function the input force has to be determined. Recent generator works either force-controlled (with a constant input force over a broad frequency range) as well as vibration velocity controlled.

To achieve a constant force-input and to avoid a take-off of the vibration device by passing the frequency sweep in some frequencies ranges a constant contact to the track-system or rail is required. Therefor the vibration generator should be fixed to the rails.

For the use in railway tracks, force amplitudes in a range of 5-20 kN are recommended [4].

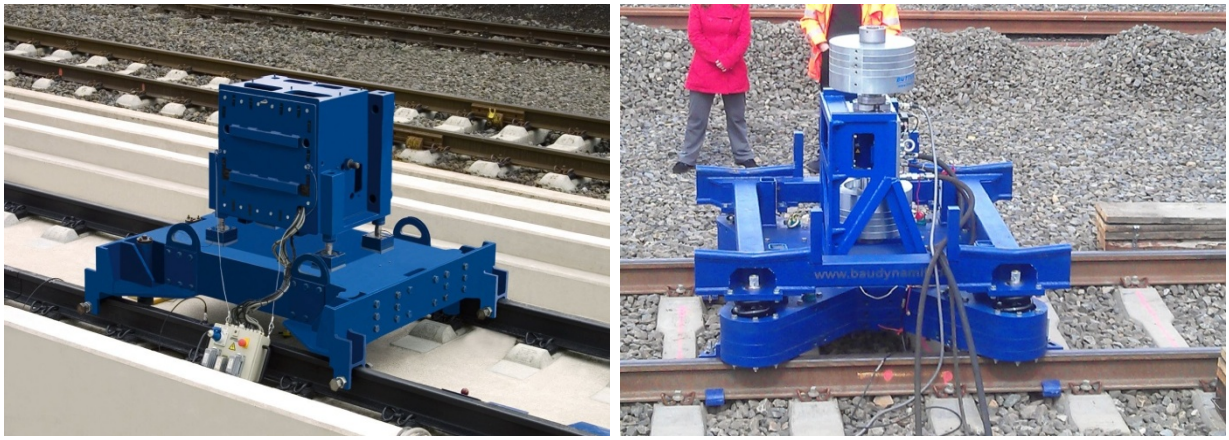

Figure 4-4: The unbalanced mass vibration generator DYNAQ® (left) and the hydraulic shaker BUTTERFLY ® at the right as examples for harmonic vibration excitation (pictures R. Garburg)

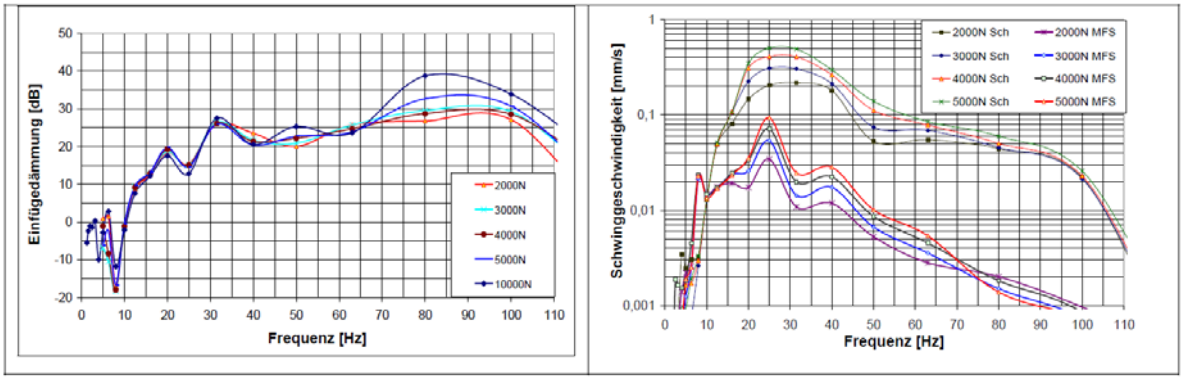

Figure 4-5: Example for determination of the IL at a low tuned floating slab system with the unbalanced mass generator DYNAQ® with IL at the left diagram and vibration velocities beside the track of Floating Slab and reference track for different load conditions at right diagram, as reported in [5].

Particular for vibration prediction of railway tunnels, vibration generators like the self-driven generator VibroScan (www.vibroscan.at) are used. It works generally directly on the ground or at tunnel foundation; an application directly on rails of a track is not reported yet.

Figure 4-6: VibroScan vibration generator in tunnel for determination of vibration transfer-functions in vibration prediction (picture, R. Garburg)

Stochastic excitation

For stochastic vibration excitation, conventional vibratory plate compactor as used as standard machine at construction sites can be used in different forms (Figure 4-7). They are easy to handle and available.

In contrast to the other methods, it is generally not possible to measure the input force in a direct way. Therefore determination of transfer-mobility functions is not accomplishable.

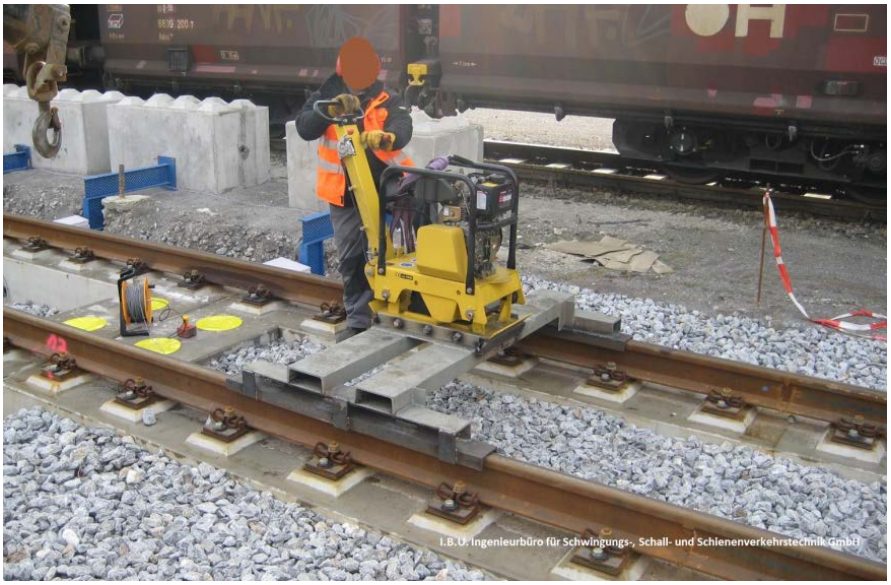

Figure 4-7: Example for stochastic excitation with vibration-plate and a cross-beam for the load distribution into the rails [4], (picture source: I.B.U GmbH, Essen)

4.4 PROCEDURES WITH ARTIFICIAL EXCITATION TESTED WITHIN RIVAS

4.4.1 Field measurements with harmonic stationary excitation

To determine the transfer mobility function from the head of the rail to the point of interest beside the track a stationary vibration excitation with specific requirements was needed:

- force controlled vibration generation which is able to operate a vibration sweep over a broad range of frequency
- applicable to large scale test in test rig as well for investigations at commercial tracks
- quick ready for action in track (< 1 h) to minimize the track possession
- suitable for work on rails at different track systems, under power cables and easy access to tracks
- Ssmulation of different load conditions for the un-sprung and sprung masses

The special hydraulic harmonic shaker BUTTERFLY® fulfilled these requirements. It can operate force or velocity-controlled over a frequency range of about 0-110 Hz with a maximum dynamic excitation force of 21 kN.

Figure 4-8: BUTTERFLY® test setup with 400 kg oscillating weight
(picture source: Ingenieuerbüro Dr. Heiland)

The shaker can operate in the frequency range 0 – 110 Hz with a maximum dynamic excitation force up to 21 kN. Its oscillating mass is 400 kg.

The technical details of the artificial excitation by the shaker are summarized in the following table.

Actual dynamic force amplitude	7500 N (0 – P)
Excitation frequency	Frequency sweep in the range 5 – 110 Hz
Oscillating mass	400 kg
Unsprung mass	2,3 t steel foundation 0,35 t shaker (without oscillating mass)
Static load due to excavator weight	See Figure 5-11

Table 4-1: Technical details of the shaker tests

Within the investigation in RIVAS the shaker *BUTTERFLY*® operates generally force-controlled. Figure 4-9 shows an exemplarily load curve over a frequency sweep from 5 to 110 Hz.

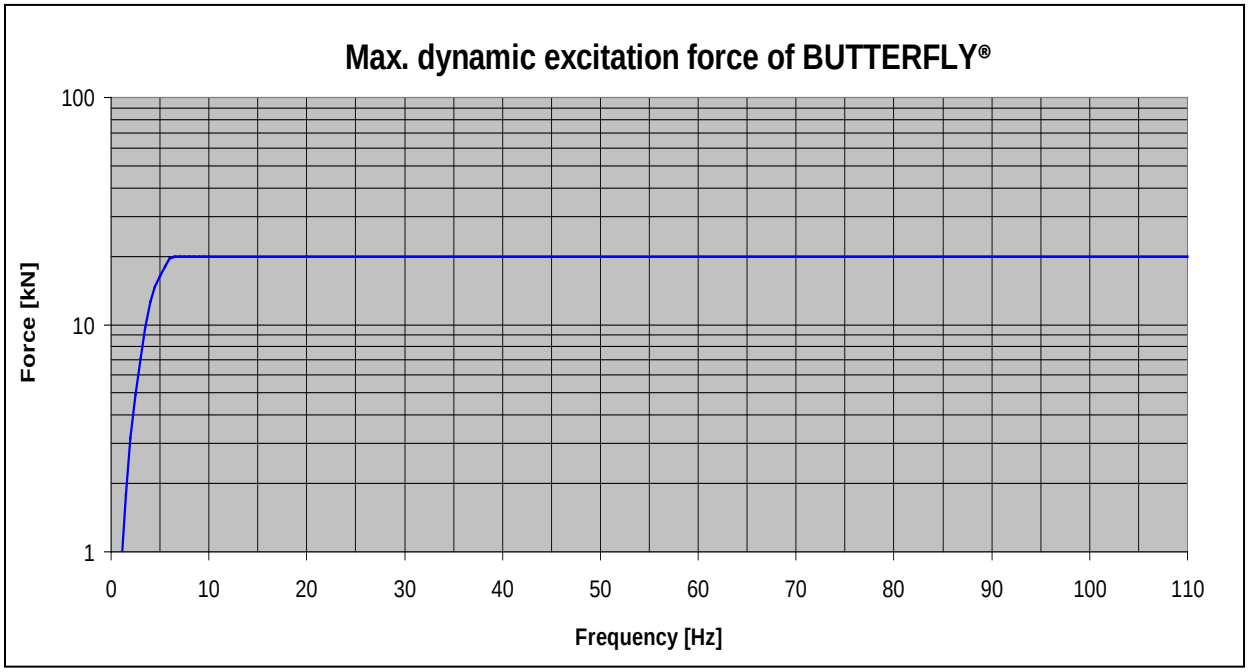

Figure 4-9: Input force over frequency for the BUTERFLY shaker

The frequency is increased continuously during a sweep from 5 Hz to 110 Hz. For each measuring section two tests with different rates of frequency increase are performed:

1. 0,1 Hz per 0,1 sec
2. 0,1 Hz per 0,2 sec

Figure 4-10 presents exemplarily a representative time history of one sweep. The seven measuring channels contain the shaker force, the current frequency, vibration response of the unsprung mass and at the three parallel 8 m points and for the 16 m measuring point.

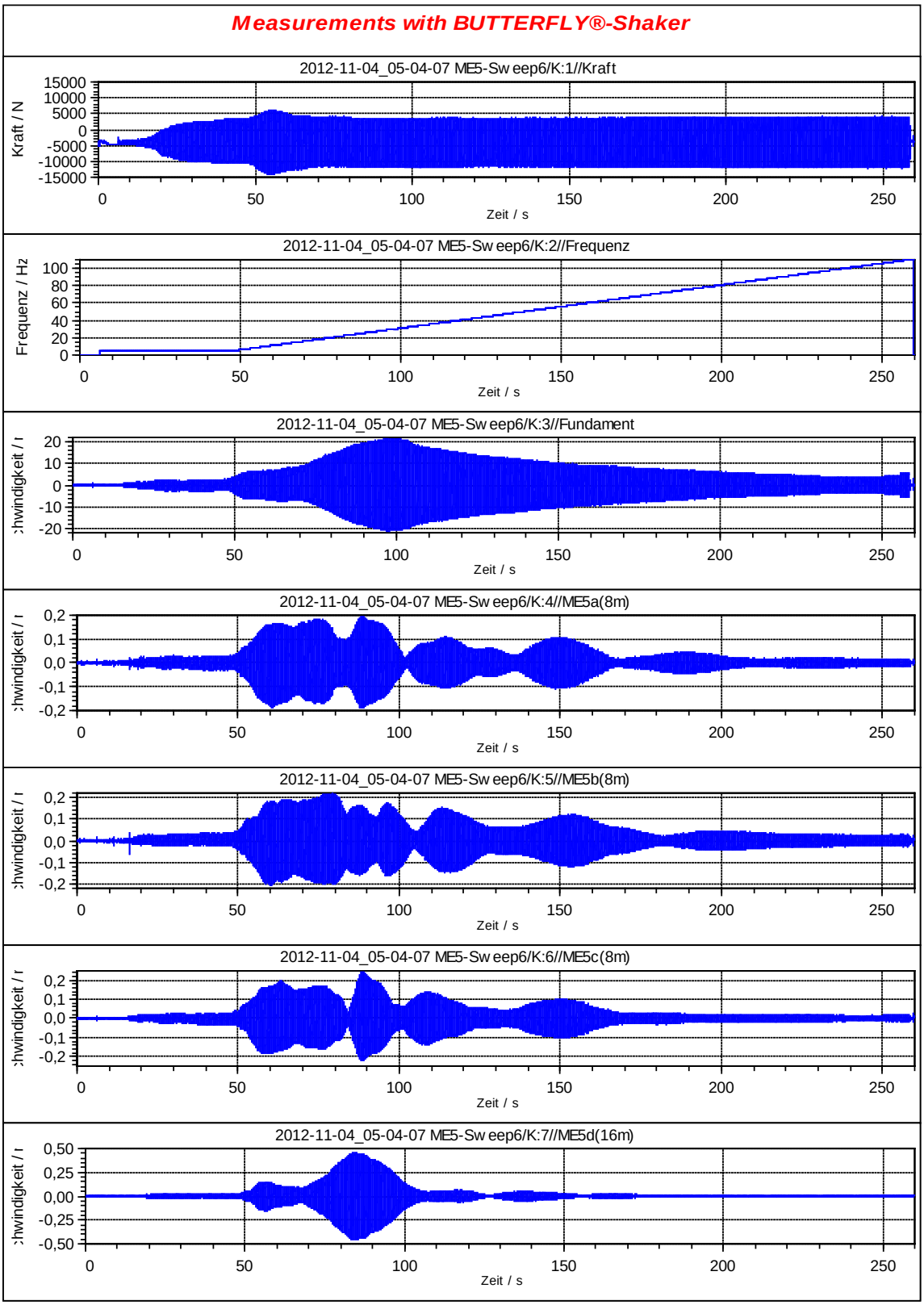

Figure 4-10: Time history of the shaker force, frequency, vibration response of the unsprung mass and at 8m and 16m measuring point (raw data of sweep6, ME5, exemplarily)

Although the shaker force is nearly constant, the vibration response of the unsprung mass depends strongly on the excitation frequency. In Figure 4-10, the eigenfrequency of the track

system is about 30 Hz. In comparison, the reference section shows its resonance behaviour at 80 Hz, see Figure 4-11.

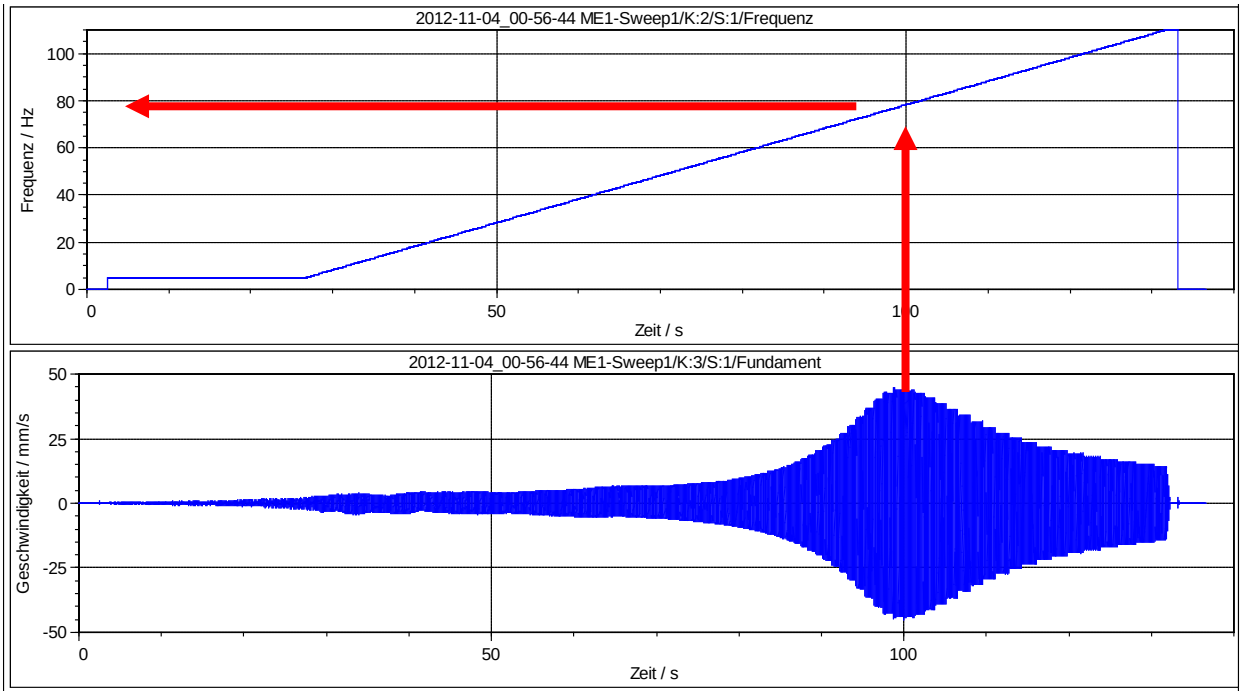

Figure 4-11: Time history of the excitation frequency and vibration response of the unsprung mass at the reference section ME1 (raw data of sweep1, ME1)

4.4.2 Laboratory measurements with simulation of train passages

The laboratory measurements were performed at the CEDEX track box which is a 21 m long, 5 m wide and 4 m deep experimental box built for testing complete railway track sections of conventional and high speed lines (1:1 scale).

The track box has been constructed with nine fix steel frames distributed in three different zones (Zone 0, Zone 1 and Zone 2) as sketched in the right hand side of Figure 4-12. They give support, in each zone, to a movable reaction system constituted by three large horizontal beams equipped, each one of them, with a couple of 250 kN (50 Hz) MTS cylinders of the 224.31S type with a piston stroke of 150 mm (see the left hand side of Figure 4-13). The cylinders are operated, either independently or simultaneously, by a computer controlled VTI electronic system which commands a servo-hydraulic system provided with three step servo-valves that require a flow rate of 1,800 litres per minute and a pressure of 21,000 kPa.

The RIVAS track systems described in chapter 5.3.1 were all tested in the central zone of the track box (Zone 0 in Figure 4-12) which at the time the tests were performed consisted of 0.35 m of ballast over 0.12 m of bituminous sub-ballast and 0.60 m of granular form layer overlying an upper subgrade 1.20 m thick and a lower subgrade with a thickness of 1.40 m, as sketched in the right hand side of Figure 4-12. Static tests run before having subjected that track box zone to several millions of high speed and conventional axle loads, along the last two years, led to a track stiffness value of 120 kN/mm.

The loading reaction frames in each testing zone have been thoroughly investigated, both theoretically and experimentally, to ensure that their natural frequencies under vertical loads are well beyond the frequencies associated to the pass by of bogies and loading axles of high

speed trains circulating at speeds up to 400 km/h. Because of the large dimensions of the box, no significant effects of its boundaries (which are not fully rigid) have been detected in the Finite Element studies carried out so far to assess their influence in the behavior of the track under quasi-static and dynamic loading conditions (see the left hand side of Figure 4-12).

Recently, the facility has been implemented with a set of two 20 kN (300 Hz) PISHA piezoelectric shakers (see the right hand side of Figure 4-13) that operating with inertial masses up to 400 Kg and vibrating with a maximum amplitude of 0.08 mm enable the generation of high frequency dynamic loads in the track.

The track box foundation is made up by one 0.70 m thick, 25 m long and 8 m wide reinforced concrete slab resting on a hard soil of the Miocene epoch with a shear wave velocity of 450 m/s.

In Chapter 2 of RIVAS deliverable D3.7 Part A [10] a complete description of the sensor, data acquisition and measuring systems of the installation is given and in Chapter 3 of that document the cross sections of the track box zone used for the RIVAS tests are defined together with the physical properties of the material layers that constitute the part of the track (ballast, sub-ballast, form layer, upper subgrade and lower subgrade) common to all the track systems tested.

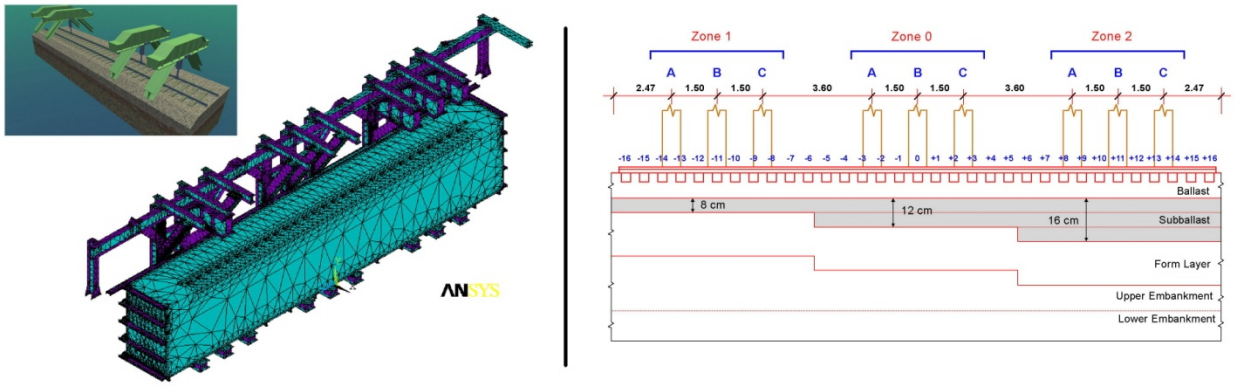

Figure 4-12: Iso-view (left) and longitudinal section view (right) of the CEDEX -track box showing the testing zones and boundary testing conditions.

In the the stationary tests run for RIVAS at the free field with the BUTTERFLY® shaker is essential to incorporate physically in the tests both the sprung and unsprung masses of the vehicles that will affect in a real line each one of the track systems tested. In the laboratory tests performed at the CEDEX track box there is no need to construct those masses since the tests performed there are based in reproducing over the track systems tested, by means of the loading systems incorporated to the track box, the following effects:

- Those induced by total loads (sum of the loads corresponding to the sprung and unsprung masses of the operating trains) either applied statically or quasi-statically simulating the pass by of trains at a certain speed.
- Those induced by dynamics loads generated by the unsprung masses of the operating trains travelling at a certain speed over well-defined track vertical irregularities.

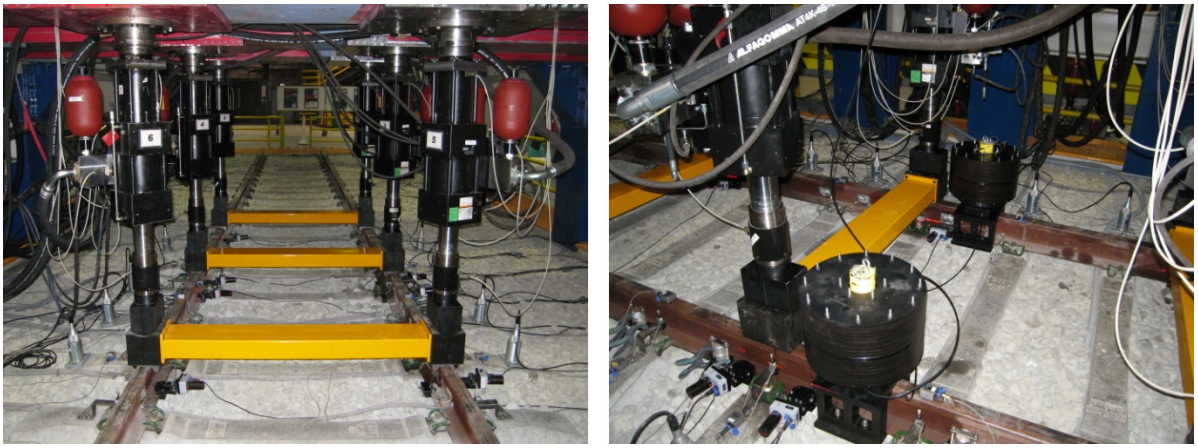

Figure 4-13: Track box loading system with MTS hydraulic cylinders (left) and PISHA piezoelectric shakers (right) (pictures CEDEX).

For reproducing those effects in the track box, its loading systems - based on the servo-hydraulic cylinders (in the first case) and the servo-hydraulic cylinders plus the piezoelectric shakers (in the second case) - must be fed previously with the appropriate load time histories. The basic principles supporting the estimation of those load time histories are described below.

The reproduction of the track effects caused by total vertical loads, applied either statically or moving horizontally at a certain speed, is based in the well-known expression of Zimmermann [11] that reproduces the track deflection "δ" bulb created by a vertical load "Q" applied statically to one rail of a track having a track stiffness "K".

Using that expression it can be checked that the deflection time history δ(t) induced in a track point previously selected, when the vertical load "Q" travelling at speed "v" passes at time t = 0 over the point in the track located at a distance "d" from the selected point such that for longer distances the moving load does not induces any deflection at the selected point, is given by the following equation:

$$\delta(t) = \frac{Q}{K} e^{-\frac{|d-vt|}{L}} \left[cos \frac{|d-vt|}{L} + sen \frac{|d-vt|}{L} \right] \quad (2)$$

The deflection time history given by that equation also represents the deflection time history that would be induced at the track point previously selected by a variable stationary load Q (t) (cylinder load at the track box) whose value at each instant "t" were given by :

$$Q(t) = K\,\delta(t) \quad (3)$$

So, after constructing in the laboratory a full scale model having a track stiffness "K" similar to the one of a real track, it is possible to reproduce the deflection time history that a total vertical load "Q" travelling at speed "v" would induce in a point of that track. To achieve that goal, it is only necessary to feed each one of the servo-hydraulic cylinder that makes a pair with half the load time history provided by equation (3), since assuming that the three parameters "Q", "K" and "v" are known, the parameters "L" and "d" in equation (2) are given in terms of "K" by the following expressions:

$$L = \sqrt[3]{\frac{8EI}{K}} \tag{4}$$

$$d = \frac{3}{4}\pi L \tag{5}$$

in which EI represents the bending stiffness of the rail.

Although the stationary load time history given by equation (3) is capable to reproduce correctly in a track point the effect of a vertical load moving horizontally at a certain speed, it does not take into account neither the effects induced in the adjacent track points by the travelling of that load nor the rotation of principal stresses induced at the point by the load approaching, passing over it and getting away.

In Chapter 2.2 of [10] it is shown how to use three pairs of cylinders, separated 1.5 m of each other, to reproduce over seven consecutive sleepers the effects of both a single vertical load and a bogie travelling at a certain speed. In that process it is necessary to incorporate a time delay, between adjacent pairs of cylinders, which depends on the travelling velocity simulated in the track box. In that way, the rotation of principal stresses that can be expected in a track cross section when an axle load or a bogie approaches it, passes over it and go away, can be taken into account [12].

Using those principles, the quasi-static load time histories illustrated on pages 34 and 35 of [10] were generated by feeding each consecutive couple of cylinders with the load time history derived from equation (3) assuming a track stiffness “K” of 120 kN/mm, a “Q” value of 85 kN (corresponding to an axle load of 170 kN) and a travelling speed “v” of 300 km/h for the first case (passenger train) and the same track stiffness “K”, a “Q” value of 112,5 kN and a velocity “v” of 120 km/h for the second case (freight vehicle). In the first case a delay time of 18 ms was applied between consecutive pair of cylinders and a delay time of 45 ms in the second case.

The same basic principles were fulfilled in the derivation of the dynamic time history illustrated in Figure 4-13 of [10]. In that figure frequencies up to 150 Hz, generated by a freight vehicle travelling at 120 km/h over a medium quality track, can be distinguished. For the obtainment of that load time history an unsprung mid-wheelset mass of 712 kg, as referenced in [40], and a geometric damping ratio of 0.30, as justified in 4.3 of [10], were adopted. The whole derivation procedure has been fully described in Chapter 4.3 of [10].

5. EVALUATION OF MEASUREMENT PROCEDURES

In chapter 5.1 the evaluation procedure is based on a measurement campaign comparing results obtained with artificial vibration excitation and with train passages at the same site with different track configurations on a commercial track. The measurement campaign consists of the three following steps:

- Determination of vibrations within the different sections by field measurements during train passages (passenger and freight trains).
- Determination of the transfer mobility of the subsoil of each track sections by defined impact tests to evaluate and correct different subsoil conditions.
- Determination of the transfer mobility within the three sections for a stationary artificial excitation by the hydraulic shaker.

The target was to compare ILs measured with stationary artificial vibration generation with ILs measured in real situations with passing trains and, hence, to validate the full procedure.

In chapter 5.2 the same procedure was used to determine the different influencing parameters of sleepers and under-sleeper-pads on a special full-scale test rig.

In chapter 5.3, an investigation performed in the CEDEX laboratory with a special test-rig is described.

5.1 FIELD TESTS AT AN EXISTING DB TEST SITE

5.1.1 Description of the test site

For the comparison of the measurements of vibration excitations due to train passages and due to artificial vibration excitation on the same site, a track in south-east of Germany near Regensburg was used as test field. Here different under sleeper pads (USP) were installed in a track on a length of about 700 m. As a reference site, an adjacent section without USP could be used.

This test track was built in a former innovation-project LZarG (Leiser Zug auf realem Gleis) under the national project funding of “Leiser Verkehr” [13]. The track was some years under operation and therefore well consolidated. It is used by freight traffic but regional (mainly electric powered railcars) and long-distance trains as well.

Three different measuring sections were installed:

- One reference section: Standard ballast track with German type B70 sleepers without under-sleeper pads (**ME1**)
- Two measuring sections with installation of elastic under-sleeper pads (USP), (**ME3** and **ME5**)
  - **ME3**: USP type G03
    nominal static bedding modulus: $c_{stat1} = 0.15\ ^{N}/_{mm^3}$
  - **ME5:** USP type G04
    nominal static bedding modulus: $c_{stat1} = 0.10\ ^{N}/_{mm^3}$

The labelling of the measuring sections are adopted from the project LZarG („Leiser Zug auf realem Gleis“) [13].

Figure 5-1: Overview of the measuring sections

ME1	ME3	ME5

Figure 5-2**:** Pictures of the three measuring sections, with ME1 as reference (standard ballast track) and ME3 (USP type G03) and ME5 (USP type G04)

In each measuring section, four vibration sensors were installed according to the RIVAS measurement-protocol [2] and DIN45669 [14], three points at 8m distance; one point at 16m distance in relation to the middle of the track. The principle layout of the sensor positions are shown exemplarily in Figure 5-3.

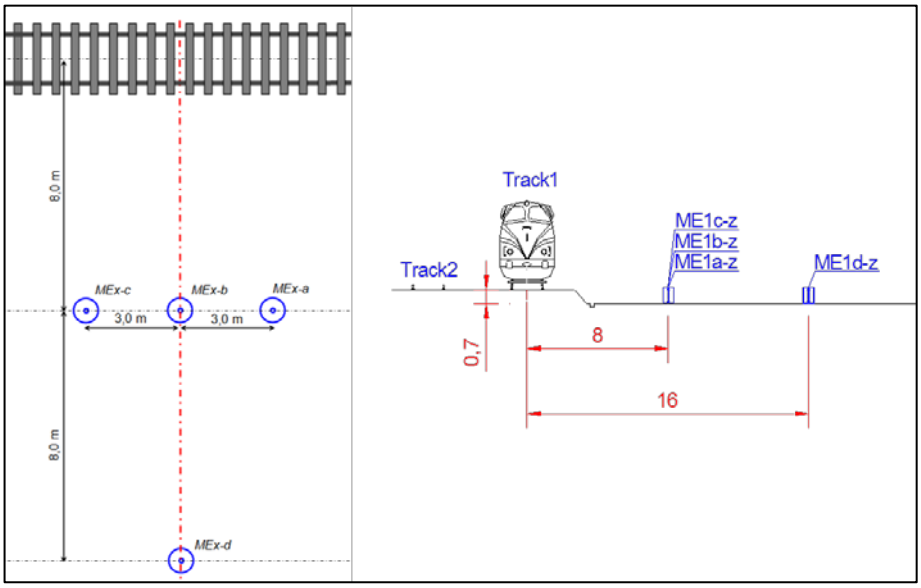

Figure 5-3: Layout and cross section of the principle sensor positions

5.1.2 Ground characterisation

To characterize the ground and soil properties at the site several tests and investigations were carried out by BAM at the sections of the site. The full description of tests with all results is documented in a separate report [15], also added as Annex B to this report here:

The aim of the tests was to determine the soil properties by seismic test methods. Therefore the wave propagation due to hammer impulses has been measured along a line of sensors perpendicular to the track. The response of the soil of each section has been analysed by different methods as described in RIVAS Deliverable D1.1 [16]:

- seismogram/time history method
- correlation function
- spectral analysis of surface waves (SASW method)
- spatial autocorrelation (SPAC) method
- wavenumber method.

In addition the attenuation curves were evaluated in order to get realistic damping values.

The sections are dominated by waves of a fast wave velocity at about 230 m/s. This stiff soil is overlaid by a softer top layer where the group wave velocity is between 130 and 200 m/s. Clear dispersion curves have been measured at section 1 and 2 and a strong decrease from 380 m/s to 130 m/s appears in the main frequency range of the measured waves. The others show less dispersion from 280 to 120 m/s at low frequencies. In these sections an additional phase velocity of v ~ 330 m/s can be observed which is assigned to the compression wave.

Frequency (Hz)	5	10	15	20	25	30	35	40
wave velocity (mm/s), SPAC method								
section 1		380	300	200	140	130		
section 2	380	325	270	180	130	130		
section 4	280	170	155	145	145	140		
section 5	280	220	170	165	160	150		
wave velocity (mm/s), SASW method								
section 1		350	280	200	160	140	140	140
section 2		350	280	180	140	130	130	130
section 4		180	140	140	130	130	130	130
section 5		200	200	180	150	150	150	150
Wave length method								
section 1	380	380	300	210	140	130	125	125
section 2	380	350	270	180	130	125	120	120
section 4	280	180	155	140	140	140	140	140
section 5	380	220	185	170	170	160	150	

Table 5-1: Comparison of the determined wave velocity of each frequency, sections and methods

The damping value D for the different sections varies between ~ 4 % (section 1), and ~ 6.5 % (section 2). The damping value in section 4 and 5 is D ~ 6.0 %. For the determining of the damping ratio a wave velocity of v = 230 m/s and a geometrical attenuation of q = 0.5 was used. The damping ratio of the softer layer on top of the soil would be lower than these values.

As a consequence of the stronger dispersion for sites 1 and 2, it must be expected that the amplitudes of ground vibration are reduced at frequencies below 20 Hz compared to the

ground vibration at site 4 and 5. The ground vibrations at higher frequencies should be comparable for all four sites due to the similar stiffness and damping values.

5.1.3 Validation of the preloading process

Due to the nonlinear material behaviour of under-sleeper pads, the measurement results strongly depend on the static contact pressure on the USP. Therefore the static preload on the under-sleeper pads has to correspond to the realistic static load under a train passage.

Due to the short time of track possession which can typically be obtained in an operating track, the transportation to the site and application of a preload on the track is a complicated issue. In RIVAS this problems was solved by two rail-/road excavators which serve as the necessary weight on the track. The following test setup was developed and approved:

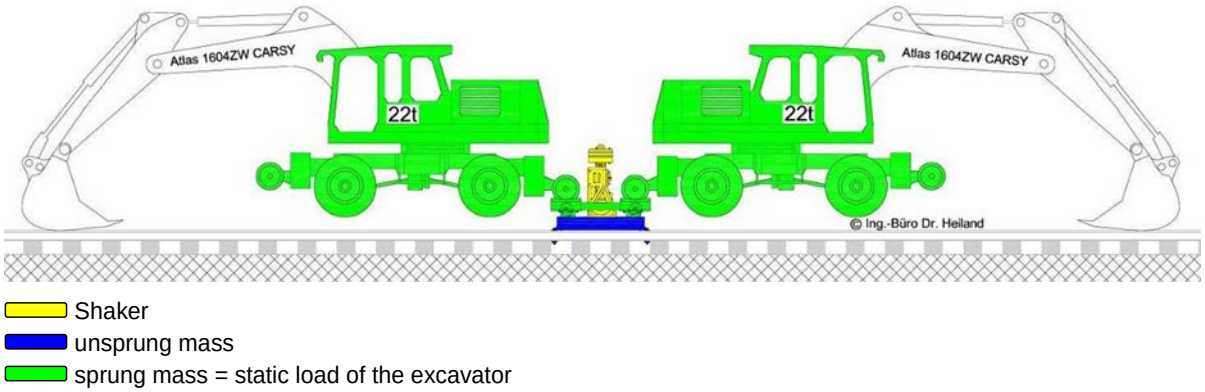

Figure 5-4: Overview of the whole test setup during the shaker tests

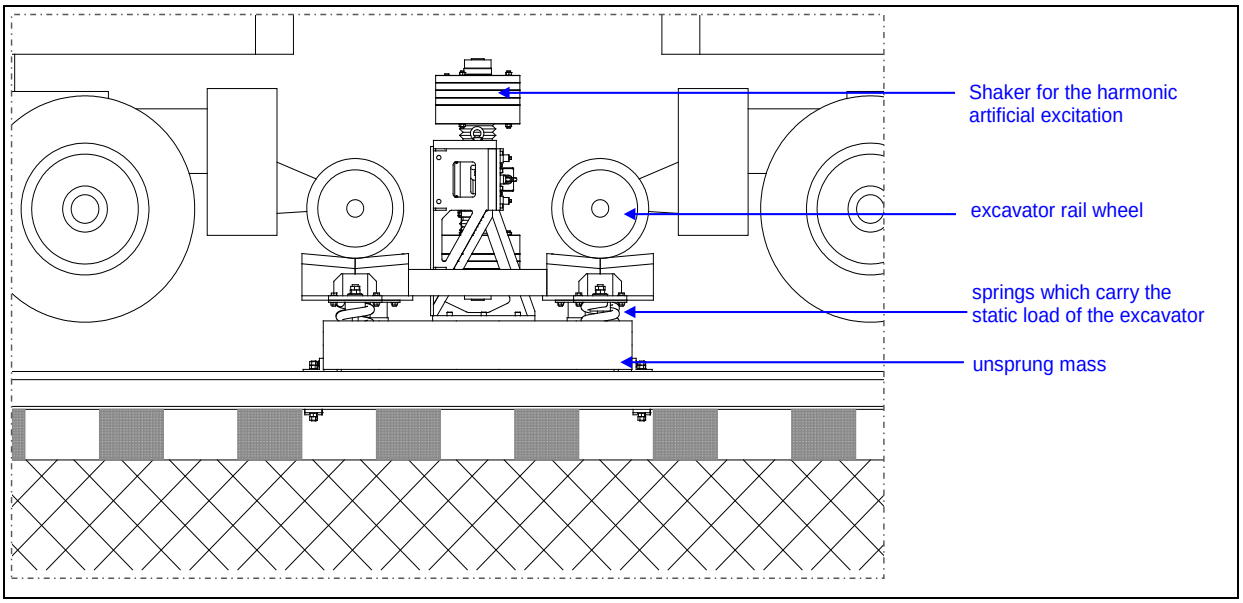

Figure 5-5: Shaker with unsprung and sprung mass

Each excavator is supported on the one side by the bucket, on the other side the excavator is supported by a steel frame which is itself supported by springs. The springs (with appropriate stiffness) are installed on the unsprung mass which is a steel plate directly coupled with the rails.

The static load depends on the position of the bucket: the force is lower for a bucket position closer to the machine body. The exact static load can be calculated from the spring deflection.

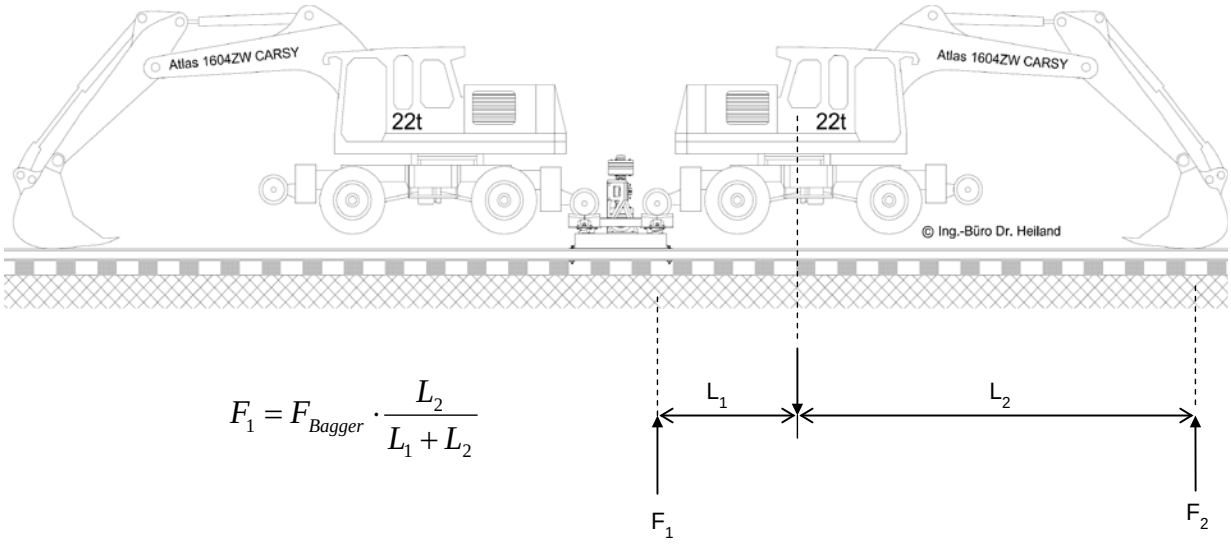

Figure 5-6: Possibility of varying the static load of the excavator

In Figure 5-6, the equation for the calculation can be found. Using an excavator of 22 t, the maximum load F1 is ~ 16 t, if the bucket is moved to the limit position. In this case, the eigenfrequency of sprung mass of the shaker is below 3 Hz.

Validation for the artificial source measurement

In order to check the realistic static pressure/load due to the excavators, the rail deflections due to train passages are calculated and compared to the rail deflection due to the suggested test setup with a exemplarily spring stiffness of 52 kN/mm per rail fastener.

In the first step, the static load (F1) is kept constant and the distance “d” of the support points of the unsprung mass (steel foundation) is investigated.

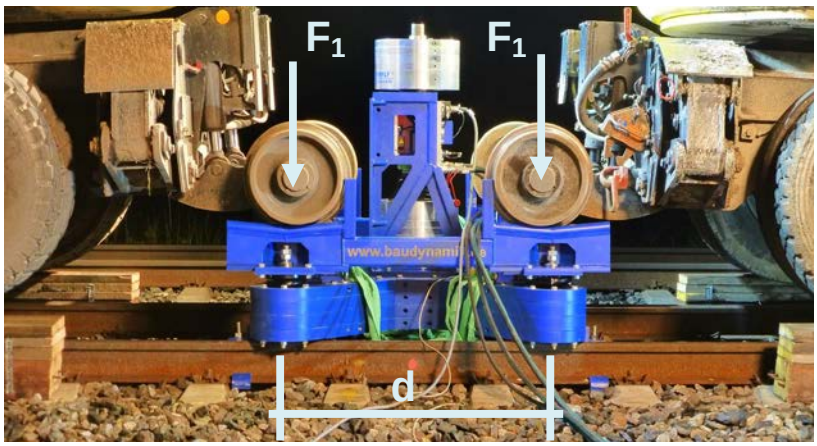

Figure 5-7: static loading F1 and distance d of the support points of the unsprung mass
(picture source: Ingenieuerbüro Dr. Heiland)

“d” varies from d= 110 cm to 150 cm. If d = 130 cm, then the rail deflection and therefore the averaged USP pressure respectively is more or less constant in the point of interest, see Figure 5-8.

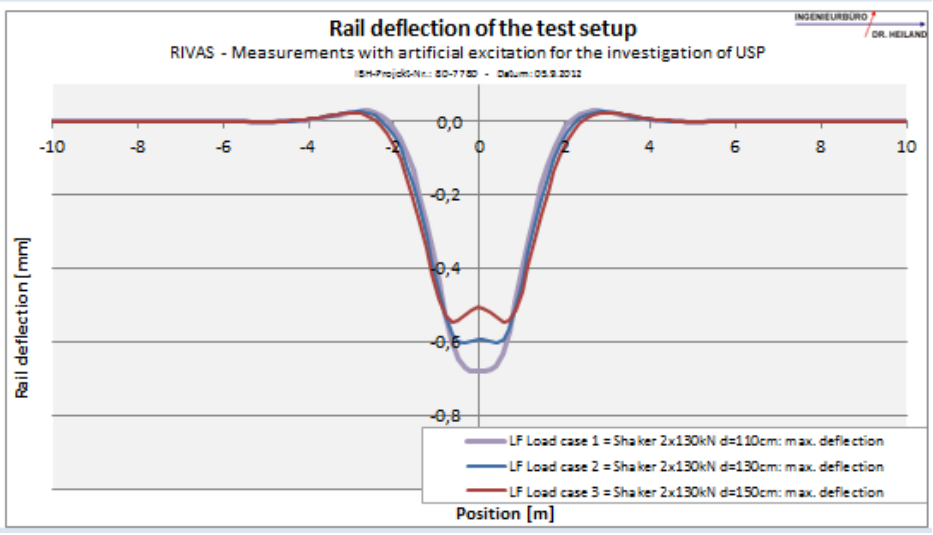

Figure 5-8: Rail deflection of the test setup - different distances d of the support points of the unsprung mass

In a second step, the rail support point interval "d" was kept constant and the static loading (2 x F1) varies between 2 x 100 kN, 2 x 120 kN and 2 x 140 kN. The calculation shows that the rail deflections of the test setup can cover the whole range of rail deflection due to ICE passing.

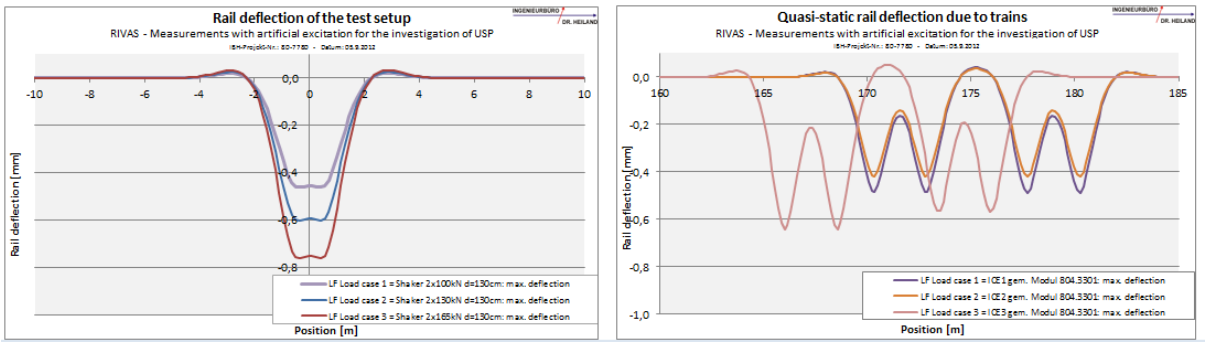

Figure 5-9: Rail deflection of the test setup in comparison to the static rail deflection of different ICE wagons

As already mentioned, F1 can achieve a value up to ~160 kN, if the bucket is moved to the closer limit. In this case the rail deflection of the test setup corresponds to the rail deflection of freight trains, see the next figure.

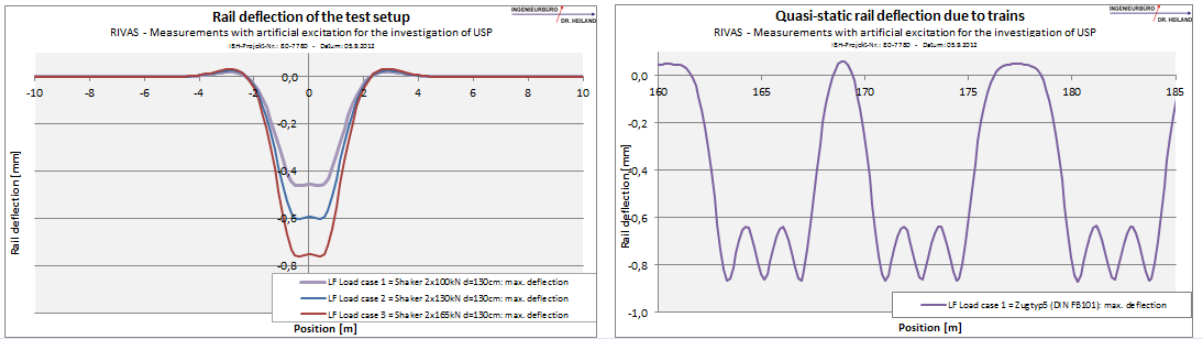

Figure 5-10: Rail deflection of the test setup in comparison to the static rail deflection of freight trains

Investigated load cases (LC)

To investigate the impact of different pre-loads all measurements were carried out with three different load cases (LC1 –LC3) in a range between 304 kN to 5 kN. These load-cases were achieved with different bucket-position as described before. Further details are given in Figure 5-11.

Load case or Position	**Bucket position**
LC1 ≈ 304 kN	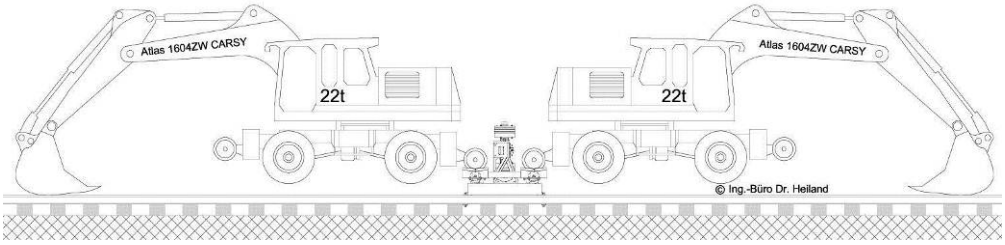
LC2 ≈ 221 kN	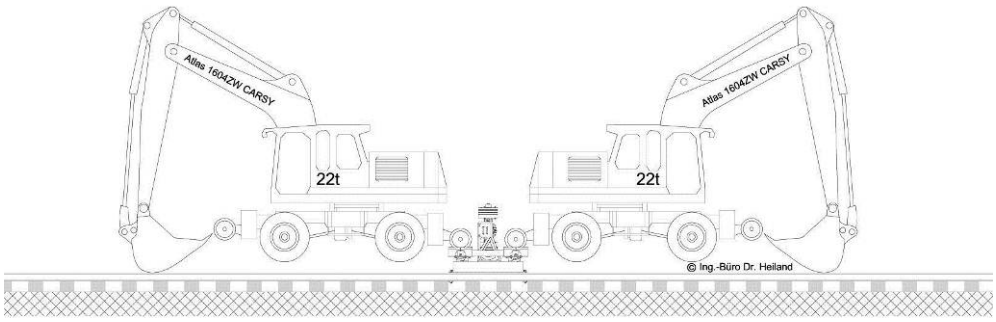
LC3 (without excavators) ≈ 5 kN	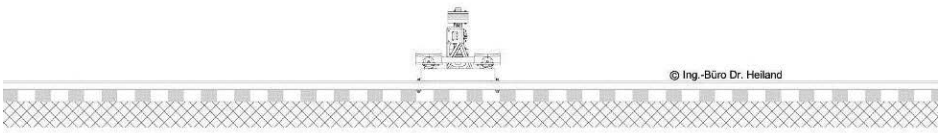

Figure 5-11: Determination of the three Load Cases (LC1-LC3) by three different bucket positions

Experiences and instructions for practical realisation on site

After extensive testing the following instructions and experiences for a future practical realisation on site can be given:

a) Before entering the track under train operating-conditions with limited track possession times, the practicability and feasibility have to be tested and the excavator operators have to be instructed and trained. The photos in Figure 5-12 present the main steps for the installation and assembling the vibration device and the preload on the track. They are taken at the campaign at the ER test-site, but the same procedure was used at the DB site near Regensburg.

b) The chosen excavators have to be approved for work in track under operating railway conditions. That means e.g. that the maximum of bucking lifting has to be limited to

avoid conflicts with the overhead-line-equipment. If trains at the opposite track are running during the investigation, the rotational movement of excavators have to be restricted in this case, that the minimum clearance outline of the opposite track is not hindered.

c) The electricity in overhead-line-equipment has to be switched of.

d) Depending on the local situation the possibilities of access to the track with the rail-road excavators has to be clarified and the running time from track access point to the site has to be calculated. Adjacent level-crossings are optimum points to serve for track access with rail-road excavators.

e) The vibration generator and the foundation device have to be prepared beside the track and preassembled as much as possible. All installation of measurement equipment has to be preinstalled and tested before.

f) For the practical realisation of tests with different frequency sweeps and the three load-cases a time shift of about 45 minutes per measurement site was sufficient. This includes the time of mounting the steel-foundation, assembling the vibration-generator in track, the vibration-sweeps and dismantling all equipment and clearing the track. Additional time is needed for the access of the excavators to the site, according to the distance of track-access point and site.

a) Positioning and fixing of the steel foundation frame on the track

b) Assembling of the shaker with the foundation frame

c) Positioning of the excavators as pre-load for the track

d) Final assembling of the shaker with foundation and the excavators resting as preload on the shaker device

Figure 5-12, a-d: Installation procedure of the foundation, the shaker and the excavators serving as dynamic uncoupled preload on the track with shaker device
(Photos Eiffage Rail, Stefan Schwieger)

5.1.4 Measurements during train passages

The principle layout of measurement points etc. were based on the RIVAS measurement protocol as described in [2] and on former investigation of the RENVIB project [17]. A detailed description of the measurements with full data annexes is given within the report [6] attached as Annex A1.

For the data evaluation, some modifications were made. This concerned mainly the following points:

- The train passages were evaluated by means of “fast”- weighted, max-hold 1/3 octave band spectra L_{vFmax} (f_{Tn}) according to DIN45672-2 [17] and VDI 3837 [19], the so-called “maximum third speed spectrum” was used.
- The graphs in the report used a different reference velocity ($v_0 = 1 \cdot 10^{-9}$ instead of $5 \cdot 10^{-8}$ [m/s])

It was assumed that the different evaluation procedures have not a significant influence but is much easier to carry out. Within a later stage of the project, the evaluation of measurements was re-assessed and the two evaluation procedures compared. This is shortly described in chapter 6 of this deliverable, respectively more exhaustive in the report [7] as given as annex A2 to this RIVAS deliverable.

Figure 5-13 gives an overview on the vibration-velocity spectra measured during train passage in a distance of 8 m from the track centre depending on the different train categories. The velocity spectra are shown to obtain an impression on the variation (statistical spread). Extreme values due to glitches, failures or train overlapping were not considered resulting in 21 regional electric railcars, 6 ICE and 33 freight trains which were finally taken into account for further analysis.

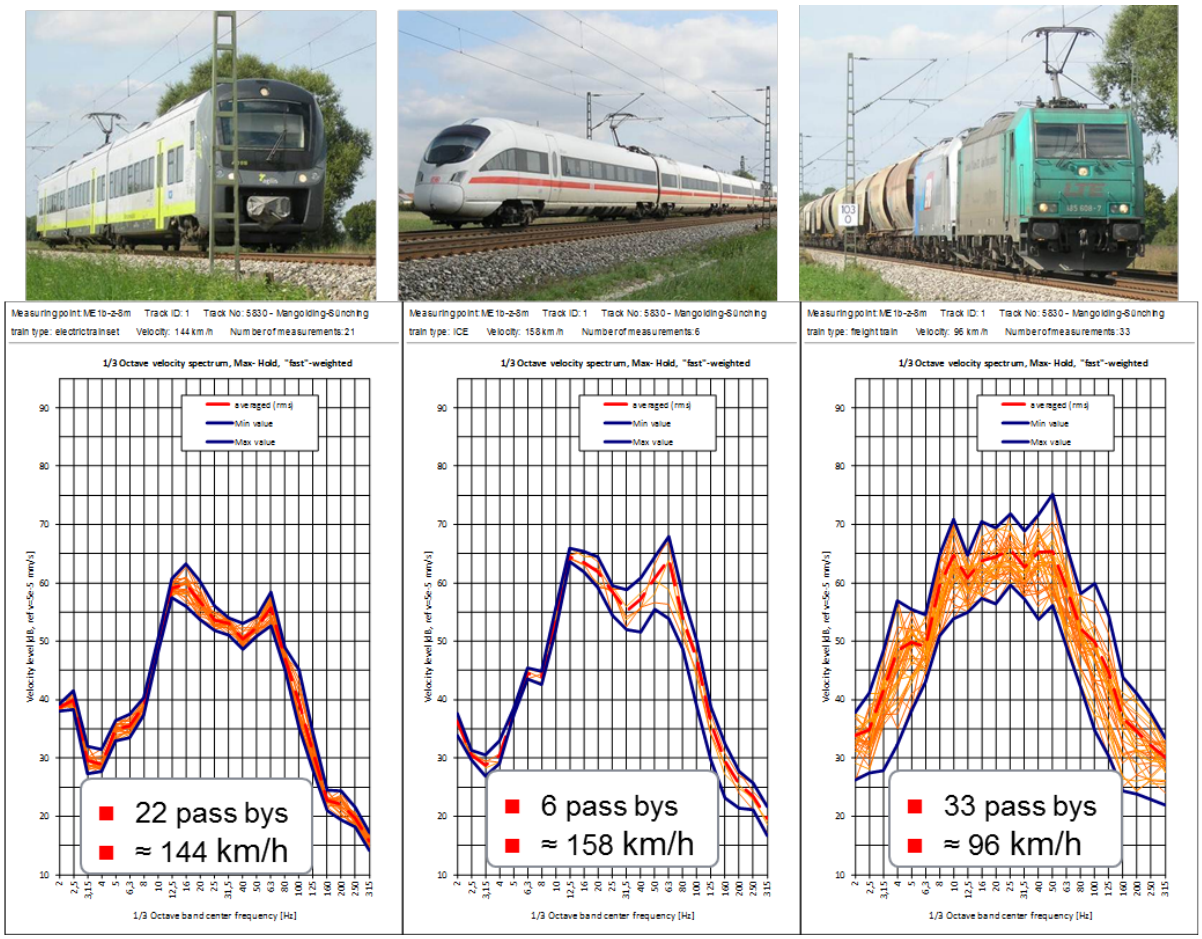

Figure 5-13: Statistical variation of vibration velocity spectra measured for the train categories (from left to right) regional rail car, ICE and freight trains at the reference measurements site ME1 for the 8 m measuring point

The figure shows that both spectra of ICE and of the electric railcars have only small deviations considering the different train passages. As expected, the spectra of freight trains result in larger deviations.

Figure 5-14 shows the spectra characteristics of the three different train types. In general, freight trains induce the highest vibration velocity level. In some specific frequency ranges, the averaged spectrum of the ICE trains has some peaks and they even exceed the averaged vibration level of the freight trains, for example at 12,5 Hz and 63 Hz. The peaks are caused by specific excitation frequencies; the peak at 63 Hz is based on the sleeper distance, the peak at 12,5 Hz – 16 Hz is based on the distance between the bogie twin axle and the out-of-roundness of the wheels respectively. All of the mentioned excitation frequencies depend on the train speed. For higher train speed, the excitation shifts to higher frequencies.

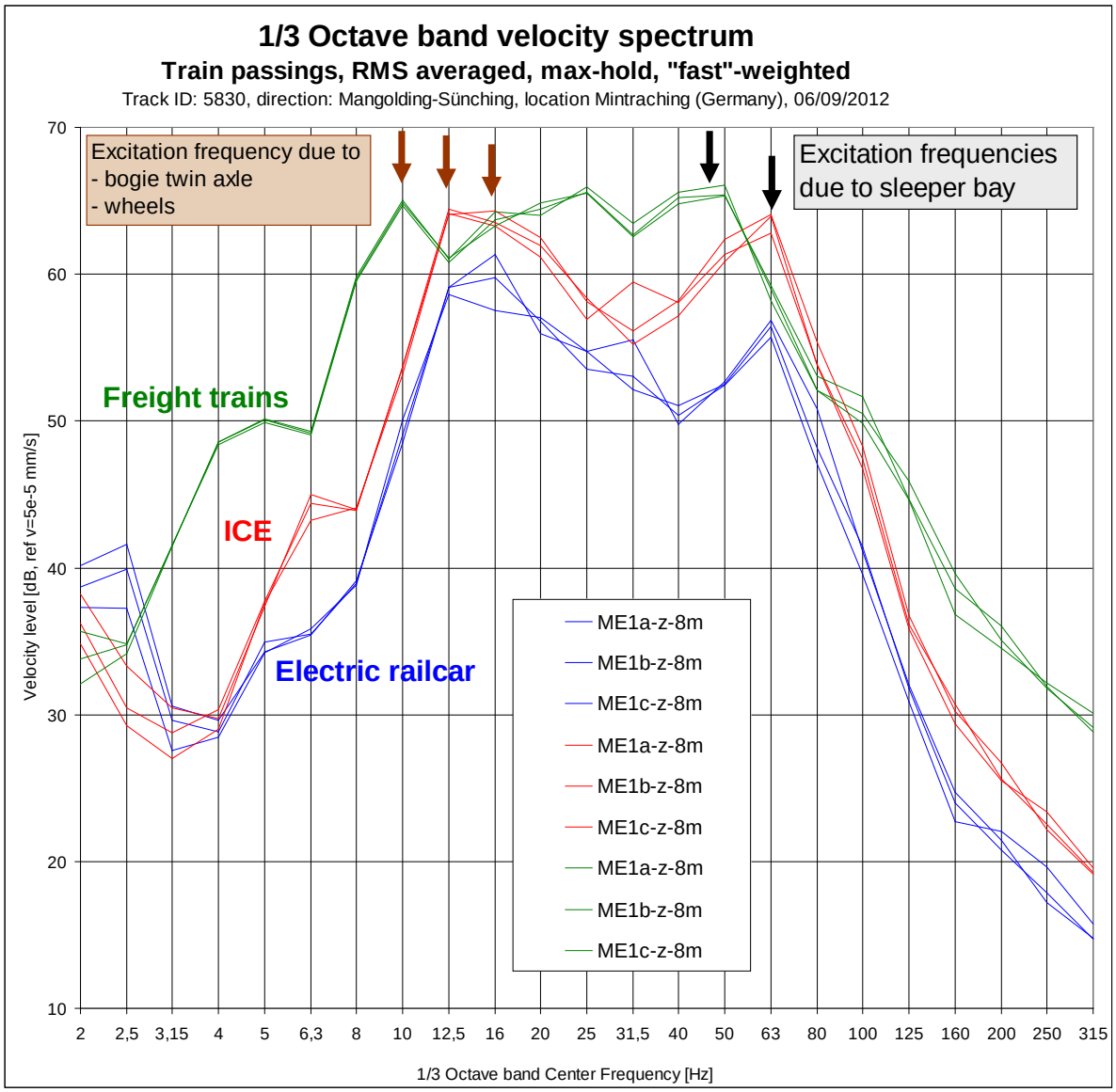

Figure 5-14: Averaged vibration velocity spectra for the three different train categories at the reference section ME1 at the 8m measuring point

5.1.5 Correction of different soil conditions

For determining the IL, the left/right procedure as described in chapter 4.1 had to be used because the measurements were performed at an existing test site. Therefore it was necessary to control whether the different investigated track sections have different subsoil or transmission conditions or not. Therefore, the transfer mobility functions from ballast to the measuring points at each section were determined. These were carried out by two different procedures as further described within the next paragraphs:

- Direct correction by transfer mobility function with impact load as falling mass
- Indirect soil correction based on trains running in the opposite track without mitigation measures

Although the surrounding conditions of test sections looked comparable (Figure 5-15) and fulfil the requirements given in [2], the results show that there are differences to be included

in a correction term. The transfer functions for the subsoil differ up to 13 dB between the single measuring sections. Therefore the results have to be corrected by a capable correction term.

Figure 5-15: View on the test sections pretending ideal measurement conditions
(picture: Ingenieurbüro Dr. Heiland)

Direct correction by determing of transfer mobility function with impact load as falling mass (Method I)

To compare the ground and transfer characteristics between the different sections the transfer mobility function from the ballast to the measuring points is determined by means of impact tests, using an hydraulic operated drop weight in combination with a load cell (here DYNPACT®, Figure 5-16). Ca. 15 impacts were performed at each excitation location. Figure 5-17 presents a representative time history of a single impact and the corresponding vibration response at 8 m and 16 m.

Figure 5-16: Application of the drop weight DYNPACT® in the track (reference example),
(picture: Deutsche Bahn AG, Rüdiger Garburg)

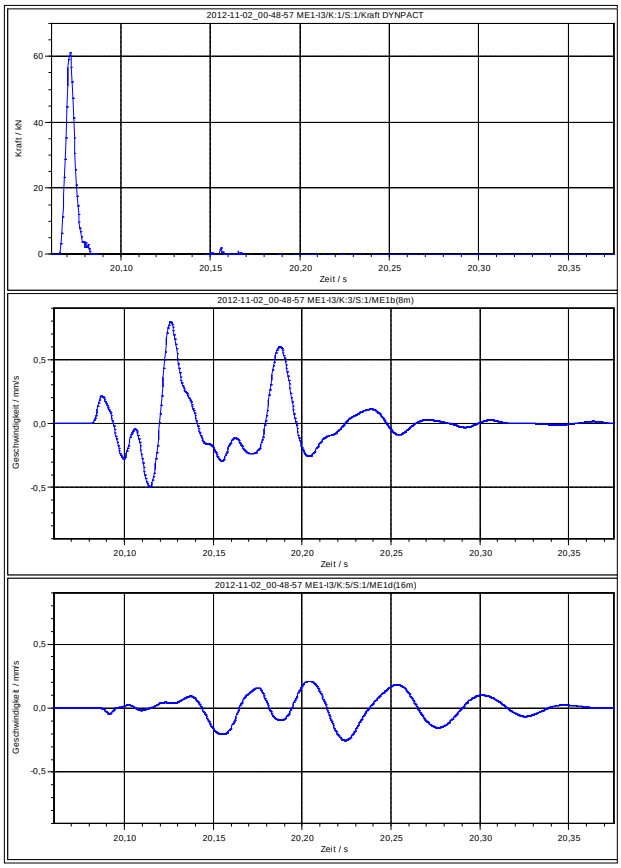

Figure 5-17: Time history of impact force and vibration response at 8 m and 16 m measuring points

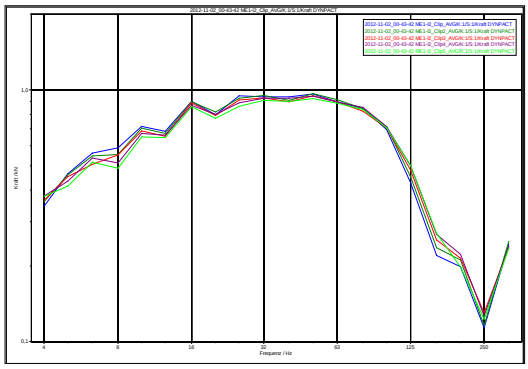

Figure 5-18: Force spectrum of five impacts

Figure 5-18 shows the force spectrum of five impacts exemplarily. It demonstrates that the variation of the induced impact was very low. Nevertheless, the transfer function was evaluated separately for each single impact. (Further details are given in [6], respectively ANNNEX A1)

The averaged transfer function of all impacts was evaluated as follows:

$$\left|\overline{TF}\right| = \sqrt{\overline{\mathrm{Re}}^2 + \overline{\mathrm{Im}}^2};\quad \overline{\Phi} = \arctan\frac{\overline{\mathrm{Im}}}{\overline{\mathrm{Re}}}$$

$$\overline{\mathrm{Re}} = \frac{\frac{1}{N}\sum_{i=1}^{N}\mathrm{Re}\left\{S_A(f)*S_E(f)^*\right\}}{\frac{1}{N}\sum_{i=1}^{N}S_E(f)*S_E(f)^*}$$

$$\overline{\mathrm{Im}} = \frac{\frac{1}{N}\sum_{i=1}^{N}\mathrm{Im}\left\{S_A(f)*S_E(f)^*\right\}}{\frac{1}{N}\sum_{i=1}^{N}S_E(f)*S_E(f)^*}$$

The next evaluation steps are listed below:

- The narrow band transfer spectrum (Δf = 0,6252 Hz) was transferred into an equivalent 1/3-octave band transfer function.
- The five 1/3-octave spectra from to the five different impact locations were arithmetically averaged.

Exemplarily, the resulting transfer mobility function of ME3 is shown in Figure 5-19.

As expected, the results at the 16 m measuring point shows lower transfer mobility than those at the 8 m measuring points due to the higher distance to the excitation point (Figure 5-19).

At the three 8 m measuring points, the same transfer mobility was observed up to 125 Hz. There was also a drop at 25 Hz of all three 8m point which is correlated to a glitch from poor coherence. The drop was adjusted for the further analysis of data.

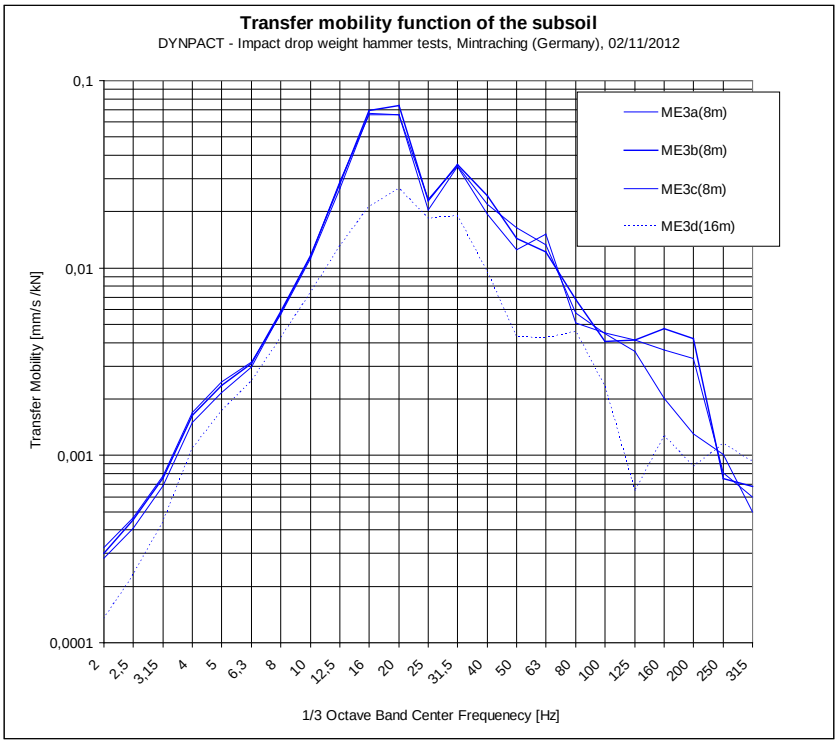

Figure 5-19: Transfer mobility function of the soil / subground for one of the test sections

The soil transfer mobility functions of all three measuring sections are shown Figure 5-20 and Figure 5-21.

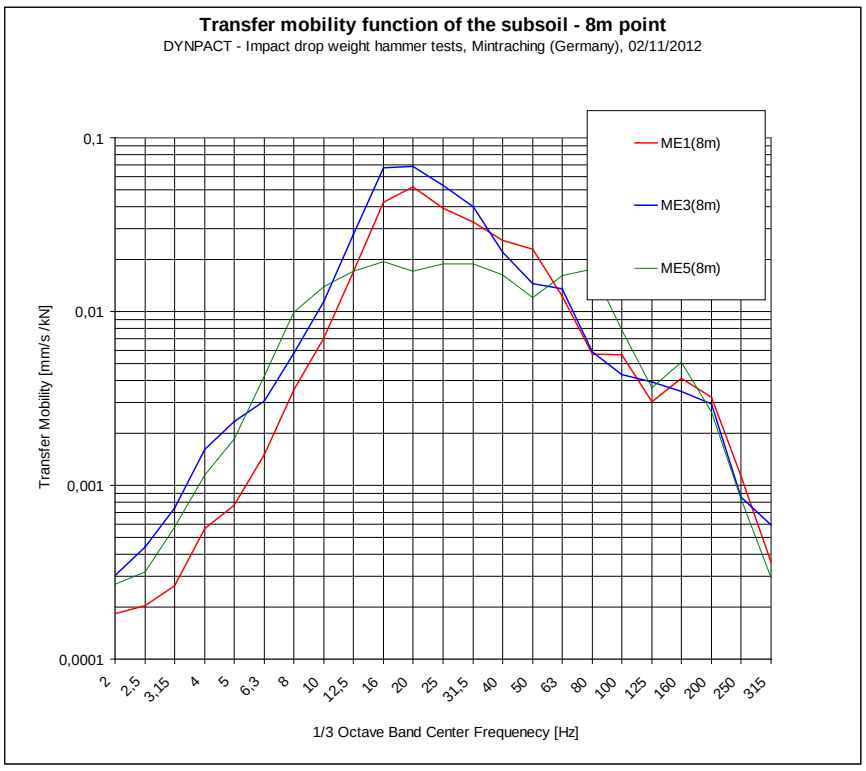

Figure 5-20: Averaged transfer mobility functions of the soil / subground for the 8 m measuring points

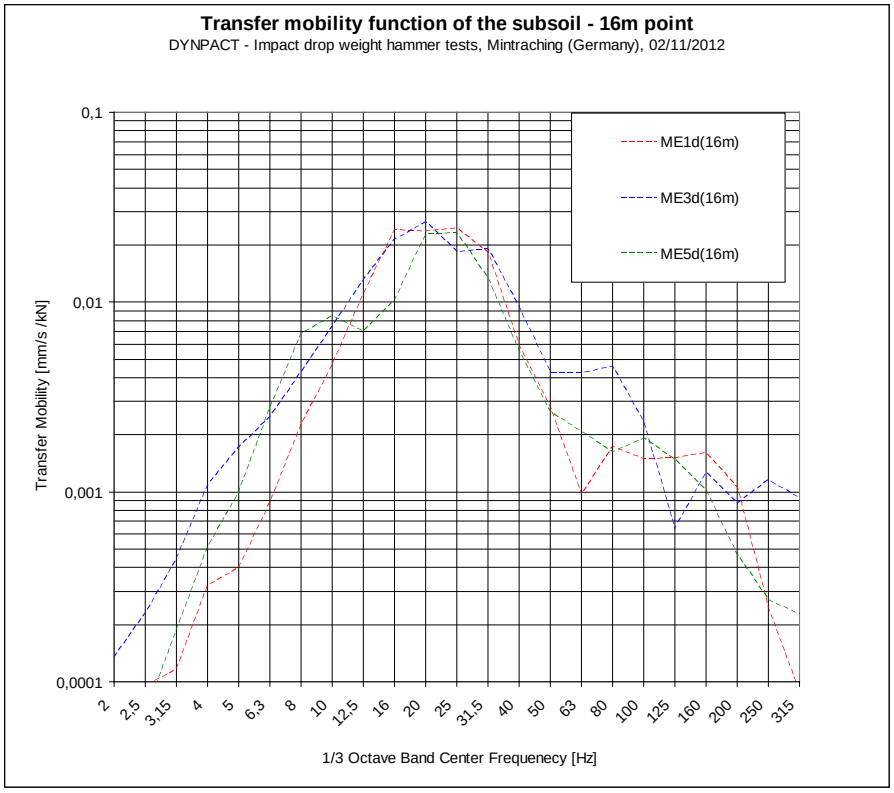

Figure 5-21: Transfer mobility functions of the subsoil for the 16m measuring points

In addition, the transfer mobilities of ME3 and ME5 were related to the reference section ME1 in the following diagram, Figure 5-22. These curves can be used as correction curves.

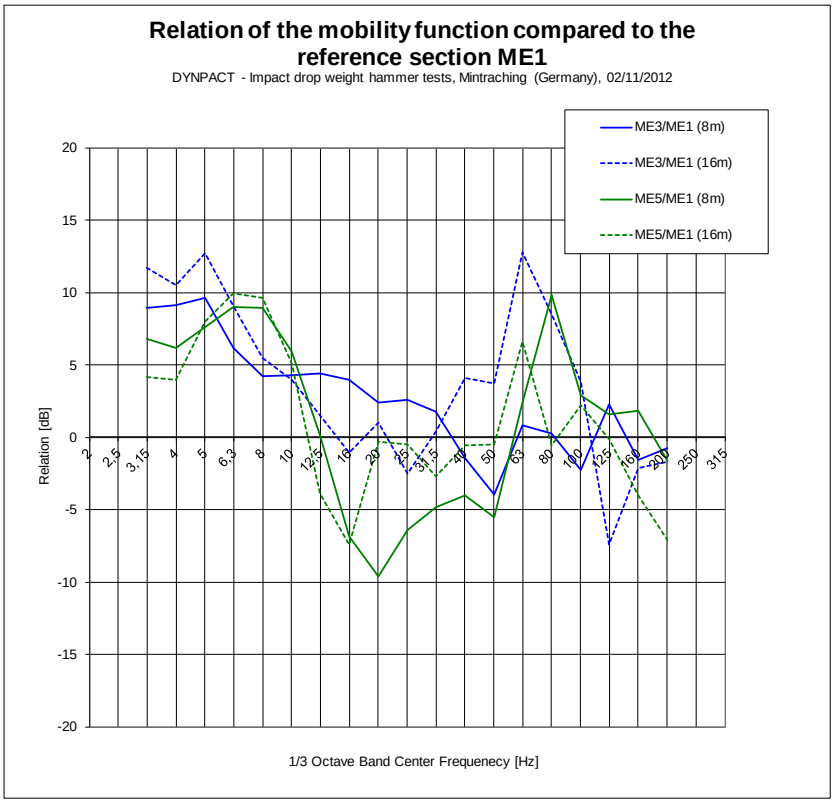

Figure 5-22: Relation of soil mobility's - ME3/M1 and M5/ME1

Indirect soil correction by trains passing in the opposite track without mitigation measures (Method II)

At this specific site only one track was equipped with different mitigation measures. The opposite track was homogenous over the whole length consisting of a track configuration with standard rail pads and standard sleepers without under-sleeper pads. It was assumed that on the whole track also the sub-ballast layer was prepared in a homogenous way as well is identical for both tracks. Under these assumptions, results measured on the opposite track could be used for the correction.

The main difference between these two methods is that method I use a point source and method II refers more to al line source excitation.

Comparison of insertion loss spectra corrected by the two different methods

In Figure 5-23 the insertion loss of electric railcars was evaluated according to subsoil correction method I and II. The red lines show the insertion loss at ME3, the blue lines show the results of ME5.

Results at the 8m measuring points are considered to be more reliable because the measuring spikes (where the sensors were installed on) were not removed during the train passage measurements and the impact measurements. The measuring spikes of the 16m measuring points had to be removed because of agricultural area in use.

In conclusion, it should be mentioned that the real insertion loss spectra should be between the two corrected curves because both methods represents an approximation.

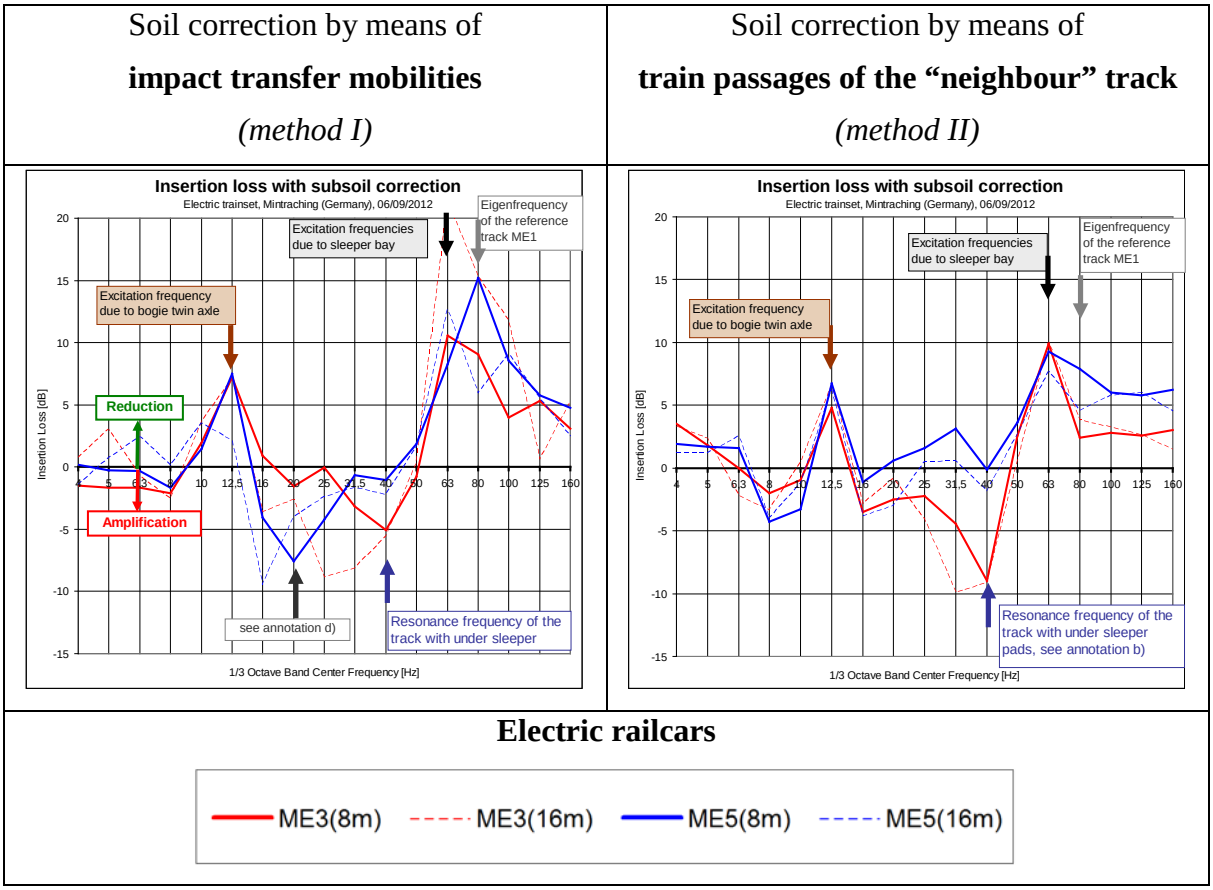

Figure 5-23: Insertion loss of electric railcar passages considering subsoil correction

From Figure 5-23, the following conclusions were drawn for the electrical railcars with an average speed of 144 km/h:

a) The insertion loss shows not only a maximum at the eigenfrequency of the reference track system at 80Hz but also at the sleeper-passing frequency at 63Hz.

b) The minimum at 40Hz corresponds to an amplification of the vibration. This peak corresponds to the peak already detected by artificial excitation. It is caused by the resonance frequency of the track system with the resilient under-sleeper pads.

c) In the lower frequency range, there is a maximum at 12,5 Hz where the vibration are reduced compared to the reference track. As explained in the previous chapter, this reduction of vibration is not caused by a dynamic spring-mass effect but it results from the fact that the under-sleeper pads homogenize the underground stiffness. Therefore, the excitation forces of the passing trains due to the bogie twin axle are reduced (soil-rail interaction).

d) The main difference in the insertion loss caused by the different correction methods (left and right side of Figure 5-23) occurs in the frequency range 20 - 25Hz for the measuring section ME5. The reason is that especially at ME5, the point source transfer mobilities leads to other results than line source transfer mobilities for this special frequency range. For the frequency range of 20-25Hz, the results of method II (right side) should be considered.

Finally, it was decided to use the insertion loss obtained by the soil correction method I (impact load). The comparison shows that the results of the railcar passages correspond quantita-

tively good to the artificial excitation results using bucket position 2 as described within the next chapter.

5.1.6 Measurement with artificial excitation

To determine the IL by the artificial excitation with the shaker the track in sections ME1, ME3 and ME5 was excited. The measured vibration velocity spectra for ME 3 and ME 5 were corrected by the subsoil correction with the transfer-mobility functions determined by the impact load as described in chapter 4.3 according Method I. The IL spectra for ME 3 and ME 5 were determined referring to the section ME 1.

- Figure 5-24 shows the resulting insertion loss with subsoil correction at 8 m measuring points.
- Figure 5-25 shows the insertion loss at 16 m measuring points.

The red lines show the insertion loss at ME3, the blue lines show the results of ME5.

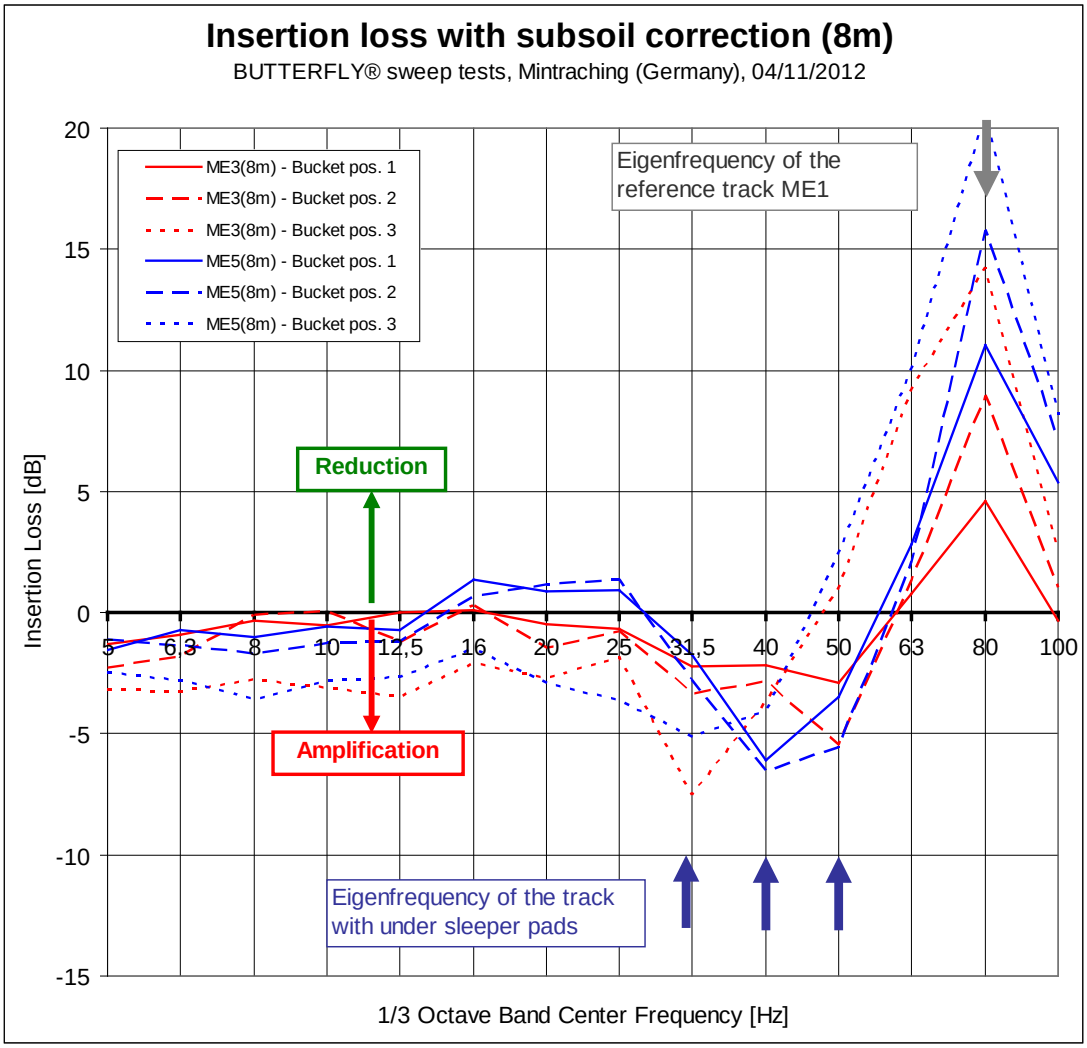

Figure 5-24: Insertion loss with subsoil correction, 8 m measuring points

As expected, the insertion loss shows the highest values in the eigenfrequency of the reference track system at 80 Hz. The lowest values are achieved at the frequency range of 31,5 –

50 Hz. This range corresponds to the eigenfrequencies of the track system with the resilient under-sleeper pads.

As already shown, the eigenfrequency of the track with under sleeper pads depends significantly on the static load of the excavator (...the lower the static load is, the lower is the eigenfrequency…), but the eigenfrequencies of the tracks with different under-sleeper pads at ME3 and ME5 were almost the same. That means that the "position" on the x-axis of the resonance frequency is more or less the same.

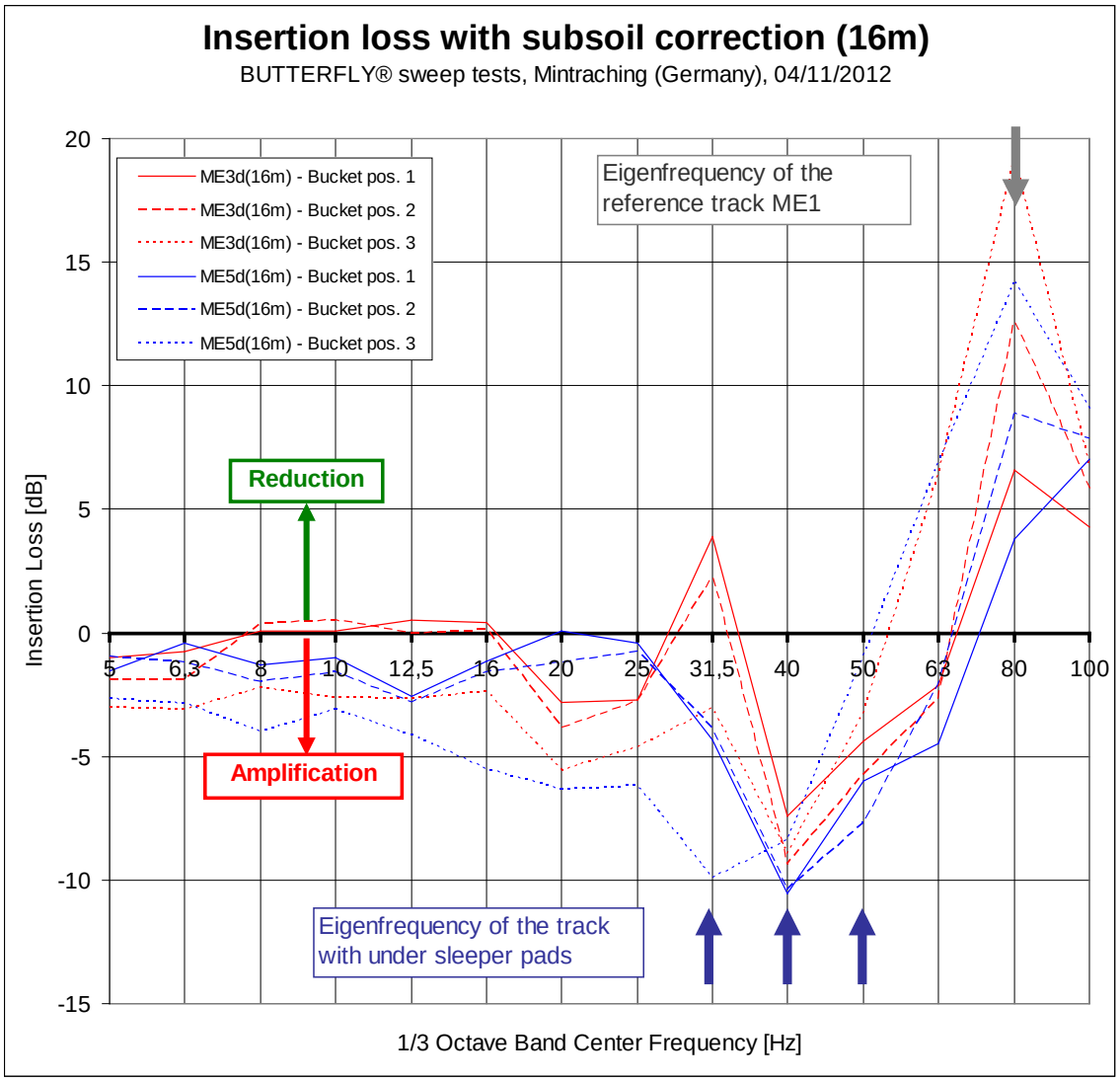

Figure 5-25: Insertion loss with subsoil correction, 16m measuring points

5.1.7 Comparison of IL by train passages and by artificial excitation

In Figure 5-26 the insertion loss by determination with the shaker excitation is compared to the determination by train passsages for the different train categories. For each the IL is corrected by the subsoil correction function with the transfer mobility of the impact load (falling mass) as described as method I in chapter 5.1.5.

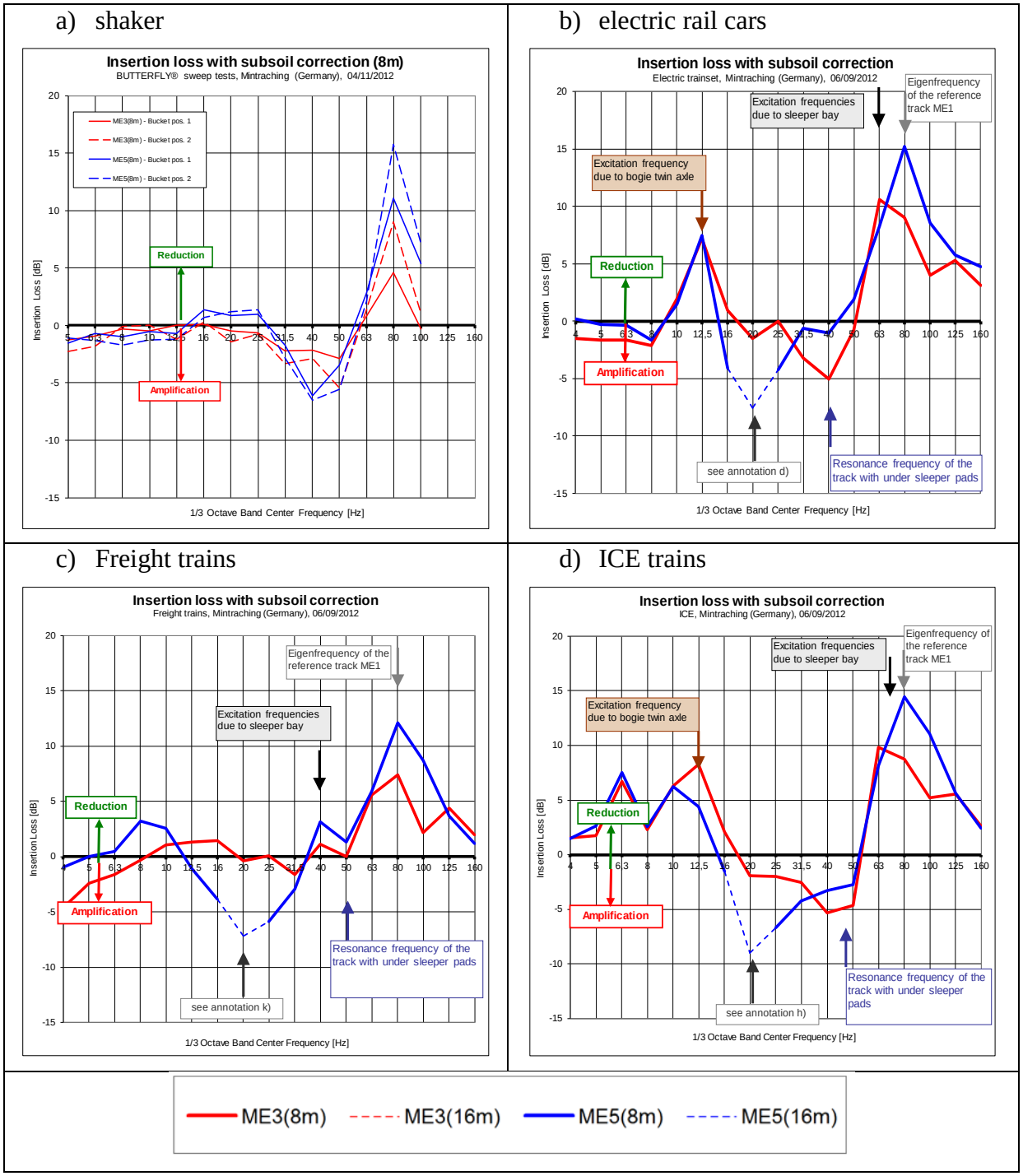

Figure 5-26: Comparison of IL by a) shaker excitation (LC1 with solid lines and LC2 with dashed lines) compared to b) electric rail cars, c) freight trains and d) ICE trains, each train passage by subsoil corrections of the impact transfer mobilities, the red lines show ME3 (USP type G03) and the blue lines ME5 (USP type G04)

5.1.8 Summary and discussion of results

The main results can be summarized as follow:

a) The developed test procedure with the artificial, force-controlled vibration excitation (including the unsprung mass and the sprung mass by means of two excavators)

turned out to be capable for the investigation of the dynamic spring-mass effect of resilient elements in track. The practicability of the used vibration exciter in particular within the track with short track possessing time was successfully approved.

b) To simulate the dead load (sprung and un-sprung masses) is an essential requirement to obtain realistic results. The tests show that the existence of the sprung mass (static load) is very important. No sprung mass (LC 3) leads to significant different result.

c) Bucket position 1 (LC 1) should be used for freight trains, bucket position 2 more for electrical railcars and ICE trains. For determination of the insertion loss, the left/right method for the investigation of the insertion loss is sensitive to the different subsoil conditions. A soil correction of the different sections (e.g. with transfer mobility functions) is essential to get reliable results.

Since the transfer mobility depends on the vibration source (point or line source), it is recommended to measure both, the point source and the line source transfer mobility, see annotation **d)**, chapter 5.1.5

d) The determination of IL by train passing's show that the determined IL is not definitely but depending significant on the different train categories.

Concerning the **passenger trains** (ICE and electric railcars), the insertion loss

- has a maximum (i.e. vibration reduction) at 12,5 Hz (speed-dependent because of the excitation frequency arising from the passage of the bogie twin axle)
- is positive for frequencies $\geq$ 63 Hz due to the dynamic spring-mass effect is negative (i.e. vibration amplification) in the resonance frequency range of 20 - 40 Hz.
- corresponds quantitatively to the results due to artificial excitation using bucket position 2.

Concerning the **freight train** passages:

- The insertion loss shows a positive effect (i.e. vibration reduction of) in the frequency range > 63 Hz, it does not show reliably the resonance effect of the under-sleeper pads (negative insertion loss).

e) The test with artificial excitation is capable to show the dynamic characteristics of a track. The results for the IL by the shaker excitation shows a good agreement with the expected results compared to calculation methods based on dynamic models with mass-spring-systems or impedance models [20]. The results of IL by train passages show particular for the lower frequency range some additional positive mitigation effects which are not possible to explain with these simplified models. This phenomenon was recognized before in several other investigations as described in [21], [22] and further publications.

f) This clearly shows that the USP have some additional positive side-effects on vibration mitigation which cannot be described with simple models as well as with the stationary harmonic artificial excitation. This mitigation effects based on mechanical behaviour e.g. due to embedding the ballast stones in resilient material with an increase of contact area together with an decrease of contact forces between ballast and sleeper [23], the better load-distribution in longitudinal direction as well as the general better track quality (e.g. avoiding of hanging sleepers) cannot be detected by stationary exci-

tation. This gives also an explanation that the mitigation effect of USP is often underestimated then using dynamic prediction models.

g) The determination of the insertion loss results compared by artificial excitation and by train passing's shows that the insertion loss is composed of two effects:

- On the one hand, the insertion loss results from the dynamic spring-mass effect. This "component" of the insertion loss can be verified by means of the artificial excitation.
- On the other hand, the soil-track interaction influences the insertion loss: The system train/track generates different dynamic forces depending on the subground, because the reference section (without under-sleeper pads) has local changes in the stiffness, whereas the under-sleeper pads homogenize the rail stiffness. That is why the moved train causes higher vibrations at the reference section than at the softer track with under-sleeper pads, especially in single excitation frequencies. This fact results in a positive effect in terms of vibration mitigation.

5.2 FIELD TEST AT THE NEW EIFFAGE TEST SITE (FULL-SCALE TEST-RIG)

To determine the insertion loss spectra of different sleeper prototype configurations , an existing track on the premises of Eiffage Rail GmbH (ER) was extended in such a way that:

- the test track was long enough to install the different systems,
- the machines such as tamping machine and road/rail excavator could be used in this test track.

Finally, a straight test track with a length of 55.25 m was constructed with certain extensions at both ends. For this purpose, masses of soil were excavated and moved. The excavation work was executed very carefully to prevent bulk blasting of the excavation bottom, which was built up of mining excavation material and consolidated for over 60 years.

These works was carried out within RIVAS WP 3.2 and is described in detail in measurement report [8] and RIVAS Deliverable D3.15. For an improved slab-track system investigated within WP 3.4, tests are described in RIVAS deliverables D3.14.

5.2.1 Description of the test site

To avoid measurement uncertainties due to different subsoil and transmission conditions the before/after procedure for determining the IL was used. In a first step, a standard reference track with B 70 sleepers was built on the whole test rig for reference and basic measurements (Figure 5-27).

In a second step, the reference track was replaced by the **test track**. For this purpose the reference track (phase 1) was removed to the top of bottom ballast and replaced by different configurations of sleepers and under-sleeper-pads.

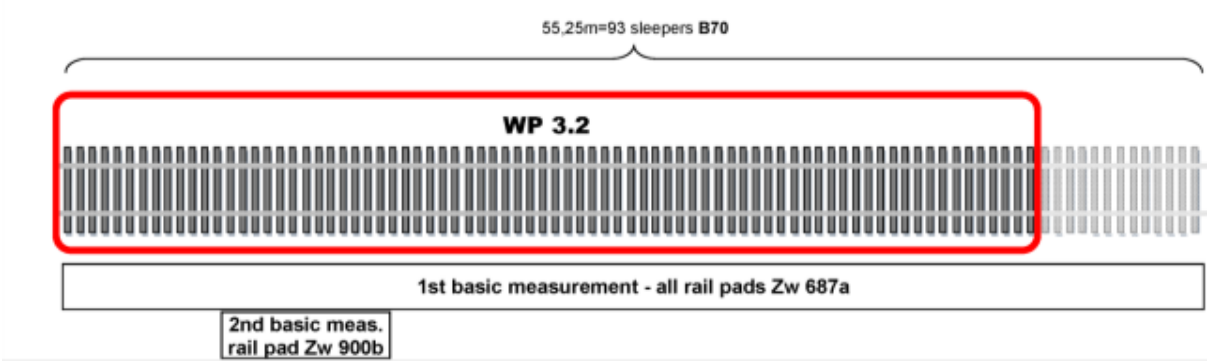

Figure 5-27 Phase 1 configuration of the basic reference track

The construction of the test track was divided into two track sections. **Track section 1** consists of 6 x 7.80 m = 46.80 m long ballasted track section. . In each of the 7.8 m long parts of the ballasted track section, 13 prototype sleepers of the same configuration were installed with a distance of 60 cm between two sleepers. **Track section 2** consists of a 8.45 m long slab-track track BBS 3.1 V2 GETRAC system track with an asphalt bearing layer (Figure 5-28 and Table 5-3).

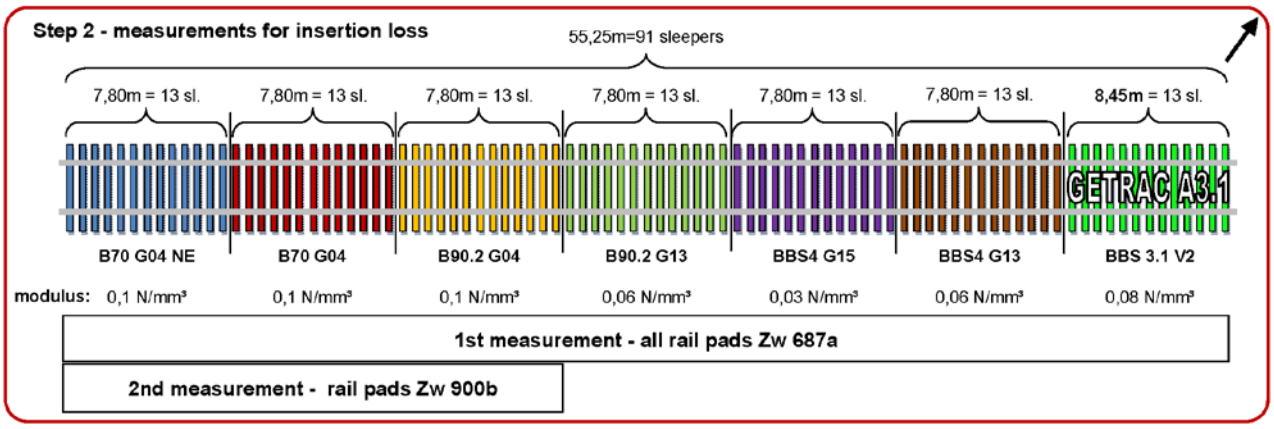

Figure 5-28: Overview of the test track sections with different USP systems, phase II (2013)

The configuration of the track sections is as follows:

- B70 G04 NE Standard sleeper without concrete edge stripes
- B70 G04 Standard sleeper (with concrete edge stripes)
- B90.2 G04 Heavy sleeper (with concrete edge stripes)
- B90.2 G13 Heavy sleeper (with concrete edge stripes)
- BBS4 G15 Wide sleeper (with concrete edge stripes)
- BBS4 G13 Wide sleeper (with concrete edge stripes)

A detailed description of different parameters is given in Table 5-2. The RIVAS deliverables D3.7 [26] gives a detailed description of the determination of the static and dynamic material characteristics.

Measuring section ID	**Short name**	**Sleeper**		**Under sleeper pad (USP)**					**Rail pad**
		Type	weight *incl. USP & fastener*	type	Supply name	Nominal static modulus	Total area	Concrete edge?	
			[kg]			[N/mm³]	[cm²]		
ME11	BBS3.1 V2	BBS 3.1	577	V-02	-	0,08	10,080	With concrete edge	Zw 687a
ME12	BBS4 G13	BBS 4	577	G-13	SLN 0613	0,06	11,820		
ME13	BBS4 G15	BBS 4	577	G-15	SLN 0315	0,03	11,820		
ME14	B90.2 G13	B 90.2	605	G-13	SLN 0613	0,06	7,122		
ME15	B90.2 G04	B 90.2	605	G-04	SLN 1010	0,10	7,122		
ME16	B70 G04	B 70	309	G-04	SLN 1010	0,10	5,900		
ME17	B70 G04 NE	B 70	309	G-04	SLN 1010	0,10	6,391	Without	
ME15	B90.2 G04 Zw900b	B 90.2	605	G-04	SLN 1010	0,10	7,122	With concrete edge	Zw 900b
ME16	B70 G04 Zw900b	B 70	309	G-04	SLN 1010	0,10	5,900		
ME17	B70 G04 NE Zw900b	B 70	309	G-04	SLN 1010	0,10	6,391	Without	

Table 5-3: Section ID and description of the investigated track configurations with sleeper type and under sleeper pads

The vibration measurements were repeated in the same way as in the Phase 1.

Figure 5-29: View on the test site at ER with the different track configurations
(photo Eiffage Rail GmbH)

5.2.2 Ground characterization

Ground characterization for the ER-test-site in Herne was carried out in the same way and according to the procedures as described for the “Regensburg-site” in chapter 5.1.2. The results can be summarised as follows:

The wave velocities were measured with v_R= 240 m/s for the Rayleigh wave and v_P= 650 m/s for the compressional wave. The dispersion curves show a dispersion (v= 350 m/s to 240 m/s) at low frequencies (f=5 to 20 Hz). At frequencies above 20 Hz, no dispersion was observed. A soil top layer of a thickness of about 8 m was determined.

The damping value was determined to be D= 8.5 %.

The attenuation of the amplitudes with distance due to hammer impacts shows a strong power-law attenuation of $v \sim r^{-q}$ with an exponent q of about 2.3 for the maximum values and 1.9 for the RMS values.

5.2.3 Evaluation procedure

The general evaluation procedure for the vibration measurements followed the same procedure as described for the test site near Regensburg. The same shaker and the same further equipment were used. The layout of measurement positions is presented in Figure 5-30. An additional measurement point was used on top of the foundation which allows to determine the input mobility at the unsprung mass directly (Figure 5-31).

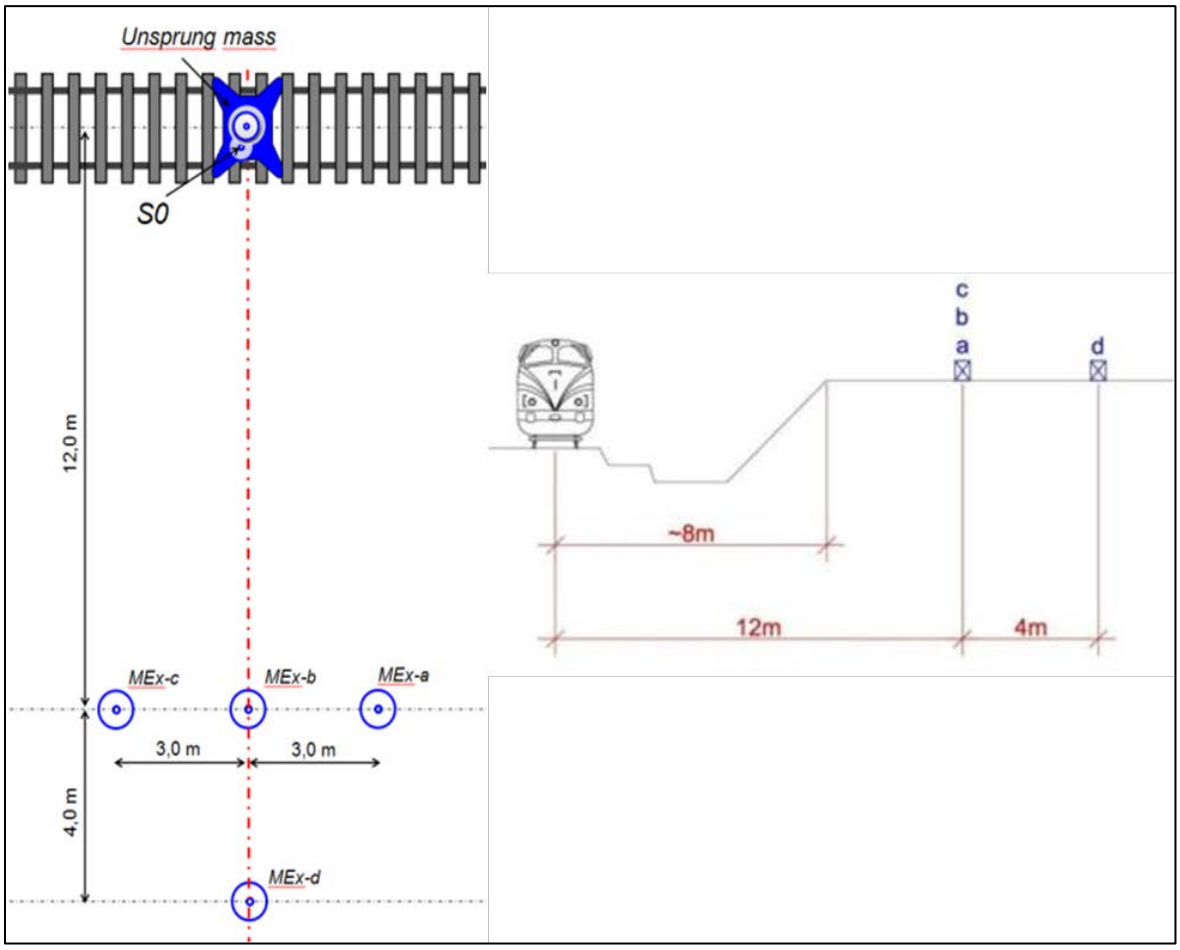

Figure 5-30 Measurement layout at ER test-site

- one measuring point on the unsprung mass (steel foundation of the hydraulic shaker, coupled with the rails)

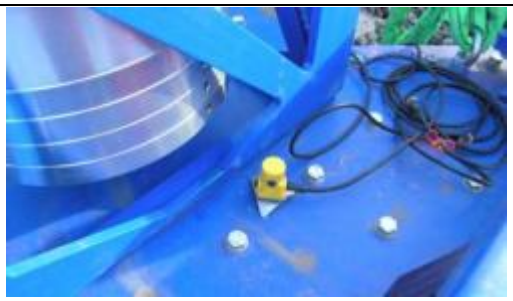

- three points at 12m distance
- one point at 16m distance from the center of the track

Figure 5-31: Arrangement of the vibration sensors on top of the unsprung mass (steel foundation coupled with rails) and beside the test track at the ground.

Figure 5-32: View on the test-site with the arrangement of the shaker and the excavators for simulation of the dead-loads at the ER test-site
(photo: M. Mistler, Ingenieurbüro Dr. Heiland)

5.2.4 Summary and discussion of results

As an example, the resulting unsprung mass (steel foundation) mobility of measuring section “B90.2 G13” (ME14) is shown in the next figure.

Mobility of the unsprung mass:

From the unsprung mass mobility, it is possible to detect the resonance frequency of the track. In Figure 5-33, the resonance frequency of the reference track (LC1) is marked by the green arrow, the resonance frequencies (depending on the static, decoupled load) of the track with USP are marked by red arrows. It shows that the dynamic behaviour of the track system

with the resilient under-sleeper pads depends on the static load of the excavator: The lower the static load is, the lower is the eigenfrequency.

- When testing with 307 kN (load case 1 (LC1)), the eigenfrequency of the measuring section “B90.2 G13” (ME14) is around 69 Hz.
- When testing with 233 kN (LC2) the eigenfrequency of “B90.2 G13” is around 58 Hz.
- The eigenfrequency of “B90.2 G13” is approximately 28 Hz without sprung mass (LC3).

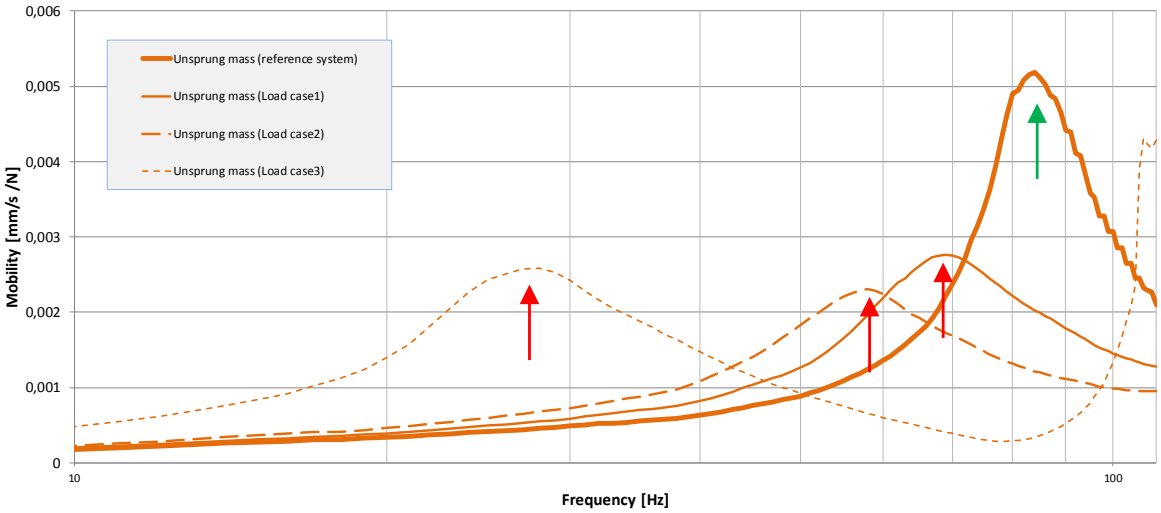

Figure 5-33: Force-controlled shaker test at measuring section “B90.2 G13” (ME14) - Mobility of the unsprung mass

Transfer mobility

The following figures show the transfer mobility from the shaker to the 12m measuring point resp. 16m measuring point. They were evaluated for each measuring point separately. Exemplarily, the averaged transfer mobility of measuring section “B90.2 G13” (ME14) is shown in the next figures as narrowband spectra.

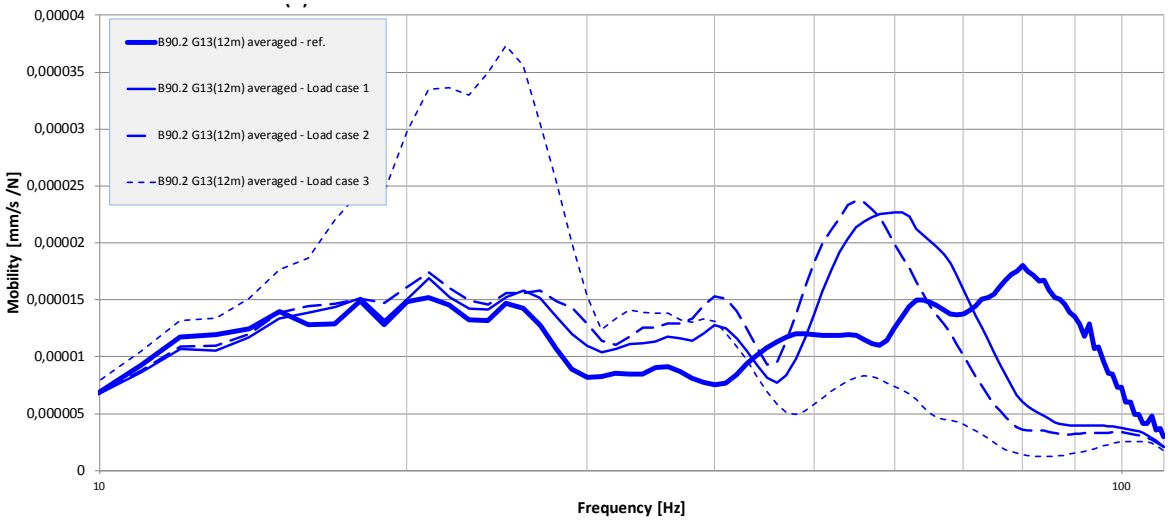

Figure 5-34: Measuring section “B90.2 G13” (ME14) – narrowband transfer mobilities from the shaker to the 12m measuring points

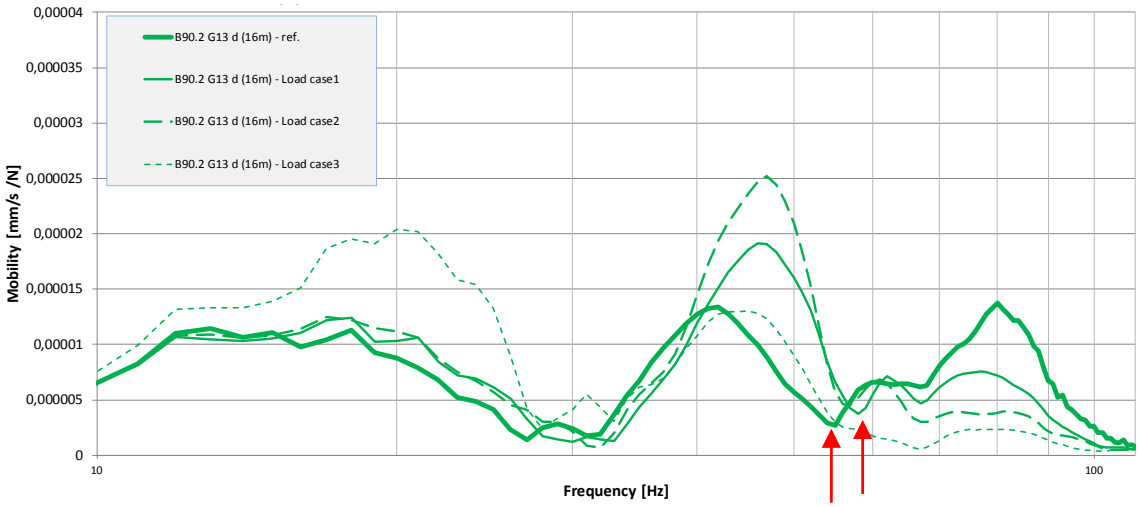

Figure 5-35: Measuring section “B90.2 G13” (ME14) - narrowband transfer mobilities from the shaker to the 16m measuring points

The thick solid line shows the mobility of the reference track.

The thin lines refer to the investigated track system:

- solid line: load case 1 (LC1)
- dashed line: load case 2 (LC2)
- dotted line: load case 3, i.e. without excavator (LC3)

As expected, the mobility of the 16 m point is lower than the mobility of the 12 m point due to the higher distance. The trend of the transfer mobility indicates that the results are very sensitive to the location, i.e. the subsoil behaviour. For example, at the excitation frequency of 55 Hz, the mobility is almost zero. But it is possible to recognize a frequency shift.

Nevertheless, this effect is not visible in the 1/3 octave spectrum, shown in the next two figures, because the shift is within the range of one 1/3 octave band.

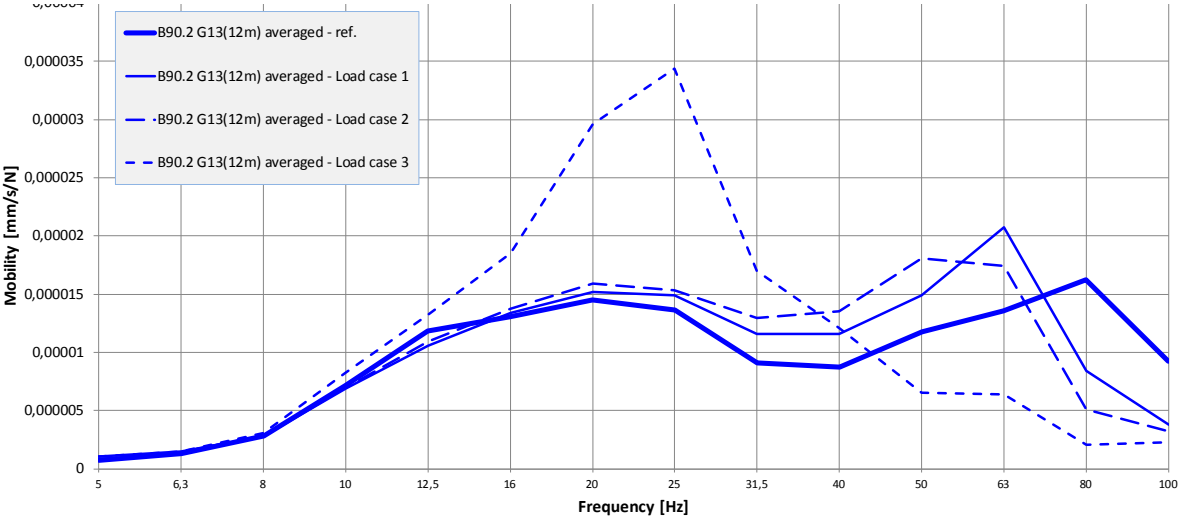

Figure 5-36: Measuring section “B90.2 G13” (ME14) - 1/3 octave band transfer mobilities from the shaker to the 12m measuring points

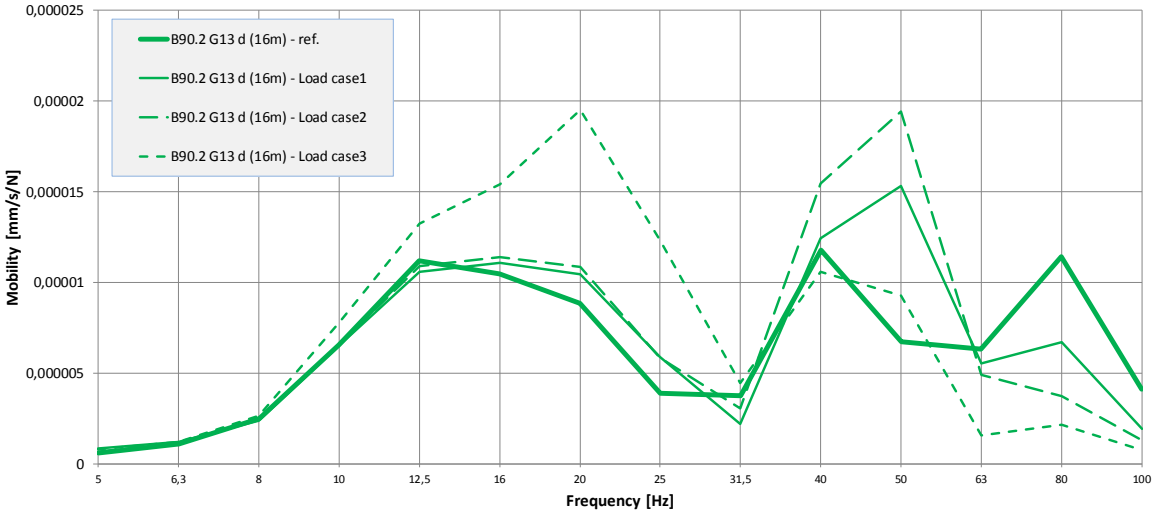

Figure 5-37: Measuring section “B90.2 G13” (ME14) - 1/3 octave band transfer mobilities from the shaker to the 16m measuring points

Insertion loss measurement

The insertion loss is assessed by dividing the transfer mobilities. It is evaluated for all three load cases (different bucket positions) in two steps:

- Step 1: First, the insertion loss is evaluated separately for each measuring point.
- Step 2: Afterwards, the results of the 12m measuring points (MP) are averaged arithmetically.

As an example, the results of measuring section “B90.2 G13” (Zw687a, ME14) are shown in the next two figures.

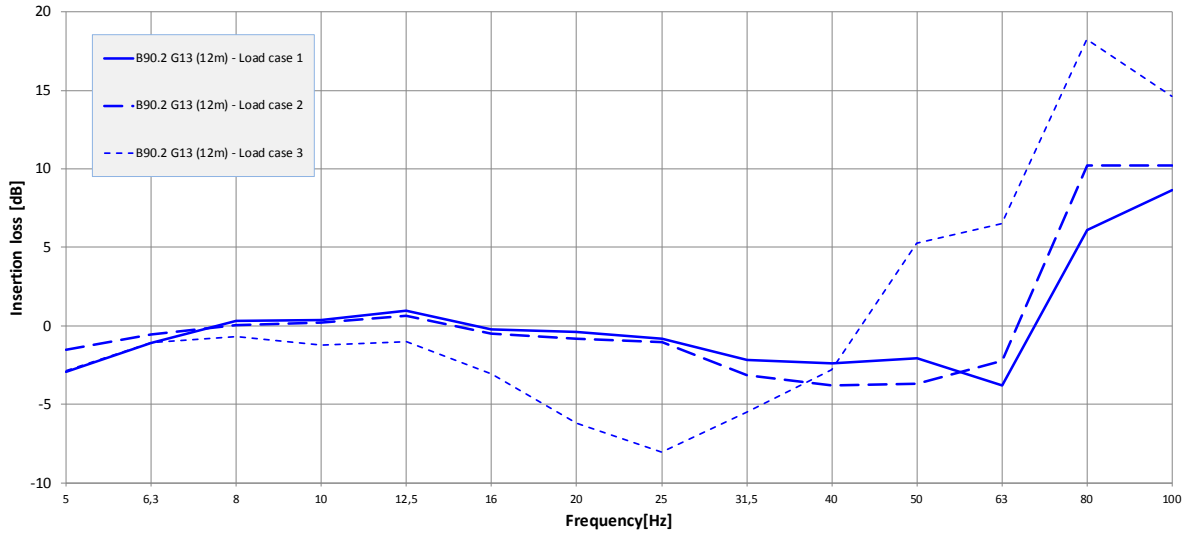

Figure 5-38: Measuring section “B90.2 G13” (Zw687a, ME14) – insertion loss at the 12 m - point

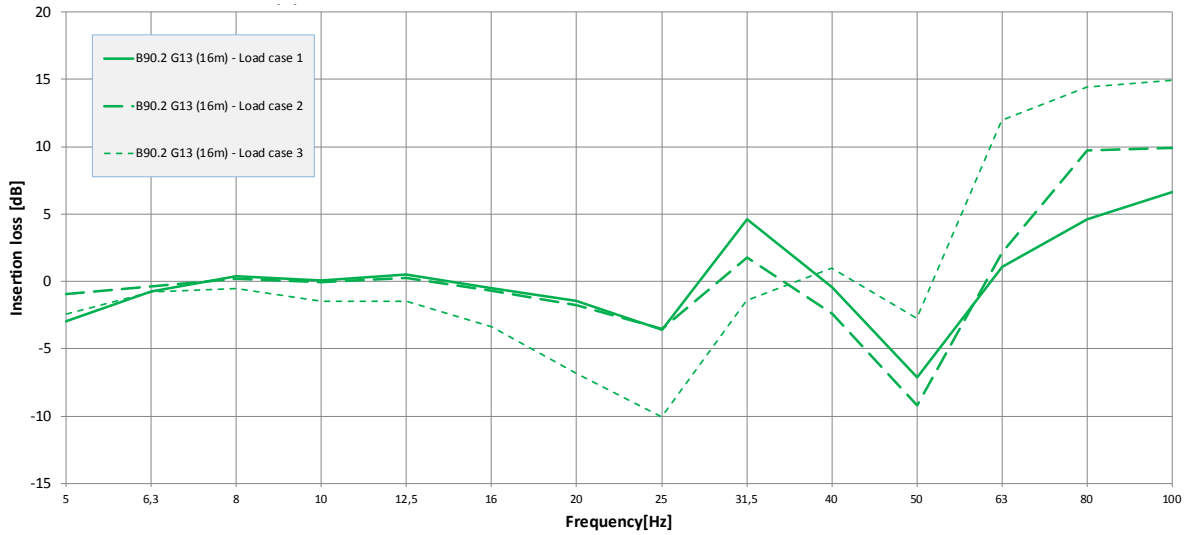

Figure 5-39: Measuring section "B90.2 G13" (Zw687a, ME14) – insertion loss at the 16 m - point

Negative values (< 0dB) means amplification, positive value (> 0dB) means reduction of vibration.

As before, the solid line refers to load case 1 (LC1), the dashed line refers to LC2; the dotted line refers to LC3, i.e. without excavator load (only the steel foundation and the shaker act as dead load).

As expected, the insertion loss is 0 dB in the lower frequency range. Generally, the insertion loss is negative in the range of the resonance frequency of the investigated track system. The best vibration reduction (highest insertion loss value) is in the range of the resonance frequency of the reference system (80 Hz).

Because of the lower resonance frequency of LC3, this situation shows the best insertion loss, but it is not representative and not realistic, because the reference track was investigated during the static load of the two excavators of together approx. 300kN.

Only LC1 and LC2 are close to reality because a realistic static load is considered.

The results of 16m measuring points show an unexpected trend of the insertion loss at 31,5 Hz. In this frequency range, the insertion loss is positive although the resonance frequency (amplification) is at 50 Hz.

We suppose that this effect is caused by changes of the soil between November 2012 and April 2013. The other sections also show this effect, particularly the measurement sections ME15 to ME17 ("B90.2 G04" / "B70 G04" / "B70 G04 NE").

As a summary, the insertion loss spectra of all track systems are shown in the next two figures. The comparison of the single systems among each other is shown and discussed in [6] as part of deliverables D3.14 and D3.15 in detail.

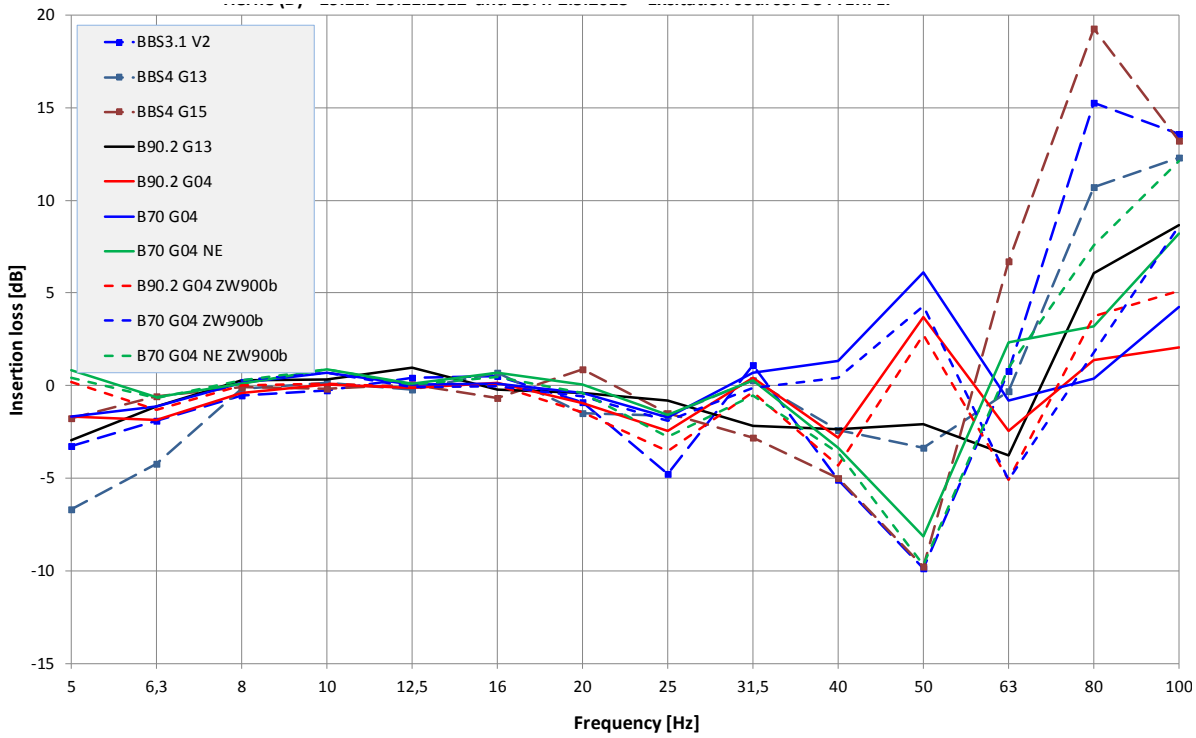

Figure 5-40: Insertion loss (LC1) of all investigated track systems

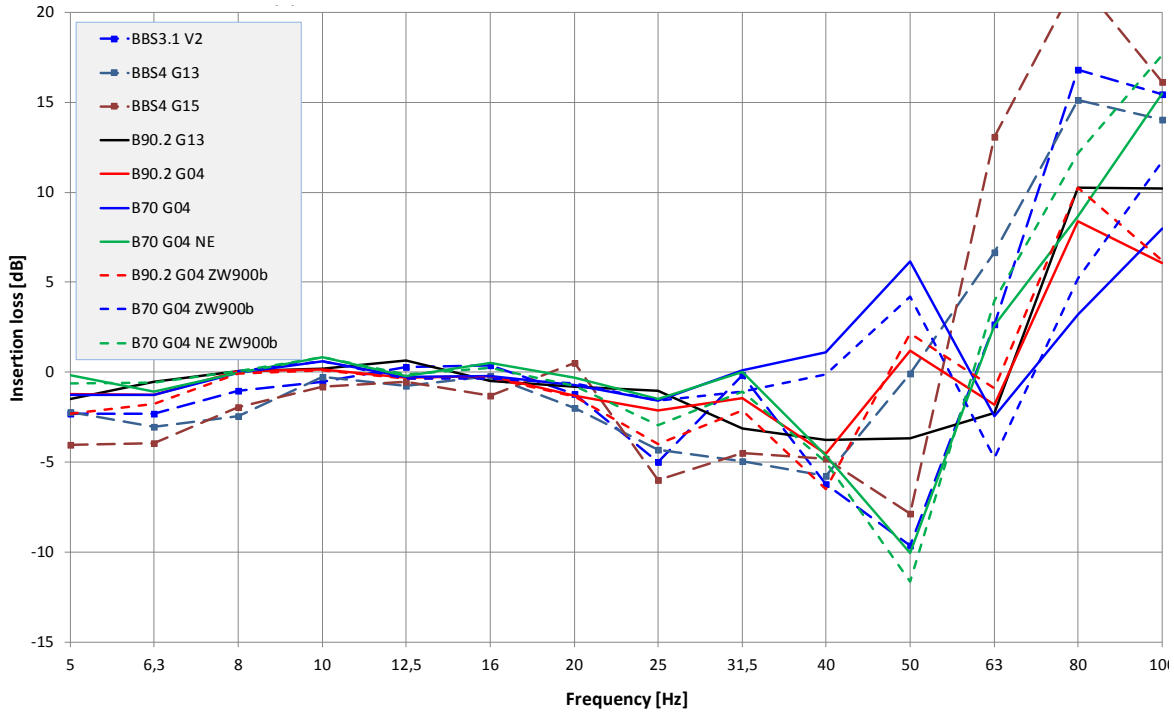

Figure 5-41: Insertion loss (LC2) of all investigated track systems

Another possibility to compare the different track system is the relation of the unsprung mass mobility at the reference track and the track of interest. This relation is not identically with insertion loss, but it seems to be a good indication for the insertion loss for each system without any soil influence. In the lower frequency range, the relation of mobility is not equal zero, but it contains the relation of track elasticity.

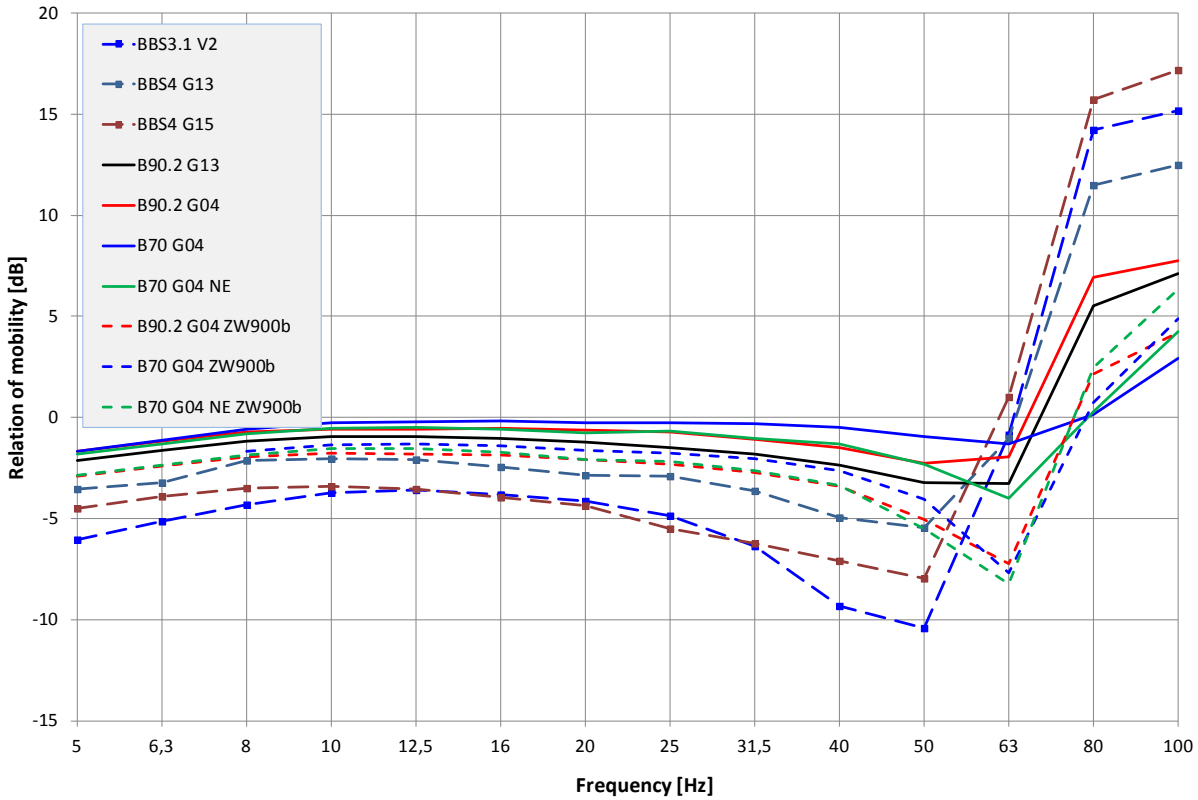

Figure 5-42: Relation of unsprung mass mobility (LC1) of all investigated track systems

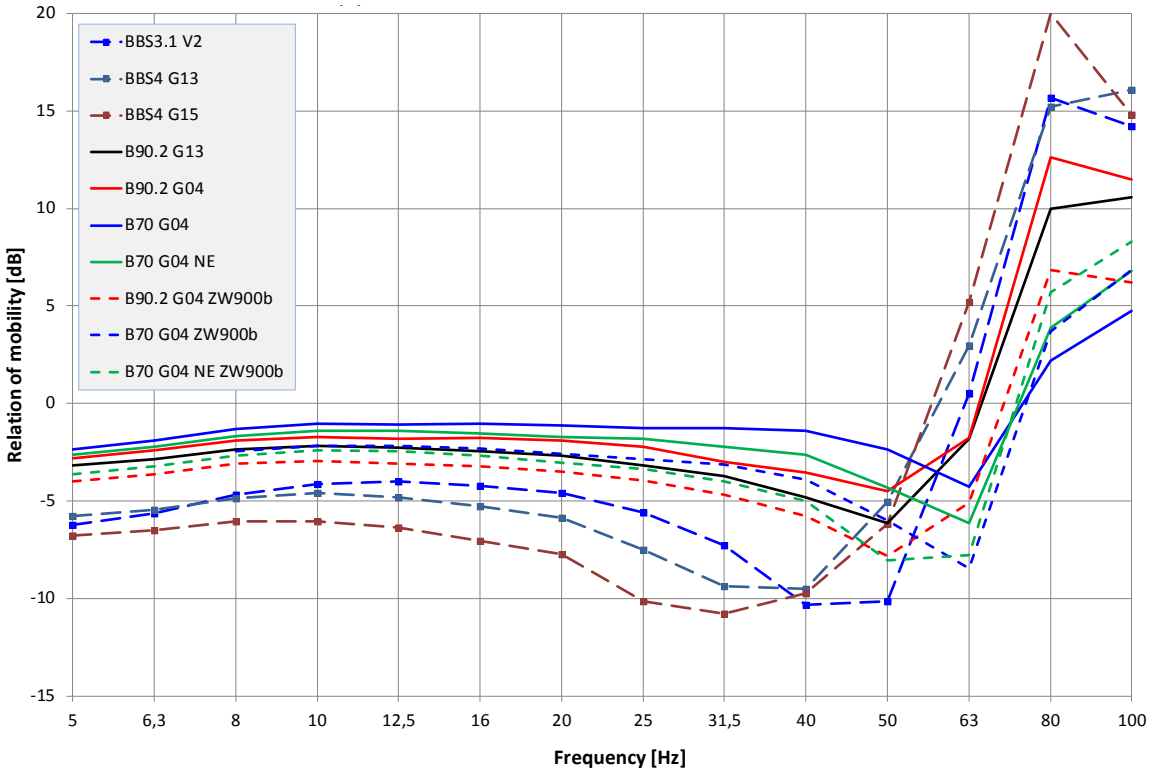

Figure 5-43: Relation of unsprung mass mobility (LC2) of all investigated track systems

In comparison with the simulations performed in the first part of the RIVAS project, the comparison of the different track configurations as measured with artificial source show reasonable results. Uncertainties mainly arise from the fact that the soil and the track was not finally consolidated.

5.3 LABORATORY TESTS AT THE CEDEX TRACK BOX

5.3.1 Description of the tested track-systems

As indicated in Chapter 5 of [10], the following track systems have been analysed in the CEDEX track box:

- TS1-BT
- TS2-BTS
- TS3-BTS
- TS1-B1M
- TS3-B1M
- TS3-B2M

A brief description of each system is given in the sequel:

- **TS1-BT**: Provided by ADIF, it is constituted by thirteen AI-99 Spanish standard sleeper (3.44 kN in weight) with PAE-2 standard rail pads (100 kN/mm stiff) in 0.35 m of tamped ballast.
- **TS2-BTS**: It is made up of thirteen AI-99 Spanish standard sleeper (3.44 kN in weight) with ZW 687a German rail pads provided by RAILONE. The ballast layer (0.35 m thick) was tamped and stabilised with 70,000 tons, equivalent to the pass by of 19 freight vehicles similar to the one described in page 35 of [10].
- **TS3-BTS**: Completely provided by RAILONE, it is made up of thirteen B90.2 German sleepers (6.10 kN in weight) with G04 (SLN 1010) under-sleeper pads (0.1 kN/mm^3 stiff) and ZW 687a rail pads. The ballast, 0.35 m thick, was tamped and stabilised in the same way that for TS2-BTS system.
- **TS1-B1M**: TS1 system after having been loaded with the pass by of 1 million axle loads (225 kN) of the freight vehicle type described in page 35 of [10].
- **TS3-B1M**: TS3 system after having been subjected to the same load time history that TS1-B1M system.
- **TS3-B2M**: TS3 system once subjected to 2 million axle loads of the freight vehicle.

All the systems described were provided with UIC rails of the E60 type and Vossloh fastening systems with rail clamps of the Skl 1 type (TS1 and TS2) and SKl 14 type (all TS3 systems). For tamping the ballast, the autonomous machine shown in Figure 5-44 was used.

Figure 5-44: Autonomous tamping machine used in CEDEX track box

5.3.2 Overview on the tests performed

Since a complete description of the different tests and sensors used in each one of the track box systems tested has already been given in Chapter 6 of [10], only the most relevant aspects of the tests playing an important role in the interpretation of the results obtained will be presented below.

For the RIVAS project, the following types of tests have been performed:

- Static tests
- Receptance tests with the track loaded and unloaded and:
    - high frequency pulses generated with:
        - ✓ hard tip 5.44 Kg hammer
        - ✓ hard tip 0.45 Kg hammer
        - ✓ soft tip 0.45 Kg hammer
    - low frequency pulses generated with hydraulic cylinders
- Quasi-static tests:
    - Short lasting
    - Long lasting
- Dynamic tests

Static tests

The step by step loading protocol to carry out the two cycle static tests performed sequentially in the three cross sections (A, B and C) of each track box system is shown in the left hand side of Figure 5-45. Two servo-hydraulic cylinders have been used simultaneously in each cross section to load the rails up to a maximum level of 112.5 kN.

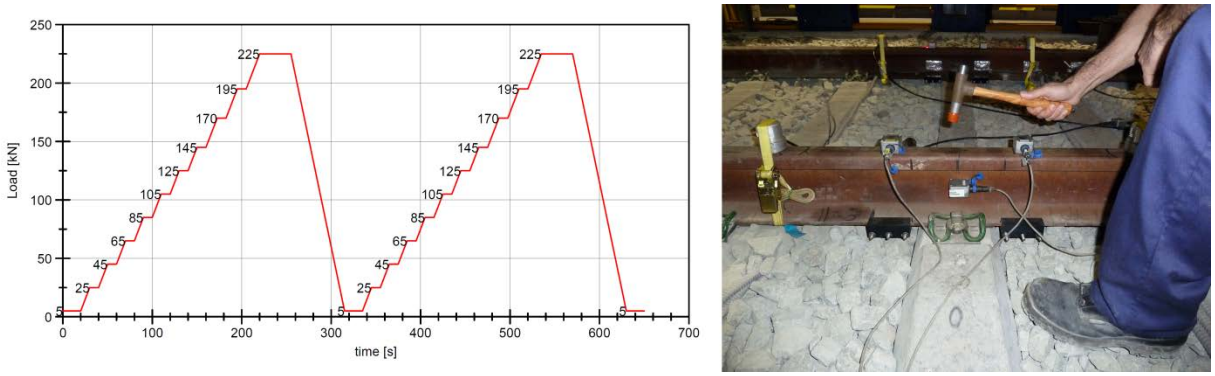

Figure 5-45: Static test wheelset loading protocol (left) and set of accelerometers used in the receptance tests (right).

Receptance tests

In the right hand side of Figure 5-45, the distribution of accelerometers used in the unloaded track box systems around the striking rail point is illustrated: the two accelerometers on the rail head were about 50 g sensors while the one in the web was about 100 g. The same distribution of sensors was adopted for the receptance tests performed in the loaded systems.

The peak forces and top frequencies generated with the different impulse sources used in the receptance tests were:

- Heavy hammer with hard tip: 2.2 kN (800 Hz)
- Slight hammer with hard tip: 8 kN (2,125 Hz)
- Slight hammer with soft tip: 2.2 kN (650 Hz)
- Hydraulic cylinders: 11 kN (40 Hz)

Quasi-static tests

Using the three pairs of hydraulic cylinders illustrated in Figure 4-13, the following quasi-static load time histories have been applied to the different track box systems:

- One corresponding to the freight vehicle, defined in Figure 4-4 of [10] constituted by 82 bogies, of the Y25 type mentioned in [40] with 225 kN axle loads travelling at 120 km/h (implying a time delay of 45 ms between each consecutive pair of cylinders)
- Another, corresponding to the passenger train of the Eurostar type, defined in Figure 4-1 of [10] circulating at 300 km/h with a time delay of 18 ms between each consecutive pair of cylinders.

Both load time histories were derived as already indicated in 4.5, assuming a track stiffness "K" of 120 kN/mm. The frequency spectra of both signals can be observed in Figures 4-5 and 4-2 of [10] respectively. Harmonics of the wagon passing frequency (2.15 Hz) with values of 6.45 Hz, 8.60 Hz, 12.90 Hz, 15.05 Hz and 19.35 Hz can be distinguished in the figure corresponding to the freight vehicle travelling at 120 km/h, and the same type of harmonics but reaching frequencies up to 40 Hz (4.60 Hz, 9.20 Hz, 18.40 Hz, 23.00 Hz, 27.60 Hz and 32.20 Hz) can be observed in the figure of the Eurostar type of train circulating at 300 km/h.

For the short lasting quasi-static tests, the testing routines illustrated in Figures 4.6 and 4.3 of [10] were used to generate 10 consecutive freight vehicles and 10 consecutive passenger trains. Out of them, only the pass by of the last three units of each series was recorded with all the displacement, velocity and acceleration sensors indicated in the corresponding chapter of [10].

The long lasting quasi-static test was carried out subjecting the TS3-BTS track system to 2 million axle loads. To accomplish that job, the same pairs of hydraulic cylinders and testing routine that those previously indicated for the short lasting test were adopted. In that way, the pass by of 11905 freight vehicles, one every 2 s, with 225 kN axle loads travelling at 120 km/h was simulated in the track box. During each working day the passing of 1,220 freight vehicles was executed making a total of 200,000 axle load applications per day. Every day, the pass by of one complete freight vehicle was recorded four times with all the internal and external sensors described in Chapter 2 of [10]. Besides, LVDT data of irreversible compressions in the ballast and the under sleeper pads have been jointly obtained along the whole test. That latter job was executed recording the pass by of vehicles 1, 4, 8, 15, 25, 37, 50 and then every 60 trains until completing the total number of 11905 units.

Dynamic tests

To carry out the dynamic tests, only the central cross section of the different track systems was loaded statically with a couple of hydraulic cylinders providing a total axle load of 225 kN. Then the two PISHA shakers were assembled to the rails at a distance of 0.35 m from the hydraulic cylinders as illustrated in the right hand side of Figure 4-13.

After feeding the piezoelectric shakers with the dynamic load time history generated as indicated in 4.3 of [10] the testing routine presented in Figure 4-14 of that document was used to reproduce the dynamics effects caused in the different track systems by the passing of three consecutive freight vehicles travelling at 120 km/h over a track with vertical irregularities. The PSD function characterizing the vertical irregularities of the track was the one identified, from the data provided by an auscultation car for a medium quality track, in [25]. At this point it is worth to outline that it is not necessary to make a separate analysis of the excitation frequencies induced by the sleeper bays, since existing in the experimental PSD, they are directly incorporated to the dynamic load time history derived from that function. In this respect, the selected PSD function was compared with others PSD functions suggested by ORE see [24] and a good agreement was found.

5.3.3 Discussion of main results

Recognising the important role played by the nonlinear behaviour of the track systems in the transmission of vibrations around the track, special emphasis was put in the text below to characterize the different track stiffness parameters that govern the mechanical behaviour of the systems under big and small loads similar to those induced by the total and unsprung masses expected in a real track.

Static tests

Figure 5-46, Figure 5-47 and Figure 5-48 show the load-track deflection curves obtained in the step by step static tests carried out in the different track systems, except track box system TS2-BTS whose load-deflection curve has been estimated from the data collected in the short lasting quasi-static tests as discussed later on.

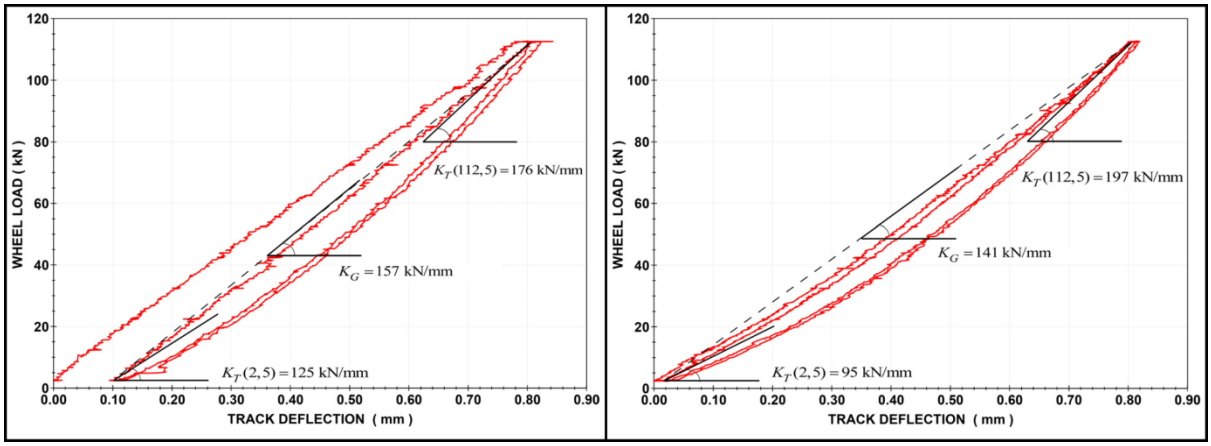

Figure 5-46: Load-deflection curves obtained in TS1-BT track system (left) and TS1-B1M track system (right)

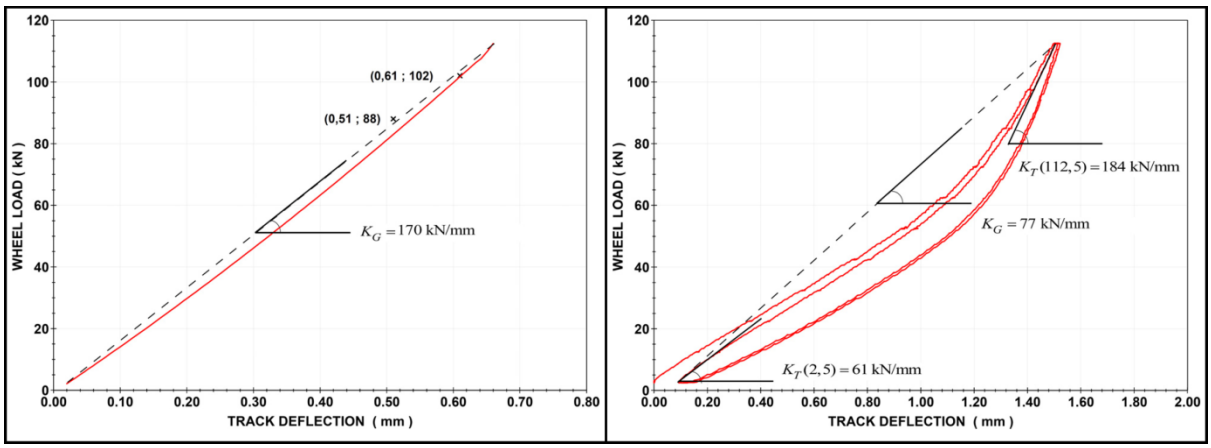

Figure 5-47: Load-deflection curves obtained in TS2-BTS track system (left) and TS3-BTS track system (right)

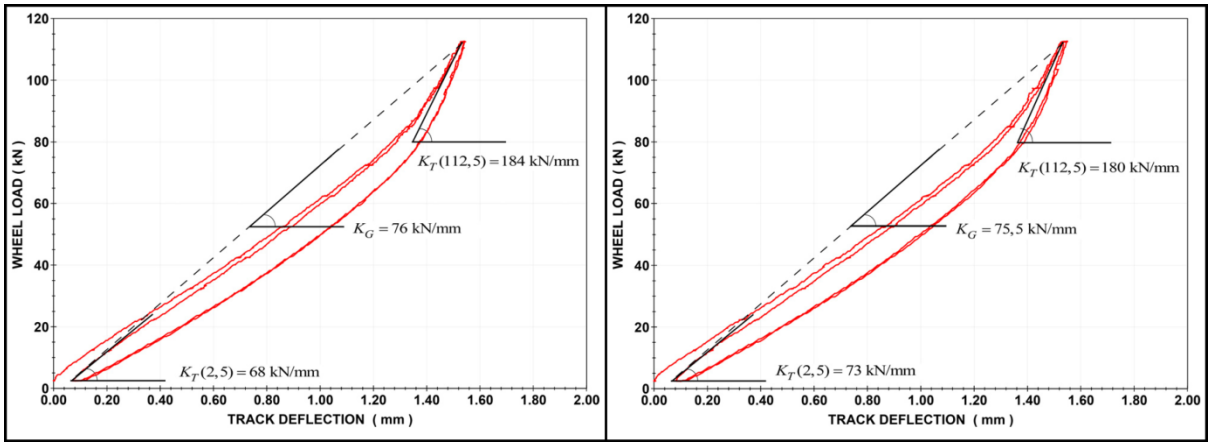

Figure 5-48: Load-deflection curves obtained in TS3-B1M track system (left) and TS3-B2M track system (right)

The global track stiffness values K_G identified in those curves (given by the slope of the secant line drawn from the origin of the second loading cycle) are considered to represent the

track stiffness of each system in the case that the sum of the unsprung and sprung static loads applied to the wheel set of the vehicle operating each track system were 225 kN. For other cases it will be necessary to draw the secants corresponding to the total wheel static load to determine the corresponding global track stiffness value K_G in each curve. Also, it can be seen that the track stiffness values obtained in the second cycle first and last steps of the loading process indicated in Figure 5-45 have been incorporated to the load-track deflection curves with the symbol K_T.

Observing the shape of the curves given in Figure 5-46, Figure 5-47 and Figure 5-48 it can be discussed that while both the TS1 and TS2 track systems initially behave almost lineally, all the TS3 track systems considered exhibit a strong nonlinear behaviour motivated by the under sleeper pads (USP). Also, after 1M axle loads the TS1 system increases its nonlinear behaviour while the TS3 system reduces it, keeping it practically constant during the application of 1M more of axle loads.

In Figure 5-49, the load-compression curves obtained for the ballast in TS1-BT track system and for the ballast plus the under sleeper pad in TS3-BTS system are given.

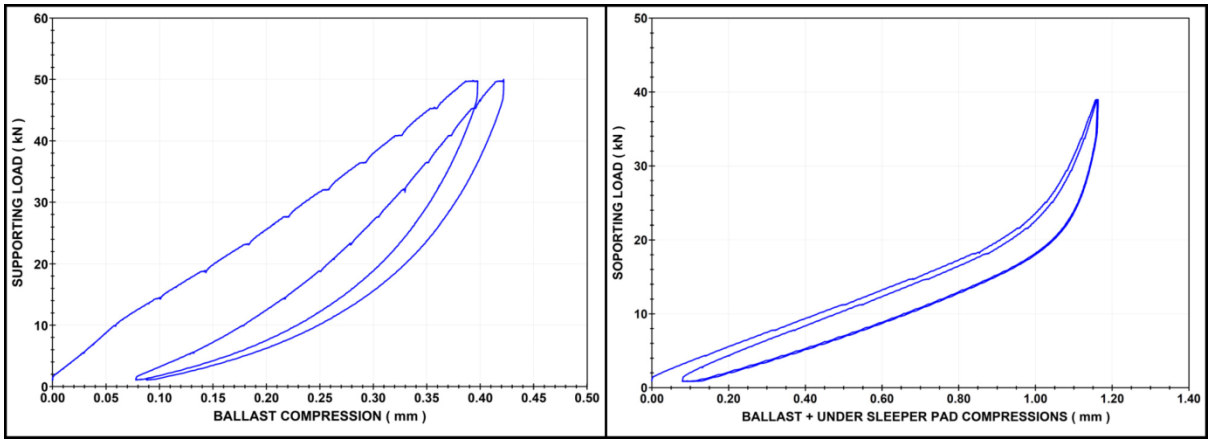

Figure 5-49: Load - compression curves obtained for ballast in TS1-BT track system (left) and for ballast plus the under sleeper pad in TS3-BTS system (right)

From the information provided by the curves represented in Figure 5-49 and the result of the measurements carried out by BAM on under sleeper pads of the SLN1010 type documented in RIVAS deliverable D3.7 report [26], important conclusions may be drawn on how both materials: ballast and USP behave when used jointly and separately.

Receptance tests

The receptance spectra curves obtained with different hammers and servo-hydraulic cylinders were collected in Appendix 2 of [10]. Unfortunately, they all correspond to the data obtained with the accelerometers located in the rail webs which were the only receptance data interpreted at the time D3.7 Part A [10] was edited. Later on, the data provided by the accelerometers at the rail heads (see Figure 5-45) have been also analysed and it was found that while the best response to the low frequency impulses generated with the hydraulic cylinders is the one provided by the accelerometers located at the rail webs, the best response obtained when striking the rails with the hammers was given by the accelerometers placed on the rail heads.

It means that from all the track receptance values compiled in Tables 7-1 to Table 7-12 of chapter 7 in [10] only the lower sets of values (those obtained for each track system with the hydraulic cylinders) and preferably those identified in the frequency range 8.9-28.2 Hz are susceptible to be used for estimating track stiffness values. As expected, it can be checked that the track stiffness values derived for each track system from those receptance values are higher than the K_T ( ) values included in Figure 5-46, Figure 5-47 and Figure 5-48. The ratios found between both sets of track stiffness values range between 1.4 and 1.6 for the loaded systems and between 1.1 and 1.2 for the unloaded ones.

In a more recent receptance test campaign performed in the track box with the different hammers and a soft tip also incorporated to the heavy one, a strong dispersion of receptance values was found for the different frequency ranges. From a comparison of the hammer-rail head accelerometer data with the best quality data available (those provided by the hydraulic cylinders striking at the track cross section in which the rail web accelerometers were installed) the following order of preference for the use of the hammers and best frequency ranges for the interpretation of the receptance spectrum data have been set up:

- Loaded track systems
    1. Heavy hammer with soft tip, within 20-45 Hz
    2. Heavy hammer with hard tip, within 20-45 Hz
    3. Slight hammer with soft tip, within 30-40 Hz
    4. Slight hammer with hard tip, within 30-40 Hz
- Unloaded track systems
    1. Heavy hammer with soft tip, within 10-45 Hz
    2. Heavy hammer with hard tip, within 10-45 Hz
    3. Slight hammer with soft tip, within 20-45 Hz
    4. Slight hammer with hard tip, within 20-45 Hz

Short lasting quasi-static tests

Only slight variations were observed in the peaks of the different time histories obtained from the passing of the last three units of each series of passenger and freight units scheduled for the short lasting quasi-static test. The mean peak values of the wheel loads and track deflections provided by the different sensors in the track box are given in Table 5-4 and Table 5-5.

Table 5-4: Mean peak values obtained from the pass by of three passenger trains at 300 km/h

PASSENGER TRAINS AT 300 km/h	TRACK BOX SYSTEM					
TRACK SYSTEM	TS1/BT	TS1/B1M	TS2/BTS	TS3/BTS	TS3/B1M	TS3/B2M
WHEEL LOAD (kN)	84	82	88	76	81	82
TRACK DEFLECTION (mm)	0.61	0.60	0.51	1.29	1.25	1.33

Table 5-5: Mean peak values obtained from the pass by of three freight vehicles at 120 km/h

FREIGHT VEHICLES AT 120 km/h	TRACK BOX SYSTEM					
TRACK SYSTEM	TS1/BT	TS1/B1M	TS2/BTS	TS3/BTS	TS3/B1M	TS3/B2M
WHEEL LOAD (kN)	112	102	102	101	100	100
TRACK DEFLECTION (mm)	0.74	0.78	0.61	1.36	1.44	1.47

Since perfect rails and rolling stock wheels are assumed in this type of test, it can be checked that the global track stiffness values K_G ( ) derived from the data presented in those tables fit well the K_G ( ) values obtained in Figure 5-46, Figure 5-47 and Figure 5-48 for the load levels given in the tables. Based on that, the data provided for TS2-BTS system in both tables were used to estimate the loading branch of the static load-deflection curve drawn for that system in Figure 5-47.

Long lasting quasi-static tests

Although not reported in [10], TS1-BT system was subjected, in the context of a previous ADIF-CEDEX contract [27], to 1 million axle loads in a long lasting test similar to the 2 million axle load test run on TS3-BTS system for the RIVAS project as described in 5.4.2 of [10].

The initial and final values of the global track stiffness obtained for TS1-BT system in those long lasting loading processes are illustrated in Figure 5-50. The same type of information is provided for TS3-BT in Figure 5-51 and Figure 5-52: Figure 5-51 reflects the evolution of the track stiffness values along the pass by of the first 6,140 freight vehicles that ADIF considers necessary to pass for the stabilization of the track and Figure 5-52 shows the track stiffness values obtained at the end of the first and second millions of axle loads.

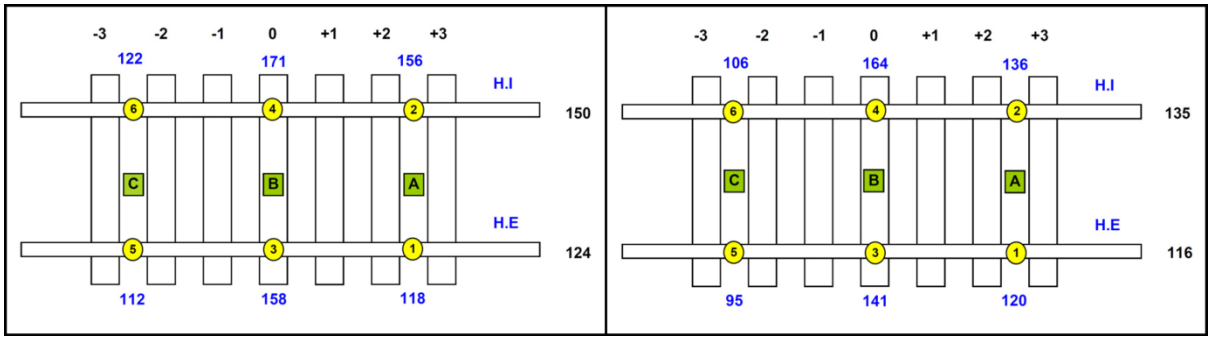

Figure 5-50: Static track stiffness values obtained at TS1-BT track system (left) and TS1-B1M track system (right)

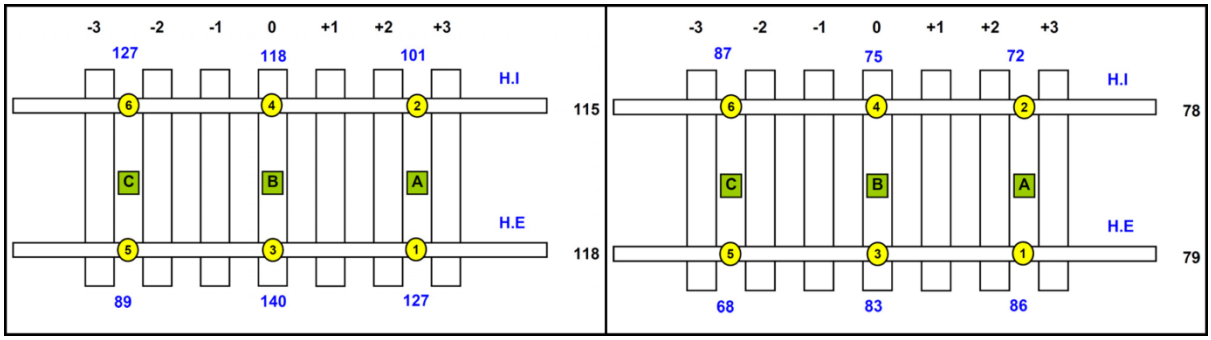

Figure 5-51: Static track stiffness values obtained at TS3-BT track system (left) and TS3-BTS track system (right)

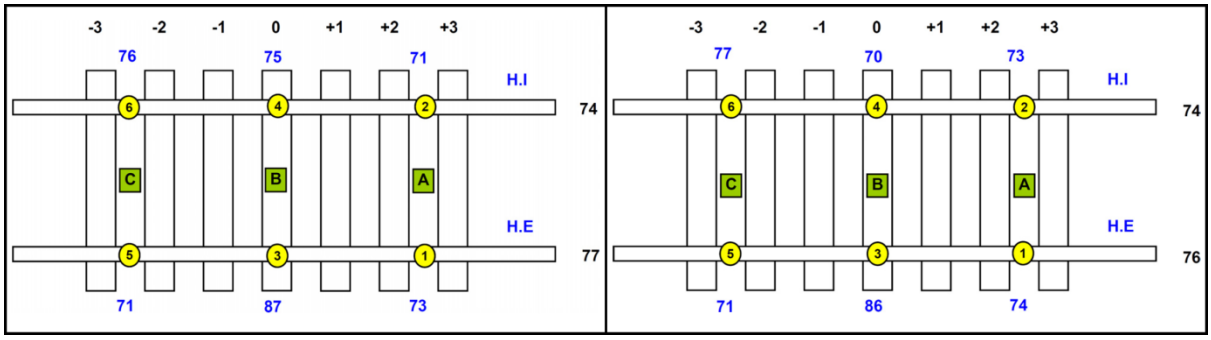

Figure 5-52: Static track stiffness values obtained at TS3-B1M track system (left) and TS3-B2M track system (right)

It can be seen from those figures that, although an increase of the static track stiffness was obtained at the end of the stabilization process of TS1-BT system (not shown in Figure 5-50), the net effect of the application of 1 million axle loads to that system is a decrease (in percentages that range from 0 to 15%) of the stiffness values along the 7 consecutive sleepers while keeping almost the same dispersion (16%) around the mean that the system had after tamping the ballast.

On the contrary, TS3-BT system exhibits a notably decrease of track stiffness (in percentages ranging from 30% to 40%) along the stabilization period (Figure 5-51). Also, after that period, it is worth to point out a notably decrease in the variations of the track stiffness's around their mean value that has led to a more homogeneous system with variations around the mean less than 8% in both rails (half the variation observed after tamping). With respect the effect of applying million axle loads to the TS3-BTS system, only a slight decrease of the track stiffness values was observed after the first million and no changes along the second million see Figure 5-51 and Figure 5-52.

Concerning the behavior of the rail pads adopted for the different track box systems, big differences have been found in the spring moduli obtained from static and quasi-static tests in the track box and the results provided by slow and quick compression tests performed on conventional testing rigs at CEDEX and BAM, see Appendix 1 of [10] and [28]. For the Spanish PAE-2 unit, spring moduli 60% higher than its nominal value (100 kN/mm) were obtained in the track box tests. For the German Zw 687a type, spring moduli higher than 570 kN/mm were obtained in the track box tests. For that unit, a spring value of 240 kN/mm was obtained in the quick compression test performed in a testing rig at CEDEX and only 130 kN/mm in the slow test (see Appendix 1 in [10]). Recent tests performed in the track box using two LVDT sensors, one on each side of the rail, instead of only one in the outside

as commonly made, have shown that those differences may be attributed to the rotation of the rail pad towards the inner part of the track when it is loaded either in the track box or in a real line.

A summary of the velocity and acceleration amplitudes reached in the superstructure elements of TS1-BT and TS3-BTS track systems induced by the pass by of freight vehicles at 120 km/h is given in Table 5-6 and Table 5-7.

Table 5-6: Velocity amplitudes (mm/s) reached in the superstructure of TS1-BT and TS3-BTS track systems under the pass by of freight vehicles at 120 km/h.

TRACK SYSTEM	RAILS AT CROSS SECTION B IN ZONE 0 OF THE TRACK BOX					
	INITIAL VALUE		AFTER 1 M AXLE LOADS		AFTER 2M AXLE LOADS	
	INNER	OUTER	INNER	OUTER	INNER	OUTER
TS1-BT	17.11	17.68	17.71	17.93	-	-
TS3-BTS	22.79	27.34	24.01	22.99	25.49	23.49
TRACK SYSTEM	SLEEPER AT CROSS SECTION B IN ZONE 0 OF THE TRACK BOX					
	INITIAL VALUE		AFTER 1 M AXLE LOADS		AFTER 2M AXLE LOADS	
	INNER	OUTER	INNER	OUTER	INNER	OUTER
TS1-BT	10.75	11.88	10.8	11.52	-	-
TS3-BTS	30.78	29.34	31.84	27.21	33.70	27.67

Table 5-7: Acceleration amplitudes (g) reached in the superstructure of TS1-BT and TS3-BTS track systems under the pass by of freight vehicles at 120 km/h

TRACK SYSTEM	RAILS AT CROSS SECTION B IN ZONE 0 OF THE TRACK BOX					
	INITIAL VALUE		AFTER 1 M AXLE LOADS		AFTER 2M AXLE LOADS	
	INNER	OUTER	INNER	OUTER	INNER	OUTER
TS1-BT	0.45	0.40	0.67	0.81	-	-
TS3-BTS	0.40	0.29	0.28	0.24	0.38	0.43
TRACK SYSTEM	SLEEPER AT CROSS SECTION B IN ZONE 0 OF THE TRACK BOX					
	INITIAL VALUE		AFTER 1 M AXLE LOADS		AFTER 2M AXLE LOADS	
	INNER	OUTER	INNER	OUTER	INNER	OUTER
TS1-BT	0.13	0.11	0.14	0.12	-	-
TS3-BTS	0.47	0.37	0.34	0.29	0.48	0.40

From the information provided in Table 5-6 and Table 5-7 it can be seen that, as expected, for TS1-BT system both velocity and acceleration amplitudes are higher in the rails than in the sleeper whereas the opposite effect was found for TS3-BTS system (higher velocities and accelerations in the sleeper than in the rails) which undoubtedly is due to the USP being the main vibrating component in TS3-BTS system.

Finally, a comparison has been made in Figure 5-53 of the permanent settlements experienced by ballast in TS1-BT and TS3-BTS systems along 1 million axle loads. A similar behavior, lacking the existence of shake-down phenomena, is observed in both track systems with permanent settlements of 0.85 mm in the first track system and 1.15 mm in the second one after 1 million axle loads. That difference may be also attributed to the effect of the USP being in direct contact with the ballast in the TS3-BTS system.

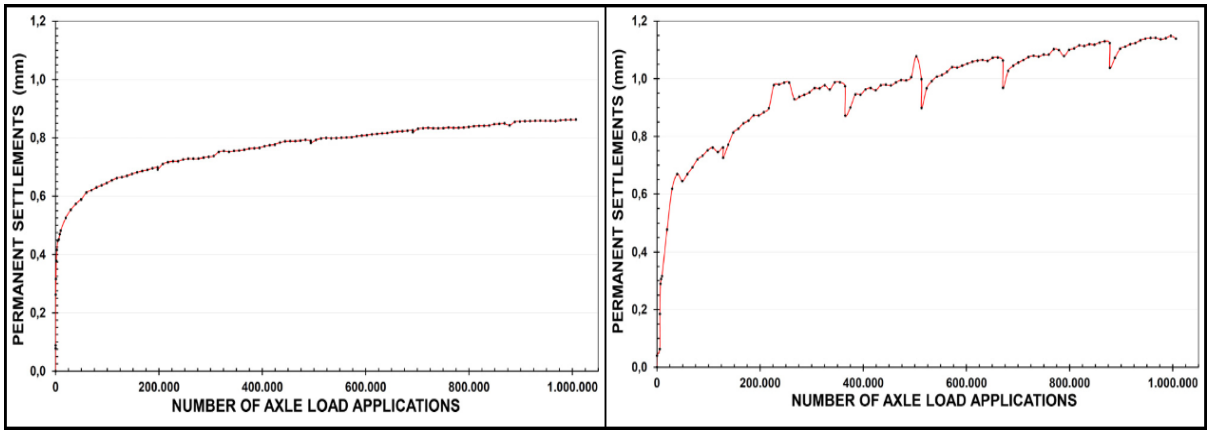

Figure 5-53: Permanent settlements of ballast in TS1-BT track system (left) and in TS3-BTS track system (right).

Dynamic tests

As already commented in 5.4.2, after loading statically each track system with an axle load of 225 kN, they have been subjected to three dynamic load time histories of the type shown in Figure 4-13 of [10]. The mean values of the peak loads and peak rail deflections, together with the corresponding track stiffness values K_T ( ) and static wheel load levels at the rail points where the PISHA shakers were installed are given in Table 5-8.

Table 5-8**:** Track stiffness values K_T ( ) obtained in the dynamic tests.

TRACK SYSTEM	TS1-BT	TS1-B1M	TS2-BTS	TS3-BTS	TS3-B1M	TS3-B2M
PEAK DYNAMIC WHEEL FORCE kN	+9.6 -12.0	+8.3 -8.5	+8.9 -9.8	+8.1 -8.7	+8.0 -7.0	+6.5 -8.0
PEAK RAIL DEFLECTION (mm)	+0.06 -0.07	+0.05 -0.06	+0.08 * -0.09 *	+0.05 -0.06	+0.06 -0.05	+0.05 -0.06
K_T ( ) (kN/mm)	166	153	110 *	153	136	131
STATIC WHEEL LOAD LEVEL (kN)	90	90	91	90	90	90

* Not reliable values

The static wheel load levels given in the last row of Table 5-8 were determined taking into account that the piezoelectric shakers were located at 0.35 m from the hydraulic cylinders. Accordingly, the static wheel load level of 112.5 kN was corrected as indicated in the following expression:

$$F(0.35) = F(0)e^{-\frac{0.35}{L}}\left[cos\frac{0.35}{L} + sen\frac{0.35}{L}\right] \quad (6)$$

where F(0) = 112.5 kN and L is given by equation (4) in 4.4.2 replacing K by K_G (112.5) as obtained for the different systems from Figure 5-46, Figure 5-47 and Figure 5-48.

Except for TS2-BTS system, in which a faulty installation of sensors was detected, all the remaining K_T stiffness values identified in the fourth row of Table 5-8 fit well the values that for increments of ±10 kN can be drawn from Figure 5-46, Figure 5-47 and Figure 5-48 for a static wheel load level of 90 kN.

5.3.4 Comparison of the CEDEX track box results with in situ dynamic tests

For the comparison of the results obtained in the tests performed at CEDEX track box with the in situ dynamic tests at DB and Eiffage sites, the following features have been taken into account:

- As indicated in chapter 3 of [10], the subgrade shear wave velocity inside the CEDEX track box range from 280 m/s (upper subgrade 1.21 m thick at a depth of 0.80 m bellow the ballast) and 380 m/s (lower subgrade 1.37 m thick). Similar range of values has been reported by BAM [29] at Eiffage site, where a constant shear wave velocity of 240 m/s was found up to depth of 4 m below the ground surface and higher values at deeper levels, reaching 350 m/s at a depth of 8 m.
- The static loads of the sprung and unsprung masses of the track systems, at both DB and Eiffage sites, and the dynamic harmonic loads generated by the BUTTERFLY® shaker in those sites are all supported in four track points: two on each rail at a distance each other of 1.30 m as indicated in Annex A1 and [8].
- In each German system the two rail static loads corresponding to the total (sprung + unsprung) mass interact each other according to a global track stiffness of the $K_G(\ )$ type defined in the load-deflection curves of the track box systems (see Figures 5-46, 5-47 and 5-48).
- In each German system the two rail static loads associated to the unsprung mass and the two rail dynamic loads generated by the BUTTERFLY® shaker interact each other respectively according to a track stiffness of the $K_T(\ )$ type defined in the abovementioned curve.
- Three different sprung mass load levels, as indicated in Annex A1 and [6] were applied to the DB and Eiffage site track systems except to the reference track system in both sites which were tested only under the higher sprung mass load level.
- An unsprung mass of 2.65 t has been applied to all DB and EIFFAGE track systems.
- The amplitude of the harmonic force generated with the shaker in all the track systems has been 7.5 kN.

For the interpretation of the velocity time histories provided in Annex A1 and the mobility spectra given in [8] the following assumptions have been made:

- Initially, and in the frame of the step by step procedure defined in the next paragraph, both German and CEDEX track box systems having similar track superstructure components are assumed to have the same wheel load-track deflection curve.
- All the four track supporting points in each German system are assumed to have the same static and dynamic track deflections.
- Each one of the DB and Eiffage track systems is assumed to be represented by one degree of freedom system (O.D.F.S.) having the same static and dynamic track deflections that one of the track supporting points.
- The stiffness of each equivalent O.D.F.S. is given by the $K_T(\ )$ value defined in the wheel load-track deflection curve of the track system by the load level induced at the supporting track point by the two rail total (sprung + unsprung) mass forces.
- The mass of each equivalent O.D.F.S is the mass corresponding to the static unsprung mass force causing at the supporting track point the same static track deflection that the two rail unsprung mass forces (see steps 2 and 3 in the following iterative procedure).

To derive the parameters (stiffness, mass and geometric damping ratio) characterizing the dynamic behaviour of the German track systems, the following step by step iterative procedure has been adopted:

1. Firstly, the total force level "F", applied to each track system is determined:

$$F = F_{SU}\ (1 + E_{SU}) \tag{7}$$

where F_{SU} is one fourth of the total mass force (sprung + unsprung) applied to the track system and E_{SU} represents the interaction effect of the two rail total mass forces. For a separation of 1.30 m between those forces that interaction effect is given by the following expression:

$$E_{SU} = e^{-\frac{1.30}{L_{SU}}}\left[cos\frac{1.30}{L_{SU}} + sin\frac{1.30}{L_{SU}}\right] \tag{8}$$

with $L_{SU} = 3\sqrt{\frac{8\,E\,I}{K_G\,(F_{SU})}}$ and $K_G\,(F_{SU})$ representing the global track stiffness value defined by F_{SU} in the system load-deflection curve.

2. In a similar way, the static unsprung mass force level F_{U0} at the supporting track point is initially obtained:

$$F_{U0} = 6.625\ [1 + E_{U0}]\ \text{kN} \tag{9}$$

where E_{U0} stands for the interaction effect of the two 6.625 kN static rail unsprung forces:

$$E_{U0} = e^{-\frac{1.30}{L_{U0}}}\left[cos\frac{1.30}{L_{U0}} + sen\frac{1.30}{L_{U0}}\right] \tag{10}$$

with $L_{U0} = 3\sqrt{\frac{8\,E\,I}{K_T\,(F)}}$ and $K_T\,(F)$ representing the track stiffness defined in the system load-deflection curve by a total mass force F and a load increment of 6.625 kN

3. Then, the initial value m_{UO} of the O.D.F.S mass is derived:

$$m_{UO} = \frac{F_{UO}}{g} \tag{11}$$

with g=9.81 m/s^2

4. Replacing the value of m_{UO} in the O.D.F.S resonance frequency equation, a new value K_{T0} is obtained:

$$K_{T0} = (2\,\pi\ f_N)^2\ m_{U0} \tag{12}$$

f_N being the track system resonance frequency obtained in the sweep frequency process of the dynamic in situ test run with the BUTTERFLY® shaker.

5. If $K_T(F)$ obtained from the track box load-deflection curve and K_{T0} are close enough, both track box and German systems are confirmed to have the same load-deflection curve and the process for obtaining the stiffness and mass of the German system is ended. On the contrary, $K_T(F)$ is replaced by K_{T0} and steps 2, 3 and 4 are repeated "n" times until K_{Tn-1} and K_{Tn} are alike. The final K_{Tn} and m_{Un} values are then adopted for the German system and K_{Tn} can be compared with the corresponding $K_T(F)$ of the track box system to judge how similar their load – deflection curves are.

6. Finally, since the velocity amplitude V of the unsprung mass at resonance is obtained by multiplying 7.5 kN by the peak mobility values provided by Figures 6.3.1 to 6.4.10 in [8] and directly from the velocity time histories given in Annex A1, the amplitude X at resonance of the unsprung mass displacement is calculated:

$$X = \frac{V}{2\,\pi\,f_N} \tag{13}$$

Then, from the standard response of O.D.F.S to harmonic loads, the damping ratio D of the system is obtained:

$$D = \frac{1}{2}\ \frac{X_0}{X} \tag{14}$$

where X_0 represents the track point deflection induced by the two rail dynamic loads (1.875 kN each) generated by the shaker, when applied statically to the track.

In the same way that for the obtainment of "F" and "F_{U0}" at steps 1 and 2, "X_0" is given by the following equation:

$$X_0 = \frac{1.875\ (\ 1 + \ E_{Un})}{K_{Tn}} \tag{15}$$

where the same interaction effect E_{Un} and the same K_{Tn} that in step 5 is are adopted.

For the track box and German systems having the same (or very similar) track superstructure components, the initial parameters F_{SU}, $K_G(F_{SU})$ and $K_T(F)$ obtained from the track box curves and the final values K_{Tn}, m_{Un}, and D identified for the German systems are given in

Table 5-9 to Table 5-12. They were derived when comparing:

- TS2-BTS track box system with reference ME15 system at EIFFAGE site (Table 5-9)
- TS3-BTS track box system with ME15 system at EIFFAGE site (Table 5-10)
- TS1-BT track box system with ME1 system at DB site (Table 5-11)
- TS3-BTS track box system with ME5 system at DB site (Table 5-12)

Table 5-9**:** TS2-BTS at CEDEX track box versus reference ME15 at EIFFAGE site

TS2-BTS (Al 99 ; Zw687a)			**Reference ME15 (B70 ; Zw687a) Sprung mass: 30 t ; Total mass: 32.65 t**							
F_{SU} (kN)	K_G (F_{SU}) (kN/mm)	K_T (F) (kN/mm)	f_N (Hz)	E_{Un} --	m_{un} (kg)	K_{Tn} (kN/mm)	V (mm/s)	X (mm)	X_0 (mm)	D --
81.6	163	184	80	0.073	706	180	40	0.079	0.011	0.07

Table 5-10**:** TS3-BTS at CEDEX track box versus ME15 at EIFFAGE site

TS3-BTS (B90.2, USP G04; Zw687a)			**ME15 (B90.2 ; USP G04 ; Zw687a) Sprung mass: 30.7 t ; Total mass: 33.35 t**							
F_{SU} (kN)	K_G (F_{SU}) (kN/mm)	K_T (F) (kN/mm)	f_N (Hz)	E_{Un} --	m_{un} (kg)	K_{Tn} (kN/mm)	V (mm/s)	X (mm)	X_0 (mm)	D --
83.4	63.2	126	68	0.121	743	135	18.8	0.044	0.0155	0.175
			Sprung mass: 23.1 t ; Total mass: 25.75 t							
64.4	56	91	61	0.154	764	112	19.12	0.05	0.019	0.19
			Sprung mass: 0.5 t ; Total mass: 3.15 t							
7.9	61	61	37	0.360	901	48	16.87	0.072	0.053	0.37

Table 5-11**:** TS1-BT at CEDEX track box versus reference ME1 at DB site

TS1-BT (Al 99 ; PAE-2)			**Reference ME1 (B70 ; Zw900) Sprung mass: 30.4 t ; Total mass: 33.05 t**							
F_{SU} (kN)	K_G (F_{SU}) (kN/mm)	K_T (F) (kN/mm)	f_N (Hz)	E_{Un} --	m_{un} (kg)	K_{Tn} (kN/mm)	V (mm/s)	X (mm)	X_0 (mm)	D --
82.6	155	165	80	0.071	709	180	45	0.0785	0.011	0.07

Table 5-12**:** TS3-BTS at CEDEX track box versus ME5 at DB site

TS3-BTS (B90.2, USP G04; Zw687a)			**ME5 (B70 ; SLN 1010 ; Zw900) Sprung mass: 30.6 t ; Total mass: 33.25 t**							
F_{SU} (kN)	K_G (F_{SU}) (kN/mm)	K_T (F) (kN/mm)	f_N (Hz)	E_{Un} --	m_{un} (kg)	K_{Tn} (kN/mm)	V (mm/s)	X (mm)	X_0 (mm)	D --
83.1	63.2	126	63	0.152	763	120	26	0.065	0.018	0.14
			Sprung mass: 23.3 t ; Total mass: 25.95 t							
64.9	56	91	63	0.152	763	120	22	0.055	0.018	0.16
			Sprung mass: 0.5 t ; Total mass: 3.15 t							
7.9	61	61	31.5	0.41	937	36	22	0.111	0.73	0.33

From Table 5-9 it can be seen that TS2-BTS at the track box is alike reference ME 15 at EIFFAGE site since K_T (F) for the track box system is almost the same that K_{Tn} for the EIFFAGE site system. Also, not significant differences arise when comparing in Table 5-10 TS3-BTS track box system with ME 15 system at EIFFAGE site, both of them having the same rail pad and sleeper plus concrete edged U.S.P. components. From the results presented

in Table 5-11 and Table 5-9 it seems that TS2-BTS track box system fits better reference ME1 system at DB site than TS1-BT track box system. That is coherent with the fact that both German reference sites: ME15 at EIFFAGE site and ME1 at DB site have the same mechanical behaviour in spite of having different Zw rail pads. Higher differences are found however in Table 5-12 when comparing, for the two lower sprung mass levels, TS3-BTS track box system with ME 5 system at DB site. They can be attributed to the different type of sleeper used.

Finally, from the definition of damping ratio "*D*" for O.D.F.S. having stiffness "*K*" and mass "*m*":

$$D = \frac{c}{c_C} \tag{16}$$

where $c_C = 2\sqrt{K \cdot m}$. In that expression "*K*" and "m" may be identified with "K_{Tn}" and "m_{Un}" in Table 5-9 to Table 5-12 after adding half the sleeper mass and the rail bay mass to the "m_{Un}" mass (206 kg for systems with the AI99 and B70 sleepers and 342 kg for systems with the B90.2 sleepers).

In Table 5-13 the "*c*" and "c_c" viscous damping coefficients derived from the abovementioned equations for the different German systems are presented.

Table 5-13: Viscous damping coefficients c_c and c for DB and EIFFAGE test sites

DAMPING PARAMETER	DB site				EIFFAGE site			
	Reference ME1	ME5			Reference ME15	ME15		
D	0,06	0,14	0,16	0,33	0,07	0,175	0,19	0,37
c_C (kN·s/m)	812	682	682	405	810	765	704	488
c (kN·s/m)	49	95	109	133	57	134	134	180

Because of the low value of the dynamic load applied through the BUTTERFLY® shaker to each one of the rail supporting points (± 1.875 kN), it can be expected that the contribution of the ballast and USP to the total energy dissipated in each loading-unloading cycle of the in situ dynamic tests considered in Table 5-13 will be relatively small when compared with the geometric damping.

No explanation has been yet found for the low *D* values obtained in both ME1 and ME5 reference systems. For the interpretation of the more logical values obtained for the ME5 and ME15 systems, the analytical model suggested by Lysmer in [30], which was also used for defining the dynamic load time history in [10], and referred to in Annex 1 of [31], has been used.

That model provides the response to a vertical dynamic load applied to a rigid circular foundation supported by an elastic half-space. From the analogy with the response of one degree of freedom system, the following expression for the half-space viscous coefficient "*c*" was derived in [30]:

$$c = \frac{3.4 r_0^2}{(1-\nu)} \sqrt{\rho G}$$

where

- r_0 represents the radius of the equivalent circular area in contact with ballast
- ν indicates the Poisson ratio of the half-space
- ρ stands for the density of the half-space
- G represents the elastic shear modulus of the half-space

Assuming an equivalent radius of 0.336 m for the B90.2 sleeper, a density of 1800 kg/m^3 for the half-space, a Poisson ratio of 0.20 for the foundation material and a shear modulus corresponding to a shear wave velocity of 240 m/s, a value c = 207 kN·s/m is obtained. To that value of c correspond, for c_c values ranging between 765 and of 488 kN·s/m, as given for ME 15 in Table 5-13, damping ratios, D, between 0.27 and 0.42 instead of the range of values (0.175 to 0.37) given in that Table. If the same half space is considered for ME 5 in DB site and an equivalent radius of 0.30 m is assumed for the B70 sleeper, a c value of 165 kN·s/m is obtained from the above equation. To that value of c correspond, for c_c values ranging between 682 and 405 kN·s/m, as given for ME 5 in Table 5-13, damping ratios, D, between 0.24 and 0.40 instead of the value range (0.14 to 0.33) given in that Table. In both cases the experimental D values are lower than the theoretical ones. That means that the assumption of a half-space below the track for estimating the dynamic loads induced by the rail irregularities should be reconsidered. In that respect, a layered half-space or an elastic layer over a half-space, providing less geometric damping than the half space, may be more appropriate.

5.3.5 IL values obtained in CEDEX track box tests

Although IL spectra in the free field near a given track cannot be obtained directly in CEDEX's track box for obvious reasons, the data collected for realistic dynamic load time histories by the velocity and acceleration sensors installed at different depths in the subgrade of the physical models constructed inside the CEDEX track box may give indications of how effective may be some measures adopted in the track superstructure (e.g.: the replacement of standard sleepers by sleepers with USP's) to abate vibrations at some distance of the track in a free field having geotechnical characteristics similar to the subgrade layers constructed inside the track box.

Up to what extent the magnifying effect of having a bed rock (bottom of the track box) at a depth of only 3.32 m below the track platform (upper surface of the sub-ballast layer, see Figure 5-54) may compensate the minimizing effect of assuming a high damping ratio (D = 0.30) to obtain IL's in the track box similar to those that can be expected in the ground surface near the track is a question that require the use of numerical modelling. Nevertheless, it is expected that the trend of the IL's obtained in CEDEX track box should be the same that in the free field.

The diagram illustrating the use of the CEDEX track box to obtain IL values representative of those that can be expected on the ground surface near the track is presented in Figure 5-54.

Firstly, the theory of random vibrations is used to combine the PSD function of the track vertical irregularities assumed with the response of ODFS travelling at speed "v" and to get the PSD function of the variable dynamic loads generated by a train wheel approaching a point in the track, passing over it and getting away. That function, as sketched in the first row of the diagram, incorporates the unsprung mid-wheelset mass "m" of the train and the dynamic track stiffness "K_T" as determined previously in a step by step static test run in the track box. Since two track box configurations (or systems) are needed to carry out an IL analyses, two

different dynamic load PSD functions: one for the reference system (R) and the other for the new track system (N) should be currently obtained in this step.

In a second step, a variable load time history (1 second long) is derived from each one of the dynamic load PSD functions previously obtained. From each one of those signals, 100,000 samples are extracted having each one of them a duration “d/v “ derived from the width “d” of the deflection bulb generated by a vertical load in each one of the two track systems already tested. Then, from the statistical analysis of their main square values (MSV’s) the wheel pass by design dynamic load time history for each system (R and N) is defined (see the second row of the diagram).

In a third step, each wheel design signal is integrated over the total number of the train wheels keeping in mind their geometric distribution and separation within each bogie. In that way, the variable dynamic load time history induced at a point of the selected track by the passage of the train considered can be sequentially obtained for both the reference (R) and the new (N) track box systems. After incorporating each of the dynamic load time histories obtained in that way to the loading system of the corresponding track system (either R or N), as indicated in the lower part of the diagram, the one-third octave analysis of the signals registered by the geophones G1, G2 and G3 and the accelerometers A1, A2 and A3 installed at different depths in the track box subgrade allows the determination of the $(IL)_v$ and $(IL)_a$ spectra at those depths.

Figure 5-55 shows for the two track box configurations indicated in the diagram and a freight vehicle travelling at v = 120 km/h, as defined in 4.5.2, with 82 bogies, a wheel separation of 1.80 m within each bogie and total loads of 225 kN/axle, the velocity and acceleration IL spectra obtained at the track box points where G1, G2, G3 geophones and A1, A2, A3 accelerometers were located. For the derivation of those spectra a mid-wheelset mass of 712 kg, a geometric damping ratio D = 0.30 and a K_T value of 120 kN/mm (for both “R” and “N” track systems) were adopted.

Although a better prediction would have been obtained for high frequencies if, instead of using the same K_T value for both “R” and “N” track systems, different K_T values had been adopted, the negative peak IL values reflected for frequencies 30-40 Hz in both the velocity and acceleration spectra given in Figure 5-54 fit well the negative peaks of the velocity spectra obtained at different distances from the track in DB site for electric train passages (see Figure 5-23) and for shaker tests (see Figure 5-24 and Figure 5-25). For frequencies less than 30-40 Hz all the spectra in Figure 5-55 provide positive IL values indicative of vibration abatement as could be expected from the use of a soft USP in the “N” track system.

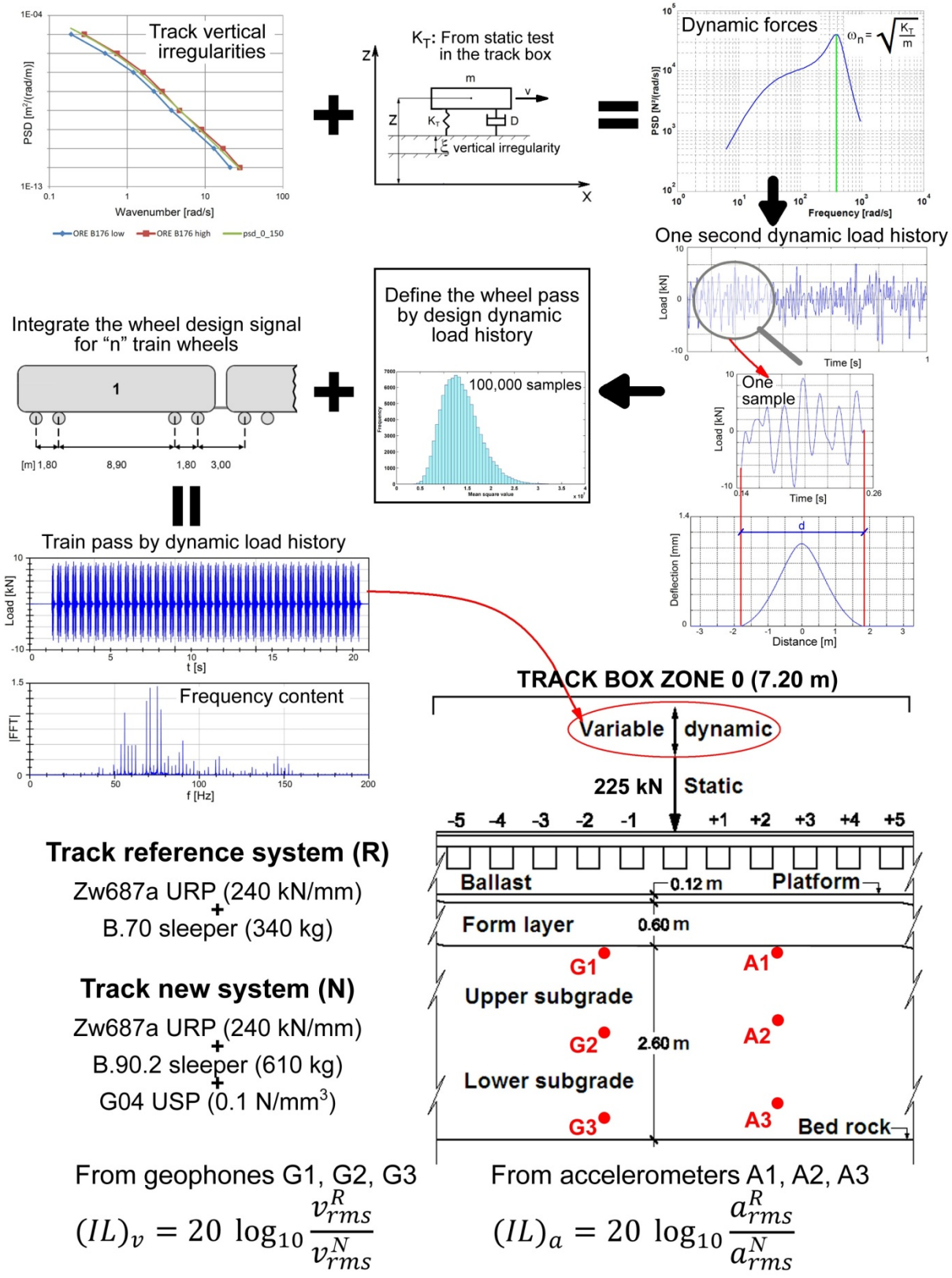

Figure 5-54: Diagram illustrating the use of CEDEX track box for the analysis of IL values

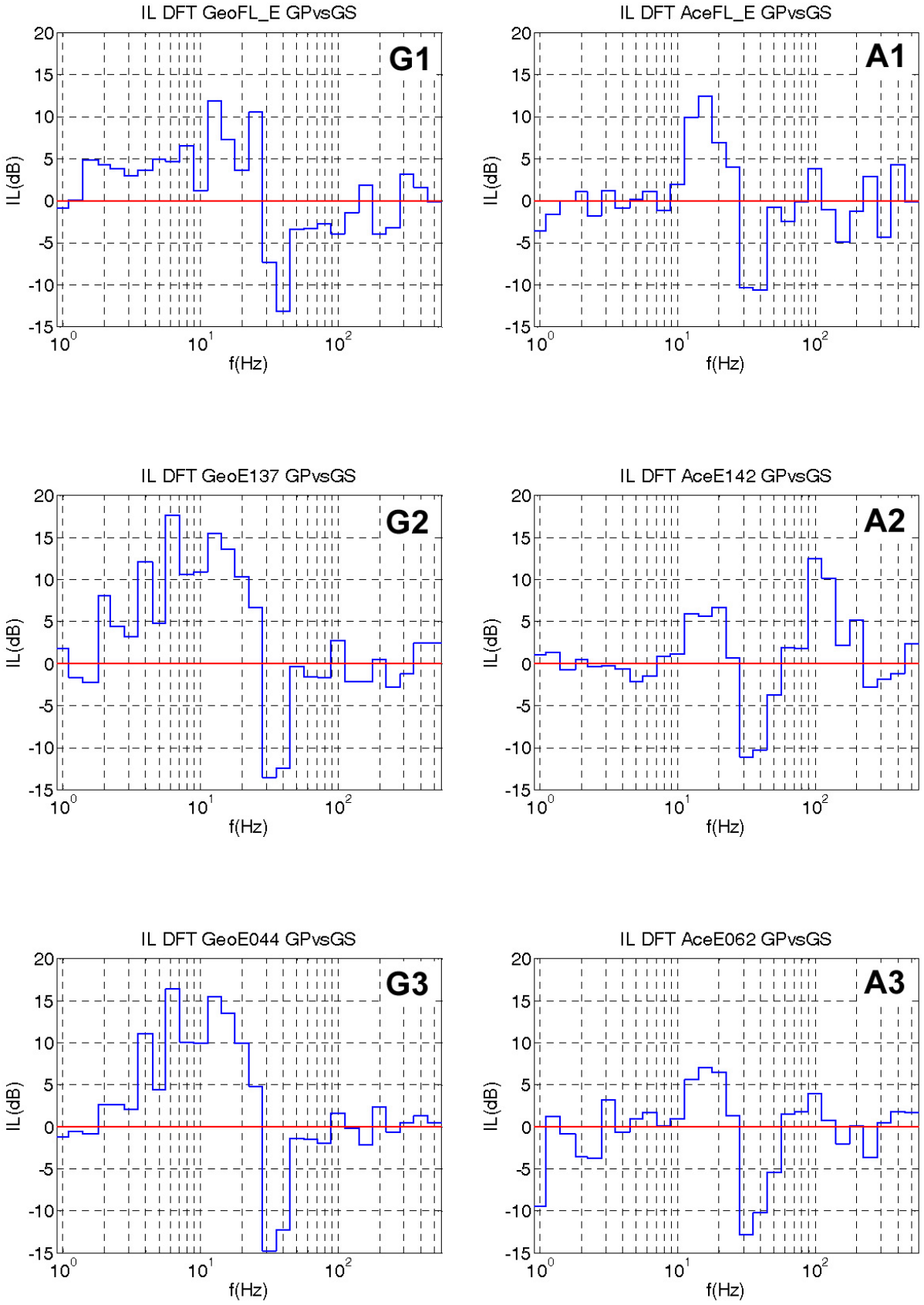

Figure 5-55 Velocity (G1, G2, G3) and acceleration (A1, A2, A3) IL spectra obtained

5.3.6 Summary and suggestions for further developments in CEDEX track box

Based on the joined interpretation of the results obtained in the laboratory tests run for the RIVAS project at CEDEX track box and the dynamic in situ tests with sprung and unsprung masses at DB and Eiffage sites, an effort has been made to incorporate in a rational way the nonlinear behavior of the track systems for the estimation of the dynamic loads and insertion loss (IL) that can be expected in ballasted tracks founded in good subgrade soils having a shear wave velocity around 250 m/s.

In the wheel load-track deflection curves obtained in the step by step static load tests run in the track box, two different types of track stiffness values have been distinguished: global track stiffness values $K_G(\ )$ governing the behavior of the track under high total mass (unsprung + sprung) loads and track stiffness values $K_T(\ )$ commanding the generation of dynamic loads and the track deflections induced by those loads and low unsprung masses when applied statically to the track. The ratio between those two types of track stiffness values characterizes the non- linear behavior of the system. In that respect, out of the different track box systems tested, TS1-BT, TS1-B1M and TS2 can be considered almost linear and TS3-BT, TS3-BTS, TS3-B1M and TS3-B2M strongly non-linear.

Depending on the nonlinear behavior of the track system and the total load level to which the track is subjected, the $K_T(\ )$ value may be higher, equal or lower than the $K_G(\ )$ value. For a track system such as the TS3 system with a soft USP and total load levels above 200 kN axle loads, the results obtained in track box show that the system may react to the dynamic loads with track stiffness values $K_T(\ )$ equal or higher than much stiffer systems without USP such as the TS1 and TS2 systems.

Results of the receptance tests carried out with the track loaded and unloaded have shown the importance of performing those tests with accelerometers located in the rail head as close as possible to the striking point. The best results for the loaded systems were obtained with heavy hammers in the 20-45 Hz range and with slight hammers in the 30-40 Hz range. As expected, the track stiffness values derived for the receptance values in those frequency ranges were higher than the $K_T(\ )$ values obtained in the step by step static test, with ratios ranging between 1.4 and 1.6 for the loaded systems and between 1.1 and 1.2 for the unloaded ones.

Concerning the short lasting quasi-static tests, it has been shown that the range of frequencies generated depends on the vehicle passage speed simulated in the test. In those tests, the harmonics of the wagon passing by frequency plays an important role. The global track stiffness derived from the data collected in this type of test agree well with the $K_G(\ )$ values obtained in the static tests.

In the long lasting quasi-static tests, the stabilization of ballast in TS3 system has led to a more homogeneous system with variations of track stiffness along seven consecutive sleepers in both rails less than 8% of the mean value. The net effect of the application of 1 M axle loads to the TS1 system has been one decrease of 15% in the static track stiffness values, while only one slight decrease was observed in the TS3 system after the application of the first 1 M axle loads and no change along the second million. On the other hand, ballast in the TS3 system has experienced higher permanent settlements along the 1M axle load process (1.15 mm) than in the TS1 system (0.85 mm). As expected, the velocities and accelerations induced in TS1 system under the pass by of freight vehicles at 120 km/h have been higher in the rails than in the sleeper whereas the opposite effect was found in TS3 system (higher ve-

locities and accelerations in the sleeper than in the rails). The sleeper being the main vibrating element in TS3 system could explain the higher level of permanent displacements.

Big differences have been found in the spring stiffness values of the rail pads (URP) when comparing the results of static and quasi-static tests in the track box and those obtained by CEDEX and BAM [26] in slow and quick compression tests run in conventional laboratory rigs. The rotation of the rail pads towards the internal part of the track when loaded vertically either in the track box or in a real line may explain those differences which require the instrumentation of the rail pads at both sides of the rail to get realistic rail pad spring stiffness values either in the track box or in a real line. For the Zw 687a rail pad, a spring stiffness of 240 kN/mm, less than the 300 kN/mm value of the Zw 900b rail pad but higher than the 100 kN/mm of the PAE-2 rail pad, has been obtained in a conventional rig quick compression test carried out in CEDEX.

Dynamic tests performed in the track box provided $K_T(\ )$ values, for the different track box systems, that confirm the $K_T(\ )$ values derived from the step by step static tests once the load level induced by the hydraulic cylinder load, at the rail point where the piezoelectric shaker was located, is taken into account.

An iterative procedure has been set up to obtain the dynamic parameters of the German in situ track systems having the same superstructure components that the track box systems. In that process the German systems have been assumed to behave as one degree of freedom systems (O.D.F.S.) with the same static and dynamic displacements that the track deflections of one of the four track points supporting the static masses and the harmonic force applied to the in situ dynamic tests. The range of track stiffness $K_T(\ )$ values obtained for the German systems has been the same that the one determined in the track box tests. The damping ratios found for the ME 5 and ME 15 German systems with standard and innovative sleepers indicate that a layered system rather than an elastic half-space should be considered to define the geometric damping needed for estimating the dynamic loads induced by the rail irregularities.

A diagram has been developed (Figure 5-54) illustrating how CEDEX track box can be used to get the trend of the IL's values that can be expected in the free field at some distances of the track. For two track box systems having the same track substructure: one with standard sleepers and the other with sleepers having USPs, the same amplifying frequencies that in DB and EIFFAGE sites under the passage of electric trains and the dynamic effect of a hydraulic shaker have been obtained. For frequencies less than those a consistent abatement effect has been obtained in all the track subgrade points instrumented in the track box.

Further improvements in the CEDEX track box will be aimed to a better characterization of the dynamic load time histories used in the dynamic tests and to improve the IL's predictions for high frequencies. To achieve those goals, the results obtained in the dynamic in situ tests run at DB and EIFFAGE sites will be taken into account and the protocol to run the static tests in the track box will be modified so that $K_T(\ )$ track stiffness values can be determined in a very reliable way and different train dynamic force time histories, according to the dynamic track stiffness of each one of the two track systems involved in the IL analysis, should always be used. Besides, the possibility to apply quasi-static high load amplitude histories and dynamic low amplitude histories simultaneously will be explored and ways to apply both hydraulic cylinder loads and piezoelectric shaker loads at the same rail point will be investigated.

6. EXCURSION I: COMPARISON OF DIFFERENT METHODS TO ANALYSE TRAIN PASSAGES MEASUREMENTS

As mentioned before in chapter 5.1.4 the performed data evaluation followed initially in some parts the German DIN standards which are slightly different from the RIVAS measurement protocol which was partly based on the former RENVIB project [17].

In the present case, measurements of train passages were evaluated by means of "fast"-weighted, max-hold 1/3 octave band spectra L_{vFmax} (f_{Tn}) according to DIN45672-2 [17] and VDI 3837 [19], the so-called "maximum third octave speed spectrum". On contrary, the RENVIB respectively RIVAS measurement protocol recommends a procedure based on the equivalent vibration level averaged over the train passage time.

The "fast"- weighted, max-hold 1/3 octave band spectra are not only much easier to evaluate but in particular within the use of vibration prediction models leading to input emission spectra on the "safe" side for the vibration prediction. For this reason, most analytical prediction models as described in e.g. in VDI 3837 [19] are based on these spectra.

It was initially assumed that the different evaluation procedure will not have a significant influence on the determination of IL. By performing an additional analysis of the existing data, the two analysis procedures were compared within RIVAS.

The next paragraphs and figures show the main conclusions, a more detailed evaluation can be found in the additional report [7], respectively added as annex A2 to this deliverable.

6.1 THE FREQUENCY DOMAIN TRANSFORMATION

According to [2] and [17] respectively, the train passage vibration measurement data have to be analyzed in the following way:

The analysis time T_a (which encloses the entire passage duration to get all the vibration energy) and the passage time T_p (which corresponds to the geometrically passage time from buffer to buffer) are determined according to Figure 6-1. According to [17] "…by experience, the passage time begins when the relative amplitude reaches about ¼ of the most frequently encountered maximum level and ends at the same level".

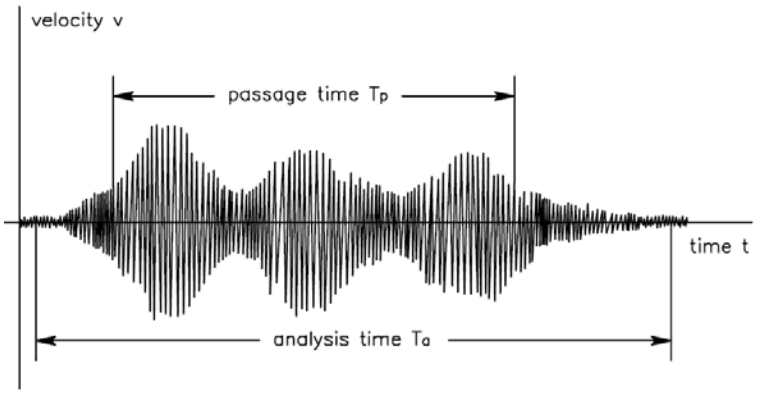

Figure 6-1: Definition of passage time T_p and analysis time T_a as given in [2] and [17]

Since the vibration from all train passages were measured simultaneously, the single passage time T_p of the three sections ME1, ME4 and ME5 have a time offset according to the distance of more than 300 m between the measurement sections, as displayed in Figure 6-2. Therefore the time histories have to be synchronized with regard to time, see Figure 6-3.

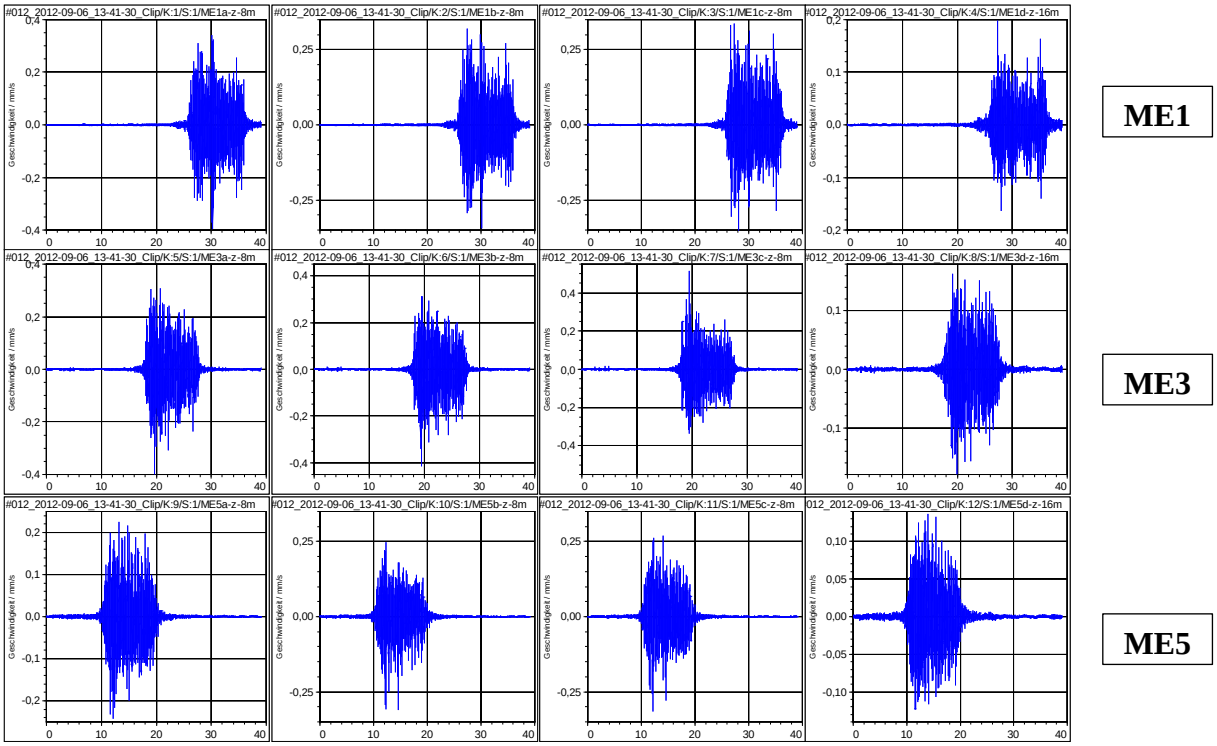

Figure 6-2: Example of an ICE passage time history

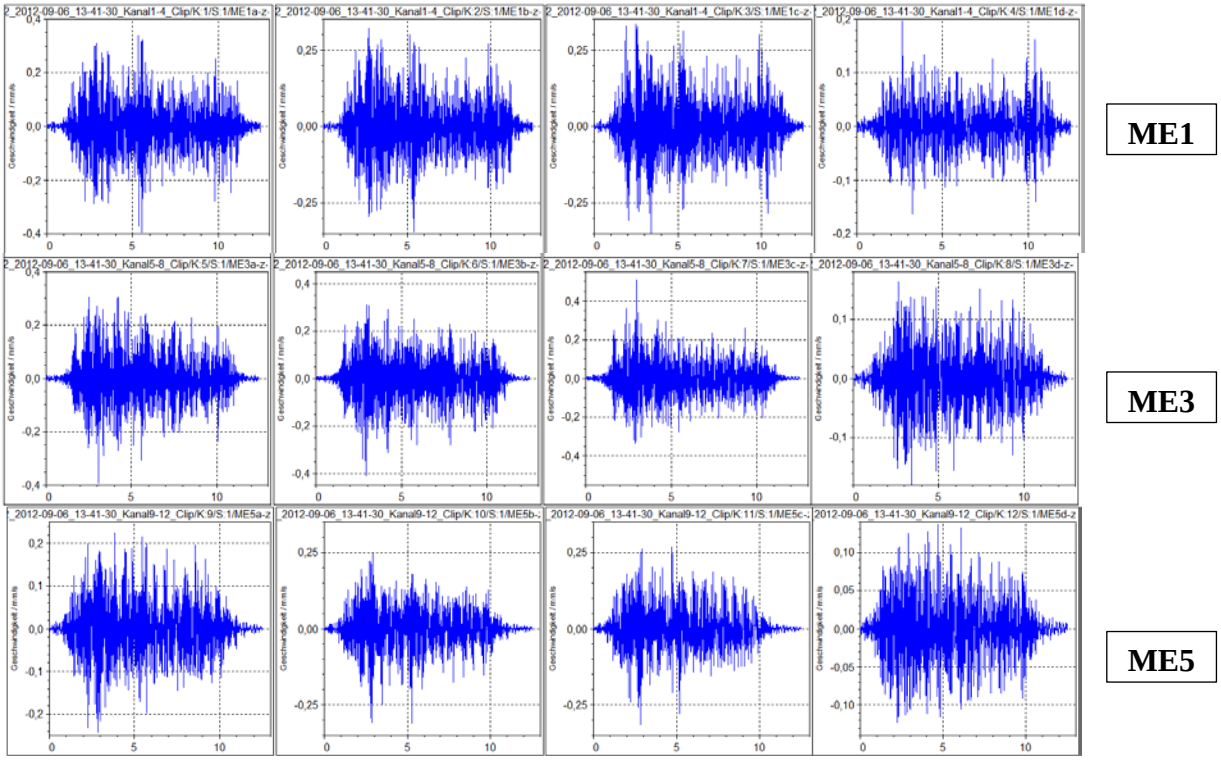

Figure 6-3: Time synchronization

Then the velocity signals within the time window T_a are transformed into frequency domain by means of FFT with Hanning weighting. The used block size is 2048, the used overlap is 75% and the single velocity spectra are averaged by means of rms (energy). Then, the spectrum is reduced to a third octave band spectrum.

This procedure leads to a third-octave spectrum of the vibration velocity for each measuring location and for each train passage. In the next step the vibration level $L_v(f)$ has to be normalized by the vibration energy to the train passage time according to the following equation

$$L_v(f) = 20\log_{10}\frac{v(f)}{v_0}dB + 10\log_{10}\frac{T_a}{T_p}dB \qquad (6.1)$$

where v_0 is a reference velocity, T_a the analysis time and T_p the passing time of each train passage.

Additionally, the spectra of the 8m measuring points at each section are averaged arithmetically. Moreover, the vibration level spectra measured during the passage of the trains belonging to the same train category are also averaged arithmetically.

Attention: The RENVIB protocol [17] specifies a reference velocity $v_0 = 1\cdot10^{-9}$ [m/s]. In contrast, the used reference velocity within the RIVAS reports [6] and [8] as well as the mentioned value of some technical standards as DIN 45672-2 [18] is $v_0 = 5\cdot10^{-8}$ [m/s]. This fact must be considered when the absolute values in this chapter are compared with the values which are listed and shown in the rest of this deliverable respectively in the reports there this deliverable is based on.

6.2 RESULTS FOR TRAIN PASSAGES SPECTRA

Figure 6-4 shows the direct comparison of the train passage spectra for the three train categories at the reference measurement section ME 1 (without USP). This is directly comparable to the Figure 5-14 of this report. The different evaluation procedures show differences by regarding the absolute values, but the characteristics values and frequencies for the different speed depending excitation mechanisms are in the same frequency ranges.

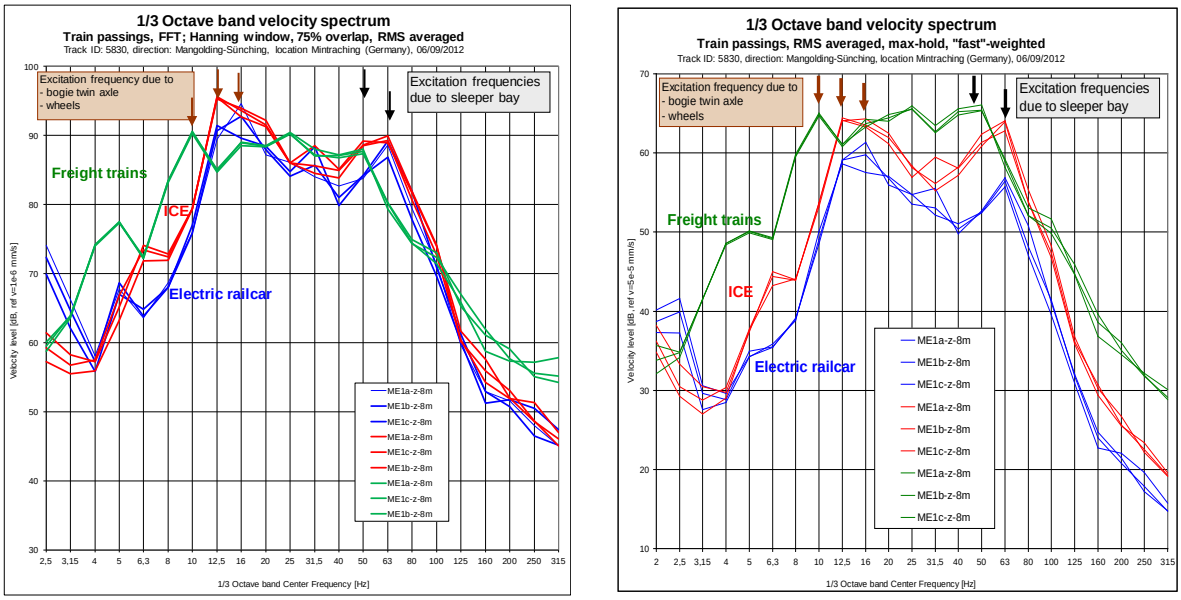

Figure 6-4: Comparison of the train passage spectra for the three train categories at the referent section ME 1. Left: evaluation according RIVAS, RENVIB measurement protocol over train passage time, right with the evaluation as the maximum third max-hold spectra, according DIN 45672-2

6.3 RESULTS FOR INSERTION LOSS SPECTRA

The insertion has to be evaluated for each single train passages separately. Since the pass by speed at all measurement sections was constant the analysis time T_a as well as the passage time T_p is identical. In this case the normalization of the spectra to the train passage time according to equation (6.1) is irrelevant in terms of the insertion loss.

Furthermore the evaluation process for determining the IL follows the same procedure as described in the previous chapters (refer chapter 5.1) including the two different methods for the subsoil corrections.

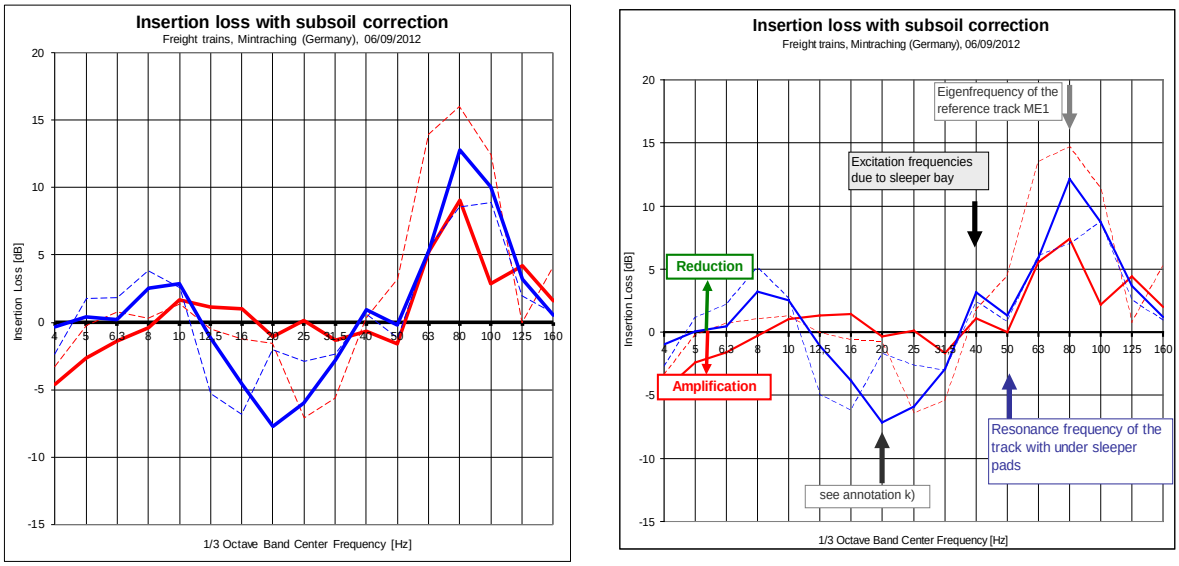

Figure 6-5: Insertion loss for freight trains with the subsoil correction method I (impact transfer mobility), at the left site according the RIVAS / RENVIB evaluation procedure and on the right side for the evaluation as the maximum third max-hold spectra, according DIN 45672-2

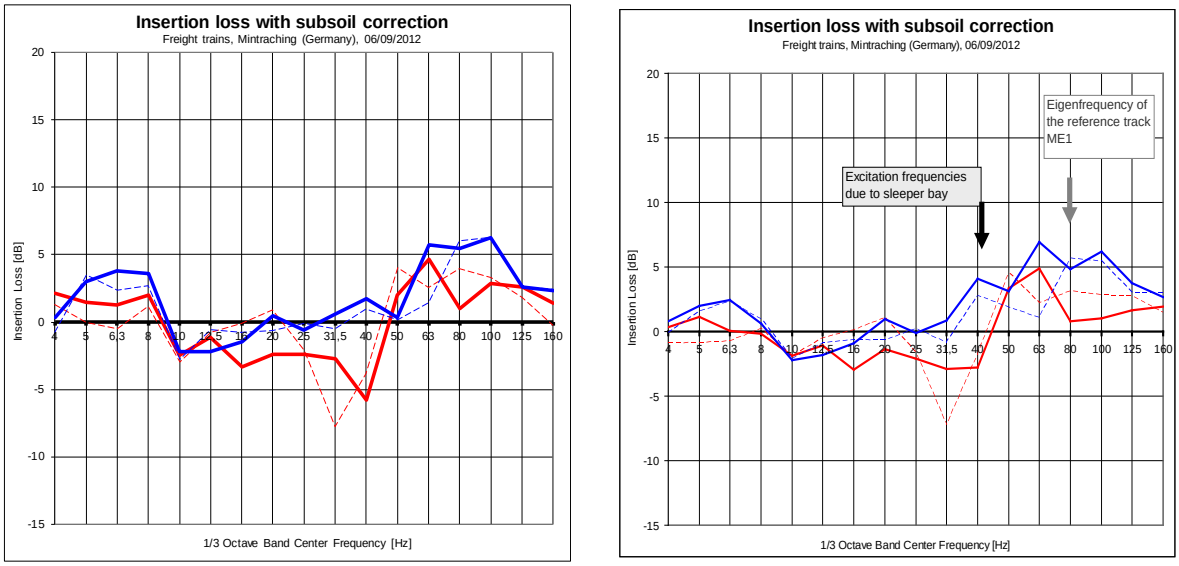

Figure 6-6: Insertion loss for freight trains with the subsoil correction method II (“train passages on neighbour track”), at the left site according the RIVAS / RENVIB evaluation procedure and on the right side for the evaluation as the maximum third max-hold spectra, according DIN 45672-2

Figure 6-5 shows the direct comparison of the IL for freight trains by the two evaluation procedures and the subsoil correction method I. Figure 6-6 shows the same but for the subsoil correction method II ("train passages on neighbour track").

The examples for the other train categories are given in the report (Annex A2, [7]).

It is obvious that the determination of the IL is not effected by the different evaluation procedures.

6.4 SUMMARY AND CONCLUSIONS

The train passage measurement data have been originally evaluated by means of "fast"-weighted, max-hold 1/3 octave band spectra (bandpass filtering in the time domain). Within an additionally evaluation process the analyses of the train passage where carried out at time histories according to [2], [17] which request a FFT analysis using rms averaging.

It is evident that the absolute values of the 1/3 octave band spectra of the train passage are different because of

- the different reference velocity ($v_0 = 1 \cdot 10^{-9}$ instead of $5 \cdot 10^{-8}$ [m/s]) and
- the need of normalization to the train passage time, see equation (6.1).

Nevertheless, the trends of the spectra as well as the dominant excitation frequencies are the same.

On the other hand, the evaluation of the insertion loss is unaffected by the specific analysis method. That is why the insertion losses of both analysis methods show comparable results.

A more detailed description of the evaluation process is given within ANNEX A2.

7. EXCURSION II: DETERMING THE SUBSOIL CORRECTION FUNCTION BY LINE TRANSFER MOBILITY MEASUREMENTS

From the measurement results for the three measurement sections ME 1, ME 3 and ME 5 in chapter 5.1, it is obvious that there is a need for an accurate determination of subsoil corrections functions. Within the first measurement campaign two different subsoil corrections were performed as described in chapter 5.1.5:

- Direct correction by transfer mobility function with impact load as falling mass (Method I)
- Indirect soil correction by trains in opposite track (Method II)[1]

The two methods lead to different results (Figure 5-23).

The main reasons for these different results lay in the different characteristic of the sources. As discussed previously in chapter 5.1.5 respectively within the measurement report [6], the transfer function by an impact load represents a well-defined “point source” while the trains on the opposite track reflect more a “line source” excitation. For using with the stationary vibration excitation, the subsoil correction by impact load may be adequate because both of them have “point source” characteristics. For subsoil corrections of train passage measurements, a procedure reflecting the line source characteristics seems to be more suited.

Thereforeit was recommended in [6] to enlarge the locations of the impact tests and therewith the length of influence, like displayed in Figure 7-1. In this way, it is possible to integrate numerically the single point source transfer mobility’s over the influence length to obtain the line source transfer mobility.

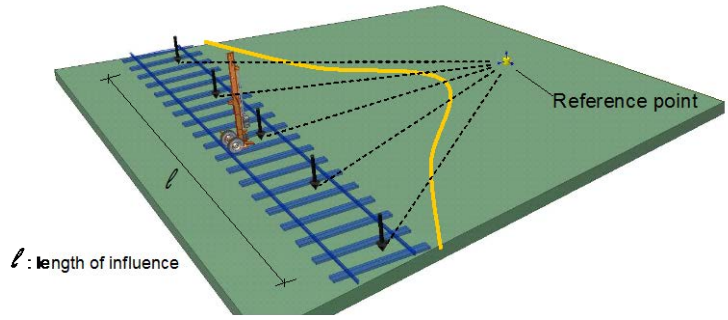

Figure 7-1: Evaluation of the line source transfer mobility by several point source excitations (sketch taken from [6])

To investigate the subsoil correction function by this line transfer mobility function, an additional measurement campaign was performed. The procedure followed the recommendation given by RIVAS deliverable D1.11 [33] and the FTA guidelines [34]. The full description of the performed investigation can be found within the report [35] which is added as annex C to this deliverable.

[1] Remark: This indirect method II with the correction by using the trains on opposite track is only possible, if the opposite track has on the whole length of the different measurement sections which are to compare, homogeneous track configuration, maintenance stage and substructure conditions. In this case it can be assumed that differences measured in the vibration points at the different measurement sections beside the track, have to be effected by a change within the soil transfer conditions and not by the excitation mechanisms of trains or the train/track interaction.

7.1 GENERAL LAYOUT OF THE MEASUREMENT AND DESCRIPTION OF PROCEDURE

For the investigations, the existing DB test site with the same three measurement section as for the previous investigation and described in chapter 5.1.1was used. For the measurements, a layout of measurement positions and exciting points as presented in Figure 7-2 was installed. Considering all measurement sections, an influence length of 120 m between the two outward exciting positions could be covered.

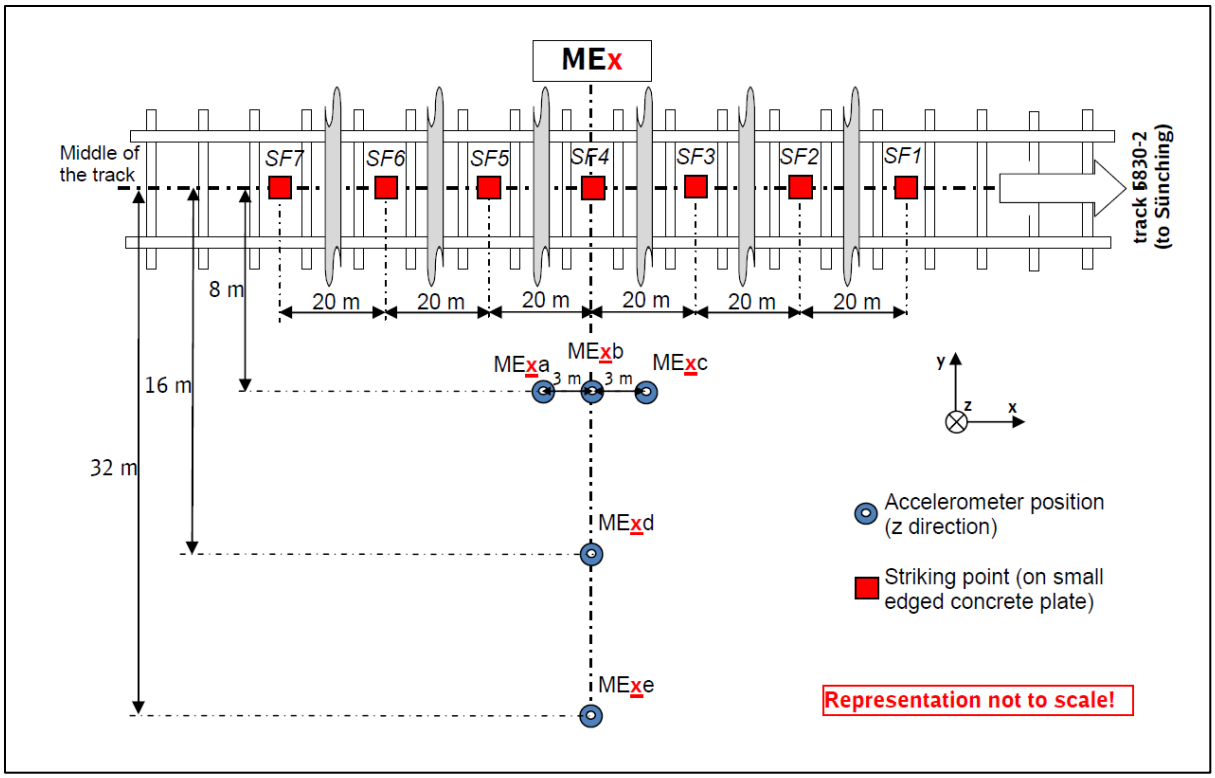

Figure 7-2: Layout of the 7 exciting positions within the track center and the respond measurements points beside the track, in each measurement section (ME 1, ME 3 and ME 5) the same layout was used

For the excitation, an impulse hammer with 5,5 kg hammer-mass was used. To get statistically robust results, a lot of exciting repetitions were carried out.

According to the recommendation given in [33] the line transfer mobility TM_L was determined for a given measurement position (MExa to MExe) by the superposition of all the point transfer mobilities along the line source (i.e. over all the impact positions of the measurement area).

In Figure 7-3 a representative example for the time history and the frequency content for the measurement section ME 1is presented.

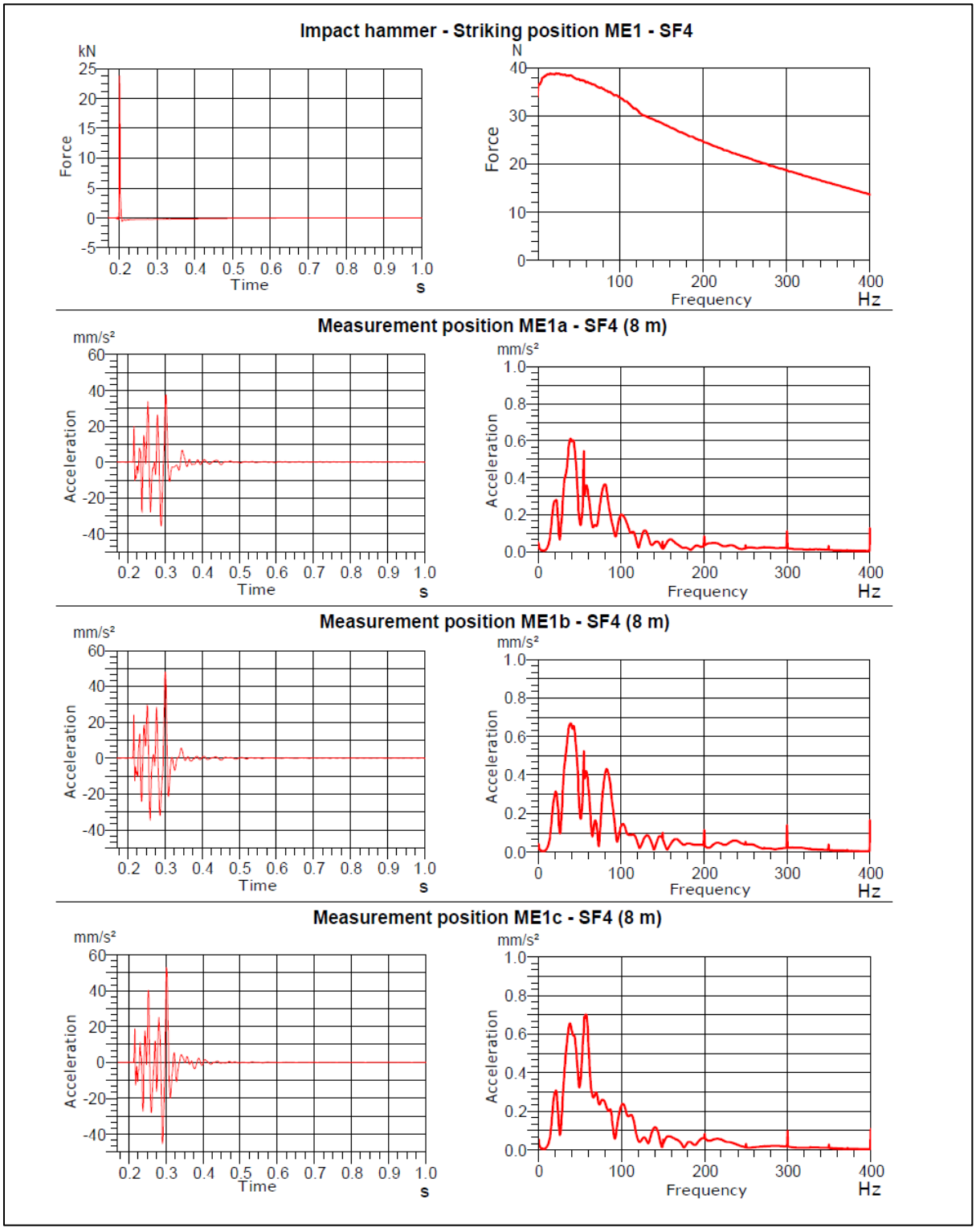

Figure 7-3: Time history and frequency contend of impact hammer and the measured free field accelerations at the 8m points

7.2 MAIN RESULTS AND COMPARISON WITH PREVIOUS INVESTIGATION

For each of the measurement sections, the calculated results of this line transfer mobility TM_L was presented. Figure 7-4 shows an example for ME 1:

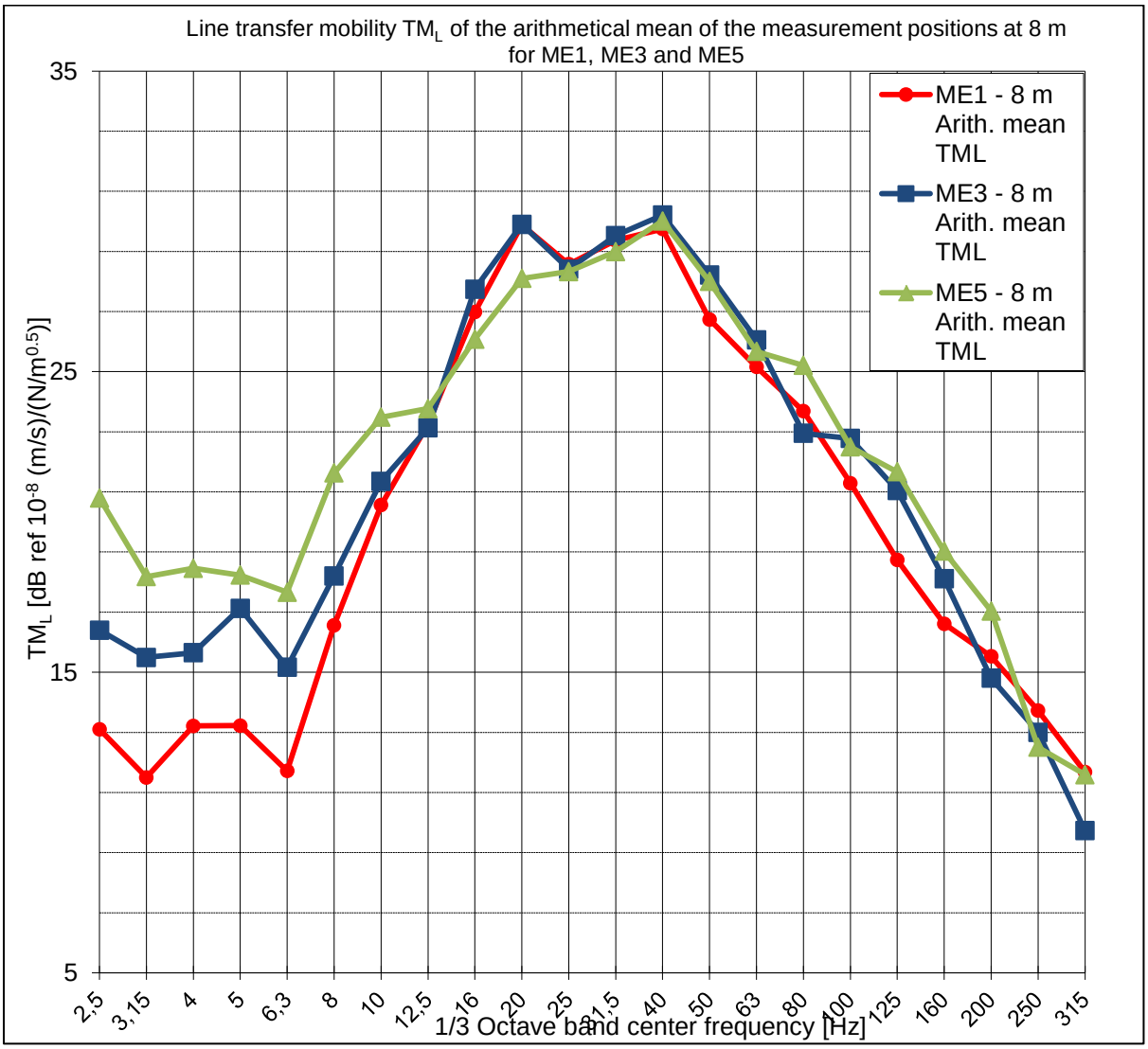

Figure 7-4: Line transfer mobility TML at ME 1 for the three positions at 8 m, the 16 m and the 32 m measurement position

Also in this example it becomes obvious that in particular the ME 5 section differs significantly but a little less distinctive from the two other measurement sections as discussed within chapter 5.1.5. This may be constitute with the longer influence length of the sections which could be into account, so that not only the line source characteristics but also impacts of very local effects are less considered as by the shorter influence-length of the point mobility.

Figure 7-5 displayed a direct comparison of the transfer mobility of ME 3 and ME 5 referred to the reference section ME 1 for the point transfer mobility with the falling mass and the line transfer mobility.

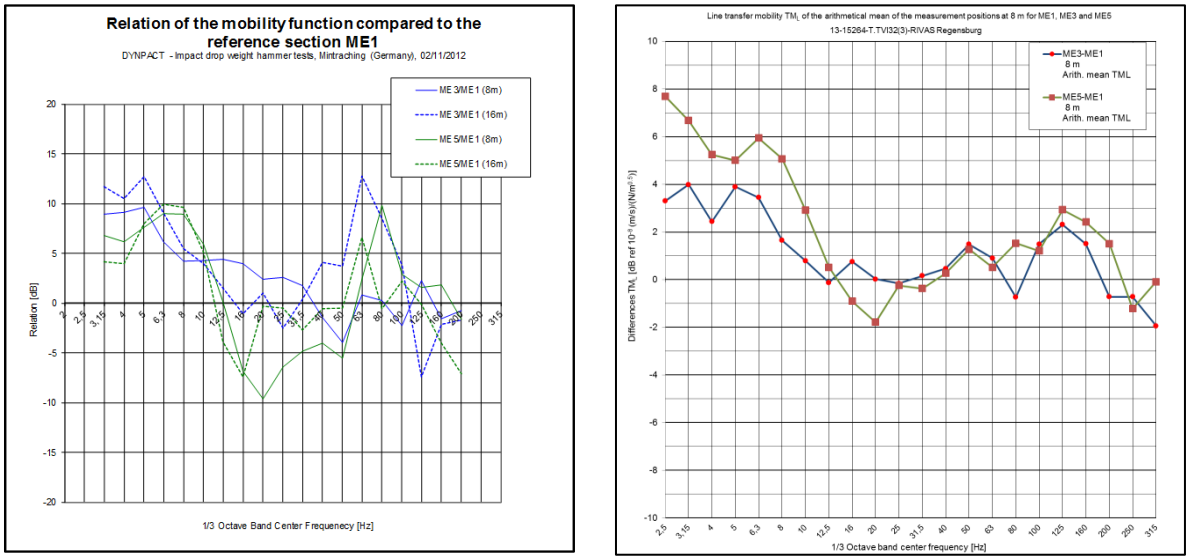

Figure 7-5: Transfer functions for ME 3 and ME 5 referred to the “reference section” ME 1, on left side for the point transfer function with the falling mass (according report [6]) and on right side for the determination of the line transfer mobility according the report [35].

8. FINAL CONCLUSIONS

The results for the determination of IL by the stationary excitation of shaker shows the expected results compared to calculation methods based on dynamic models with mass-spring systems or impedance models as described in [32].

The results of IL obtained by measurements during train passage show particular for the lower frequency range some additional positive mitigation effects which are not possible to explain with these simplified models. This phenomenon was also recognized in several other investigations as described in [36] and [37] as well as further publications.

As outlined in Chapter 4.2 the vibration generation by trains is caused by different vibration generation effects. Not all of these effects can be stimulated by a stationary vibration generation in an appropriate way to simulate train passage.

It was concluded that the USP have some additional positive side-effects on vibration mitigation which cannot be described with simple calculation models as well as with the stationary harmonic artificial excitation. This mitigation effects based on mechanical behaviour e.g. due to embedding the ballast stones in resilient material with an increase of contact area together with an decrease of contact forces between ballast and sleeper [38] and [39], the better load-distribution in longitudinal direction as well as the general better track quality (e.g. avoiding of hanging sleepers) cannot be detected by stationary excitation. This gives also an explanation that the mitigation effect of USP is often underestimated then using dynamic prediction models.

The presented investigations with the determination of insertion loss by artificial excitation compared to measurements of train passages of USP (under-sleeper pads) in tracks led to following main conclusions

- The procedure and practicability of the artificial shaker excitation in particular within the track with short track possessing time was successfully practical approved.
- To simulate the dead load (sprung and un-sprung masses) is an essential requirement to get realistic results.
- The determination of IL by train passing's show that the determined IL depends significantly on the different train categories. This is caused by the dominant influence of the parametric excitation in combination with USP. Therefore it is not possible to define one definitely reference IL for the comparison of train passages and artificial excitation.
- For determination of the insertion loss, a soil correction of the different sections (e.g. with transfer mobility functions) is essential to obtain reliable results.
- The test with artificial excitation is capable to show the dynamic characteristics of a track. The results for the IL by the stationary excitation shows a good agreement with the expected results compared to calculation methods based on dynamic models with mass-spring-systems or impedance models [20]. The results of IL by train passages show particular for the lower frequency range some additional positive mitigation effects which are not possible to explain with these simple models. This phenomenon was recognized before in several other investigations as described in [21] and [22] and further publications. Compared to other resilient elements (under ballast mats, floating slab-systems), the parametric excitation has a more dominant effect.

- This clearly shows that the USP have some additional positive side-effects on vibration mitigation which cannot be described with simple models as well as with the stationary harmonic artificial excitation. This mitigation effects based on mechanical behaviour e.g. due to embedding the ballast stones in resilient material with an increase of contact area together with an decrease of contact forces between ballast and sleeper [23], the better load-distribution in longitudinal direction as well as the general better track quality (e.g. avoiding of hanging sleepers) can`t be detected by stationary excitation. This gives also an explanation that the mitigation effect of USP is often underestimated when using dynamic prediction models.

Based on the joined interpretation of the results obtained in the laboratory tests run for the RIVAS project at CEDEX track box and the dynamic in situ tests with a hydraulic shaker provided with sprung and unsprung masses at DB and Eiffage sites, an effort has been made to incorporate in a rational way the nonlinear behavior of the track systems for the estimation of the dynamic loads and insertion loss (IL).

A diagram has been developed (Figure 5-54) illustrating how CEDEX track box can be used to get the trend of the IL's values that can be expected in the free field at some distances of the track. For two track box systems having the same track substructure: one with standard sleepers and the other with sleepers having USP's, the same amplifying frequencies that in DB and EIFFAGE sites under the passage of electric trains and the dynamic effect of a hydraulic shaker have been obtained. For frequencies less than those a consistent abatement effect has been obtained in all the track subgrade points instrumented in the track box.

The investigations will help for further improvements in the CEDEX track box with the aim of a better characterization of the dynamic load time histories used in the dynamic tests and to improve the IL's predictions for high frequencies.

9. REFERENCES

[1] RIVAS; Railway Induced Vibration Abatement Solutions, www.rivas-project.eu

[2] RIVAS, Deliverable D1.2: Stiebel, D.: Protocol for free field measurements of mitigation effects in the project RIVAS for WP 2, 3, 4, 5, (2011).

[3] RIVAS Deliverable D1.2 Annex: Stiebel, D. et.al: Measurement protocol for parameters influencing mitigation effects, (2012)

[4] DIN SPEC 45673-3 (Working draft 2013): Mechanical vibration - Resilient elements used in railway tracks - Part 3: Experimental evaluation of insertion loss from artificial excitation of mounted track systems (in a test rig and in situ). In preparation as replacement for DIN V 45673-3:2004-09.

[5] Mistler, M.; Heiland, D.: Erschütterungsprognose mit Hilfe künstlicher Anregungsmethoden, in VDI-Berichte 2063, proceedings Baudynamik Kassel, (2009)

[6] Mistler, M., Heiland, D.: Free field vibration measurements - Experimental investigation of the Insertion Loss of under-sleeper pads within the framework of RIVAS "Railway Induced Vibration Abatement Solutions - Collaborative Project", Measurement Report ID 80-7781-B1 Rev A (17.06.2013), Annex A1 of RIVAS deliverable D1.10

[7] Mistler, M., Heiland, D.: Additional data analysis of the train passage vibration measurements, Appendix to report 80-7781-B1, (13.09.2013), Annex A2 of RIVAS deliverable D1.10

[8] Mistler, M.; Heiland, D.: Free field vibration measurements - Experimental investigation of the Insertion Loss of under-sleeper pads within the framework of RIVAS "Railway Induced Vibration Abatement Solutions - Collaborative Project", Test report of vibration measurements in Herne, Measurement Report ID 80-7780-B4 (2013), Part of RIVAS deliverable D3.15

[9] Nélain, B., Vincent, N.; Lombaert, G.; Degrande, G.; Control of railway induced ground vibrations: influence of excitation mechanisms on the efficiency of resilient track layers, Proceedings of the 11. IWRN (International Workshop on Railway Noise), Udevalla (2013)

[10] RIVAS Deliverable D3.7 Part A: Cuéllar, V. et al.: Results of laboratory tests for ballasted track mitigation measures: CEDEX track box tests, (2013)

[11] Zimmermann, H.: Die Berechnung des Eisenbahnoberbaues, Berlin (1941)

[12] Moreno, J.: Reproducción mediante ensayos a escala real del efecto en la vía de la circulación ferroviaria a alta velocidad, Tesis doctoral, E.T.S. de Ingenieros de Caminos UPM, 537 pp. (2008)

[13] Behr, W.: Innovationsprojekt "Leiser Zug auf realem Gleis" (LZarG), Abschluss-Bericht, Förderkennzeichen 19 U 7020 A) (2012)

[14] DIN 45669, Measurement of vibration immission
Part 1: Vibration meters - Requirements and tests
Part 2: Measuring method

[15] Said, S.; Auersch, L.; Rücker, W.: Geotechnical data and soil characteristics of the test site in Tiefbrunn near Regensburg, Part of Deliverable D1.10, Berlin (2013)

[16] RIVAS Deliverable D1.1: Houbrechts, J. et al.: Test procedures for the determination of the dynamic soil characteristics, Deliverable D1.1 of the European research project RIVAS, “Railway induced vibration abatement solutions”, International Union of Railways (UIC), Paris, 2012

[17] RENIVIB II Phase 3, Measurement protocol vibration and ground borne noise, AEAT, 2003

[18] DIN 45672-2: Vibration measurement associated with railway traffic systems - Part 2: Evaluation method

[19] VDI 3837: Ground-borne vibration in the vicinity of at-grade rail systems - Spectral prediction method

[20] DIN 45673-4: Mechanical vibration - Resilient elements used in railway tracks - Part 4: Analytical evaluation of insertion loss of mounted track systems

[21] UIC International Union of Railways (2009), UIC Project Under Sleeper Pads - Semelles sous traverses - Schwellenbesohlungen Summarising Report, http://www.uic.org/IMG/pdf/2009-03-26_Summarising_Report_UIC-USP.pdf

[22] Loy, H.: Mitigation vibration using under sleeper pads, Railway Gazette International, April 2012

[23] Freudenstein, S.: Die Kontaktspannung zwischen elastisch besohlten Schwellen und Schotter, Eisenbahntechnische Rundschau ETR, Mai 2011, Nr. 05

[24] RIVAS Deliverable D2.1: Nielsen, J. et al.: Classification of track conditions with respect to vibration emission, (2012)

[25] Claus, H. & Schielen, W.: Modeling and simulation of railway bogie structural vibrations, Vehicle System Dynamics Suppplement 28, pp. 538-552, (1998)

[26] RIVAS Deliverable D3.7 Part B: Knothe, E.: Results of laboratory tests for ballasted track mitigation measures: Under sleeper pads (USP), (2013)

[27] Cuéllar, V. et al.: Ensayos quasi-estáticos de larga duración con trenes de mercancías en un tramo de vía de alta velocidad con 12 cm de subbalasto bituminoso construido en el Cajón del CEDEX, Encomienda de Gestión por el Administrador de Infraestructuras Ferroviarias (ADIF) al CEDEX para la realización de trabajos de investigación y desarrollo tecnológico en el cuatrienio 2010-2013, 335 pp. (2012)

[28] RIVAS Deliverable D3.7 Part C: Knothe, E.: Spanish rail pads – Spring modulus. Comparison Spanish and German tests, (2013)

[29] Said, S. et al.: Geotechnical soil properties of the test site by Eiffage Rail GmbH in Herne, Germany. Part of RIVAS Deliverables D3.14 and D3.15, (2013)

[30] Richart, F. E. et al.: Vibration of soil and foundation, Prentice-Hall, 414 pp. (1970)

[31] ORE D117/RP6/F.: Application optimale de la voie classique au trafic de l’avenir: Caractéristiques rhéologiques de la voie, (1975)

[32] DIN 45673-4: Mechanical vibration - Resilient elements used in railway tracks - Part 4: Analytical evaluation of insertion loss of mounted track systems

[33] RIVAS Deliverable D1.11: Verbraken H., Degrande G.; Lombaert G.; Stallaert B., Cuellar V.: Benchmark tests for soil properties, including recommendations for standards and guidelines (05/12/2013)

[34] C.E. Hanson, D.A. Towers, and L.D. Meister. Transit noise and vibration impact assessment. Report FTA-VA-90-1003-06, U.S. Department of Transportation, Federal Transit Admininistration, Office of Planning and Environment, May 2006.

[35] Depuis, H.: RIVAS WP1: Line transfer mobility measurements with hammer excitation of three subsoils on track 5830-2, km 102,13 to km 103,25, Report 13-15264-I.TVI32(3)-PR-Part2, DB Systemtechnik GmbH Testing laboratory Sound and vibration (08.11.2013)

[36] UIC International Union of Railways (2009), UIC Project Under Sleeper Pads - Semelles sous traverses – Schwellenbesohlungen, Summarising Report, http://www.uic.org/IMG/pdf/2009-03-26_Summarising_Report_UIC-USP.pdf

[37] Loy, H.: Mitigation vibration using under sleeper pads, Railway Gazette International, April 2012

[38] Freudenstein, S.: Die Kontaktspannung zwischen elastisch besohlten Schwellen und Schotter, Eisenbahntechnische Rundschau ETR, Mai 2011, Nr. 05

[39] Iliev, D.: Die horizontale Gleislagestabilität des Schotteroberbaus mit konventionellen und elastisch besohlten Schwellen, Mitteilungen des Prüfamtes für Verkehrswegebau der Technischen Universität München, Heft 86, München 2012

[40] Nélain, B. & Vincent, N.: Procedure for transfer of insertion loss. Guideline for RIVAS project partners, WP1, (2011)

10. ANNEXES

The following annexes are added as additional parts to this deliverable which describe the performed investigation in a more exhaustive way.

ANNEX A1: Mistler, M., Heiland, D.: Free field vibration measurements - Experimental investigation of the Insertion Loss of under-sleeper pads within the framework of RIVAS "Railway Induced Vibration Abatement Solutions - Collaborative Project", Measurement Report ID 80-7781- B1 Rev A (17.06.2013)

ANNEX A2: Mistler, M., Heiland, D.: Additional data analysis of the train passage vibration measurements, Appendix to report 80-7781-B1, (13.09.2013)

ANNEX B: Said, S.; Auersch, L.; Rücker, W.: Geotechnical data and soil characteristics of the test site in Tiefbrunn near Regensburg, Part of Deliverable D1.10, Berlin (20.02.2013)

ANNEX C: Depuis, H.: RIVAS WP1: Line transfer mobility measurements with hammer excitation of three subsoils on track 5830-2, km 102,13 to km 103,25, Report 13-15264-I.TVI32(3)-PR-Part2, DB Systemtechnik GmbH Testing laboratory Sound and vibration (08.11.2013)

10.1 ANNEX A1:

Mistler, M., Heiland, D.: Free field vibration measurements - Experimental investigation of the Insertion Loss of under-sleeper pads within the framework of RIVAS “Railway Induced Vibration Abatement Solutions - Collaborative Project”, Measurement Report ID 80-7781-B1 Rev A (17.06.2013)

10.2 ANNEX A2:

Mistler, M., Heiland, D.: Additional data analysis of the train passage vibration measurements, Appendix to report 80-7781-B1, (13.09.2013)

10.3 ANNEX B:

Said, S.; Auersch, L.; Rücker, W.: Geotechnical data and soil characteristics of the test site in Tiefbrunn near Regensburg, Part of Deliverable D1.10, Berlin (20.02.2013)

10.4 ANNEX C:

Depuis, H.: RIVAS WP1: Line transfer mobility measurements with hammer excitation of three subsoils on track 5830-2, km 102,13 to km 103,25, Report 13-15264-I.TVI32(3)-PR-Part2, DB Systemtechnik GmbH Testing laboratory Sound and vibration (08.11.2013)